

Copyright  
by  
Thomas Robert Shelite  
2014

**The Dissertation Committee for Thomas Robert Shelite Certifies that this is the  
approved version of the following dissertation:**

**DEVELOPMENT OF A MURINE MODEL OF SEVERE SCRUB  
TYPHUS AND ITS USE TO ELUCIDATE THE IMMUNE  
RESPONSE TO AND THE PATHOLOGY THAT OCCURS DURING  
*ORIENTIA TSUTSUGAMUSHI* INFECTION.**

**Committee:**

---

David H. Walker, M.D., Supervisor and  
Mentor

---

Gustavo A. Valbuena, M.D., Ph.D., Co-  
Supervisor

---

Donald H. Bouyer, Ph.D.

---

Sanjeev K. Sahni, Ph.D.

---

Peter C. Melby, M.D.

---

Daniel H. Paris, M.D., Ph.D.

---

Lynn Soong, M.D., Ph.D.

---

---

Dean, Graduate School

**DEVELOPMENT OF A MURINE MODEL OF SEVERE SCRUB  
TYPHUS AND ITS USE TO ELUCIDATE THE IMMUNE  
RESPONSE TO AND THE PATHOLOGY THAT OCCURS DURING  
*ORIENTIA TSUTSUGAMUSHI* INFECTION.**

**by**

**Thomas Robert Shelite, A.S., B.S., M.S.**

**Dissertation**

Presented to the Faculty of the Graduate School

The University of Texas Medical Branch

in Partial Fulfillment

of the Requirements

for the Degree of

**Doctor of Philosophy**

**The University of Texas Medical Branch**

**March, 2014**

## **Dedication**

For my father, I finally figured out what I am going to be when I grow up.

## Acknowledgements

First I would like to thank my mentor, Dr. David H. Walker. Dr. Walker, thank you for providing me the opportunity to prove myself in your laboratory when you had no reason to do so. You gave me guidance when needed and the freedom to explore various avenues of interest even when you didn't agree with my hypothesis. As my research "Father," you allowed me to pursue this project that will provide the foundation of my scientific career.

Next I would like to thank my committee members, Drs. Donald H. Bouyer, Peter C. Melby, Daniel H. Paris, Sanjeev K. Sahni, Lynn Soong, and Gustavo Valbuena. Strength in numbers is an adapt description of our committee. Each of you eagerly served on my committee and brought your expertise to each meeting throughout your tenure on this project. Thank you all for your guidance during this atypical journey and seeing this dissertation through to the end.

I want to thank all the past and present members of the Walker laboratory, as well as the Bouyer and Valbuena laboratories who have been like family to me as well as colleagues. I would like to thank Dr. Rong Fang for training in the ABSL3 and BSL3 facilities early in my career. Without her training this project would not have been possible, Dr. Lijun Xin whose guidance in the laboratory and life has provided a constant heading in this endeavor, Patricia Valdes for providing guidance and laboratory assistance, and Dr. Tais B. Saito for experimental assistance and playing "devil's advocate" with my research questions. In addition, I would like thank Eric Carlsen for his flow cytometry assistance in determining the efficiency of PMN depletion (**Chapter 5**) and Dr. Hui Wang for expert assistance in all of the RNA studies and preparation of figures (**Chapter 4, Figures 4.10-4.16, Table 4.4**) as well as her excellent immunohistochemical staining for PMNs and *Orientia* (**Chapter 5, Figures 5.1-5.3**).

Next, I would like to thank my family, especially, Mom, Dad, and Lendell for their support; even if they don't entirely understand what it is that I do. Although not related by blood, I would like to thank other members of my "family," Allison McMullen, Kimberly Roberts, Dr. Bin Gong, Sherrill Hebert, Nicole Mendell, and Guang Xu for all of the support and friendship. You all will never know how much it has meant to me and how proud I am to call you family. I will keep all of you in my mind and heart in all of my future endeavors.

**DEVELOPMENT OF A MURINE MODEL OF SEVERE SCRUB TYPHUS AND ITS USE TO ELUCIDATE THE IMMUNE RESPONSE TO AND THE PATHOLOGY THAT OCCURS DURING *ORIENTIA TSUTSUGAMUSHI* INFECTION.**

Publication No. \_\_\_\_\_

Thomas Robert Shelite, Ph.D.

The University of Texas Medical Branch, 2013

Supervisor: David H. Walker

Scrub typhus is an often lethal infection that threatens one billion persons globally and causes illness in one million people annually. There is no vaccine for scrub typhus, and the mechanisms of protective immunity are poorly understood. Scrub typhus is a disseminated infection of endothelial cells by the obligately intracellular bacterium *Orientia tsutsugamushi*. Mechanistic studies of immunity have been performed primarily in intraperitoneally inoculated mice in which *Orientia* is largely confined to the peritoneal cavity rather than causing disseminated endothelial infection and multifocal vasculitis that occur in scrub typhus in humans. There is a critical need for a valid endothelial-target mouse model of scrub typhus to enable determination of the mechanisms of protective immunity against *Orientia*.

The first objective was to develop a disease model that demonstrates pathology and cellular tropism similar to those of human disease. Development of this model allows for investigation of the immunological mechanisms that mediate protective immunity in scrub typhus infections. C57BL/6 (B6) mice were determined to be susceptible to intravenous

challenge by *Orientia* with overt signs of illness with a dose-dependent time of onset. Immunohistochemical staining of *Orientia* antigens demonstrated extensive endothelial infection, most notably in the brain and lungs. The histopathology revealed cerebral perivascular lymphohistiocytic infiltrates, focal hemorrhage, meningoencephalitis, and interstitial pneumonia, resembling that of human scrub typhus.

The second objective was to address the role of neutrophils in scrub typhus. All scrub typhus case studies that report blood cell counts, describe neutrophilia during the course of infection and observed in our model, suggesting key a role in scrub typhus. To determine the role of neutrophils in this infection, mice were lethally challenged, and neutrophils were depleted one day prior to and six days post infection. Early depletion resulted in more severe pathology with earlier onset and disease progression similar to non-depleted animals but with increased survival. Animals depleted at 6 dpi recovered weight and had less severe signs of illness. Signs of illness had resolved by 12 dpi. These data suggest a dual role of neutrophils in bacterial clearance and tissue pathology during scrub typhus infection.



# TABLE OF CONTENTS

List of Tables.....	xi
List of Figures .....	xii
List of Abbreviations .....	xiv
Chapter 1 .....	1
Introduction.....	1
Structural comparison and delineation of Rickettsiaceae .....	1
Geographical distribution.....	3
Clinical manifestations .....	4
Current research models .....	7
Scrub typhus immunology .....	11
Chapter 2 .....	15
Specific Aims .....	15
Specific aim 1.....	16
Specific aim 2.....	17
Innovation, outcomes, and benefits .....	17
Expected outcomes .....	18
Significance .....	18
Chapter 3 .....	19
Materials and Methods .....	19
Bacterial culture.....	19
Focus forming assays (FFA).....	20
Quantitative oriental viability assay .....	21
Mouse strain comparison .....	22
Characterization of lethal and sublethal mouse models of <i>Orientia</i> <i>tsutsugamushi</i> infections.....	23
Histopathology and immunohistochemistry .....	23
Bacterial load determination.....	25
Blood cell counts .....	25

Transmission electron microscopy .....	26
Serum chemokine/cytokine measurements .....	26
Quantitative reverse transcriptase PCR (qRT-PCR) analysis .....	27
Chapter 4 .....	29
Development of a hematogenously disseminated mouse model for scrub typhus. ...	29
Specific aim 1 .....	29
Hypothesis .....	29
Rationale.....	29
Sub-aim 1: Characterize and compare the course and histopathology of the classic intraperitoneally inoculated and novel intravenous inoculation mouse models of scrub typhus. ....	29
Mouse strain comparison .....	30
Characterization of lethal i.v. and same dose i.p. <i>Orientia</i> infection in C57BL/6 mice .....	31
Disease progression of intraperitoneally inoculated mice:.....	32
Disease progression of intravenously inoculated mice:.....	34
Circulating blood cell counts .....	38
Characterization of the sublethal i.v. and same dose i.p. <i>Orientia</i> infection in C57BL/6 mice .....	40
Discussion.....	44
Sub-aim 2: Characterize the cytokine response during lethal scrub typhus using a hematogenously disseminated murine model of disease. ..	47
Results-Sub-aim 2 .....	52
Disease progression:.....	52
Cytokine expression during <i>Orientia</i> infection: .....	53
Serum cytokine and chemokine levels:.....	59
Discussion.....	61
Chapter 5 .....	64
Janus-like behavior of neutrophils during lethal <i>Orientia</i> infection. ....	64
Specific aim 2.....	64
Hypothesis .....	64
Rationale.....	64
Characterization of the role of PMNs during <i>Orientia</i> infection .....	65

Part 1 Experimental design .....	65
Part 2 Experimental design .....	66
Results .....	67
Part 1: Neutrophil localization .....	67
Part 2: Neutrophil depletion and disease progression .....	71
Discussion .....	81
Chapter 6 .....	86
Conclusions and Future Studies .....	86
Summary .....	86
Future studies .....	92
References .....	97
Vita .....	108

## List of Tables

Table 1.1. Mouse strains used in <i>Orientia</i> research and strain susceptibility.....	9
Table 3.1. Selected secreted endothelial proteins and chemokine/cytokines.....	26
Table 3.2. Primers of murine genes for real time PCR.....	28
Table 4.1. Bacterial load (47 kDa gene copies/pg of DNA or $\mu$ L of blood) kinetics of 1.25 x 10 <sup>6</sup> FFU-challenged C57BL/6 mice.....	39
Table 4.2. Summary of disease manifestations.....	41
Table 4.3. Bacterial load (47 kDa gene copies/pg of DNA or $\mu$ L of blood) kinetics of 1.25 x 10 <sup>4</sup> FFU-challenged C57BL/6 mice.....	43
Table 4.4. Cytokine expression profile summary.....	63

## List of Figures

Figure 1.1: Cell wall composition of <i>Rickettsia</i> and <i>Orientia</i> .....	2
Figure 1.2: Geographic distribution of <i>Orientia</i> and <i>Orientia</i> -like agents.....	4
Figure 1.3: Scrub typhus transmission cycle.....	5
Figure 1.4: Immunohistochemical staining of <i>Orientia</i> in human lung tissue.....	6
Figure 4.1: Survival and body weight change of mice inoculated intraperitoneally or intravenously with <i>O. tsutsugamushi</i> .....	31
Figure 4.2: Histopathology in mice following $1.25 \times 10^6$ <i>Orientia</i> intraperitoneal challenge at days 6 and 9 pi.....	33
Figure 4.3: Histopathology in mice following $1.25 \times 10^6$ <i>Orientia</i> intravenous challenge at 6 dpi.....	34
Figure 4.4: Pulmonary endothelial infection by <i>Orientia</i> .....	35
Figure 4.5: Histopathology of mice following lethal <i>Orientia</i> intravenous challenge at days 9 and 12 pi.....	37
Figure 4.6: Histopathology of the lung following $1.25 \times 10^4$ <i>Orientia</i> challenge.....	44
Figure 4.7: Serum cytokine levels during lethal <i>Orientia</i> infection.....	49
Figure 4.8: Soluble cellular adhesion molecules in serum during lethal <i>Orientia</i> infection.....	50
Figure 4.9: Experimental design for cytokine analysis.....	51
Figure 4.10: IHC staining of liver and lung from mice lethally challenged with <i>Orientia</i> .....	52
Figure 4.11: Relative mRNA levels of selected cytokines and chemokines at 2 dpi with <i>Orientia</i> .....	54
Figure 4.12: Relative mRNA levels of selected cytokines and chemokines in the liver and lung at 6 dpi with <i>Orientia</i> .....	56
Figure 4.13: Relative mRNA levels of selected cytokines and chemokines in the kidney and spleen at 6 dpi with <i>Orientia</i> .....	57

<b>Figure 4.14: Distinct repression of type 2 responses and activation of type 1 responses at 10 dpi with <i>Orientia</i>.....</b>	<b>58</b>
<b>Figure 4.15: Liver cytokine levels during <i>Orientia</i> infection.....</b>	<b>58</b>
<b>Figure 4.16: Serum cytokine levels expressed as signal intensity in mice challenged with <i>Orientia</i>.....</b>	<b>60</b>
<b>Figure 5.1: IHC staining of PMNs in the spleen of mice lethally challenged with <i>Orientia</i>.....</b>	<b>68</b>
<b>Figure 5.2: IHC staining of liver from mice lethally challenged with <i>Orientia</i>.....</b>	<b>69</b>
<b>Figure 5.3: IHC staining of lung from mice lethally challenged with <i>Orientia</i>.....</b>	<b>70</b>
<b>Figure 5.4: Percent body weight change of mice following lethal challenge with <i>Orientia</i> and PMN depletion.....</b>	<b>71</b>
<b>Figure 5.5: Percent survival following lethal challenge with <i>Orientia</i> and PMN depletion.....</b>	<b>72</b>
<b>Figure 5.6: <i>Orientia</i> 47 kD gene copies/pg of DNA at 19 dpi following neutrophil depletion.....</b>	<b>73</b>
<b>Figure 5.7: Histopathology of the lung at 6 dpi of mice inoculated with <i>Orientia tsutsugamushi</i> following neutrophil depletion on day 1.....</b>	<b>74</b>
<b>Figure 5.8: Hepatic histopathology at 6 dpi of mice inoculated with <i>Orientia tsutsugamushi</i> following neutrophil depletion on day 1.....</b>	<b>75</b>
<b>Figure 5.9: Histopathology of the lung at 12 dpi of mice inoculated with <i>Orientia tsutsugamushi</i> following neutrophil depletion on day 6.....</b>	<b>77</b>
<b>Figure 5.10: Dual immunofluorescence staining for PMNs (red) and <i>Orientia</i> (green) in the lung of mice inoculated with <i>Orientia tsutsugamushi</i> following neutrophil depletion on day 6.....</b>	<b>78</b>
<b>Figure 5.11: Hepatic histopathology at 12 dpi of mice inoculated with <i>Orientia tsutsugamushi</i> following neutrophil depletion on day 6.....</b>	<b>79</b>
<b>Figure 5.12: Dual immunofluorescence staining for PMNs (red) and <i>Orientia</i> (green) in the liver of mice inoculated with <i>Orientia tsutsugamushi</i> following neutrophil depletion on day 12.....</b>	<b>80</b>
<b>Figure 6.1: The role of ILCs in promotion of a Th-1 response in scrub typhus.....</b>	<b>96</b>

## **List of Abbreviations**

ARDS	Acute respiratory distress syndrome
BSA	Bovine serum albumin
BSL	Biosafety level
CBC	Complete blood count
CCL	Chemokine (C-C motif) ligand
CTL	Cytotoxic T lymphocyte
CNS	Central nervous system
CXCL	Chemokine (C-X-C motif) ligand
DC	Dendritic cell
DIC	Disseminated intravascular coagulation
DMEM	Dulbecco's Modified Eagle's Medium
dpi	Days post infection
DPBS	Dulbecco's PBS
FBS	Fetal bovine serum
FFA	Focus forming assay
FFU	Focus forming unit
GATA-3	GATA-binding protein transcription factor
G-CSF	Granulocyte colony-stimulating factor
GM-CSF	Granulocyte macrophage colony-stimulating factor
H & E	Hematoxylin and eosin
i.c.	Intracranial

IFN	Interferon
IHC	Immunohistochemistry
IL	Interleukin
ILC	Innate lymphoid cells
i.m.	Intramuscular
i.p.	Intraperitoneal
i.v.	Intravenous
KC	Cytokine-induced neutrophil-attracting chemokine
LPS	Lipopolysaccharide
MadCAM	Mucosal vascular addressin cell adhesion molecule 1
MCP	Monocyte chemoattractant protein
MIP	Macrophage inflammatory protein
MPO	Myeloperoxidase
NHP	Non-human primate
PBS	Phosphate buffered saline
PCR	Polymerase chain reaction
PMN	Polymorphonuclear cell/ neutrophil
RANTES	Regulated on activation, normal T cell expressed and secreted
RBC	Red blood cells
ROR- $\gamma$	Retinoic acid receptor-related orphan receptor- $\gamma$
sCAM	Soluble adhesion molecules
SPG	Sucrose-phosphate-glutamate
s.q.	Subcutaneous



sTNFR	Soluble TNF receptor
T-bet	Th-1 cell-associated transcription factor
TIMP1	Tissue inhibitor of metalloproteinases
TGF-	Transforming growth factor
TNF-	Tumor necrosis factor
VEGF	Vascular endothelial growth factor
WBC	White blood cells

## CHAPTER 1

### Introduction

Scrub typhus is a mite-transmitted infection of endothelial cells by the obligately intracellular bacterium *O. tsutsugamushi* (formerly *Rickettsia orientalis* and *Rickettsia tsutsugamushi*) (Tamura 1995, Ohashi 1994). Mechanistic studies of immunity have been performed primarily in intraperitoneally inoculated mice in which *O. tsutsugamushi* is largely confined to the peritoneal cavity and infects peritoneal macrophages (Kundin 1964) rather than causing disseminated endothelial infection and multifocal vasculitis affecting the brain, lungs, and other organs as occurs in scrub typhus in humans (Allen and Spitz 1945, Berman and Kundin 1973, Levine 1946, Sayen 1946). Most mechanistic research on immunity to scrub typhus was performed more than 25 years ago when many contemporary tools and concepts of immunology had not been developed (Kundin 1964 and 1972, Jerrells and others 1981-83, Rollwagen 1986).

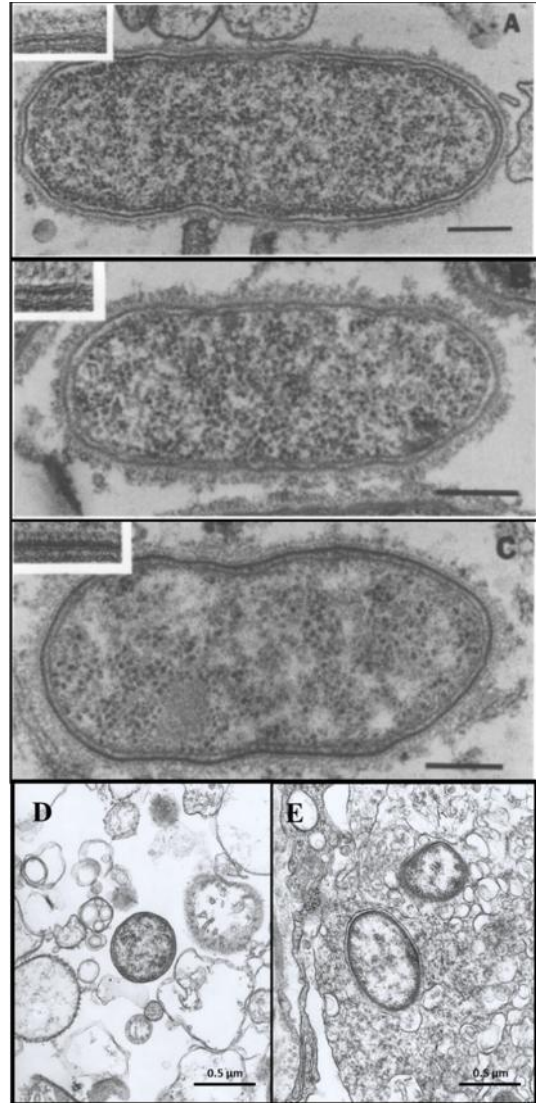
### Structural comparison and delineation of Rickettsiaceae

The etiologic agent of scrub typhus has been referred to as both a bacterium and a virus as well as by several different names: *Rickettsia orientalis* (1920-1930), *Rickettsia tsutsugamushi* (1918-1995), and finally, *Orientia tsutsugamushi* (1995-present) (Nagoya 1917, Fox 1948, Tamura 1995). *Orientia* belongs to the Rickettsiaceae family and is phylogenetically 90.2 to 90.6% similar to the *Rickettsia* genus based on 16S rRNA sequences (Ohashi 1995). The genetic difference between *Rickettsia tsutsugamushi* and

the other members of the genus as well as morphological differences (**Figure 1.1**) led to the creation of a new genus, *Orientia*, with the sole member, at the time, being *Orientia tsutsugamushi* (Silverman and Wisseman 1978, Ohashi 1995, Tamura 1995).

**Figure 1.1: Cell wall composition of *Rickettsia* and *Orientia*.<sup>1</sup>**

The cell wall of *Rickettsia prowazekii* (A), *R. rickettsii* (B), and *O. tsutsugamushi* (C-E) are considerably different. *Orientia* completely lacks peptidoglycan and lipopolysaccharides as well as not possessing any homologous outer membrane proteins to either *Rickettsia* group (Image modified from Silverman and Wisseman 1978 A-C). D and E show extracellular and intracellular *Orientia*, respectively, in Vero E6 cells.



The second member of this genus was isolated from a febrile woman returning from Dubai, UAE. She had been bitten by a mite while visiting a market in Dubai, and later developed an eschar, 11 days after leaving Dubai, followed by fever ~18 days after being bitten. Samples were collected and an isolate obtained. After an extensive workup, this isolate was found to be significantly different from the ~150 strains of *O. tsutsugamushi*, and therefore christened as *Orientia chuto* (sp. nov.) (**Figure 1.2**) (Kelley 2009, Izzard 2010). To date, there are only two species in the

<sup>1</sup> Modified from Silverman and Wisseman 1978 with permission from ASM. ASM authorizes an advanced degree candidate to republish the requested material in his/her doctoral thesis or dissertation.

genus *Orientia*, but *O. tsutsugamushi* consists of ~150 antigenically and genetically diverse strains isolated from humans, mites and rodents (Kelley 2009).

### **Geographical distribution**

Scrub typhus is a serious public health problem in Asia and islands of the western Pacific and Indian Oceans including Korea, Japan, China, Phillipines, Taiwan, Indonesia, India, Sri Lanka, and Thailand, which threatens one billion persons globally and causes illness in one million people each year (Kelly 2009) (**Figure 1.2**). Historically, *Orientia* isolates were made in the “Tsutsugamushi Triangle,” but there is growing evidence that *Orientia*-like agents may be found globally. In two separate reports, travelers returning from Africa presented to their local hospitals with signs and symptoms of scrub typhus. Serology demonstrated that they had antibodies reactive with *O. tsutsugamushi* and began to recover after receiving appropriate antibiotics (Osuga 1991, Ghorbani 1997). In 2006, even stronger evidence for scrub typhus-like agents outside the established range of distribution was discovered. On Chiloe Island, Chile a man presented with a febrile illness that included a rash and a wound that resembled an eschar. Serology was negative for endemic viral agents as well as rickettsiosis. The patient’s sera contained antibodies that reacted with *Orientia*, and an electron micrograph of the eschar revealed an organism that had a cellular structure like *O. tsutsugamushi*. Unfortunately, the group reporting this case has not cultivated an isolate for further identification (Balcells 2011). Interestingly, the primary vector has not been determined in Chile, and the eschar was present at the site where a leach had attached, indicating a possible different vector in the Western hemisphere (Balcells 2011).

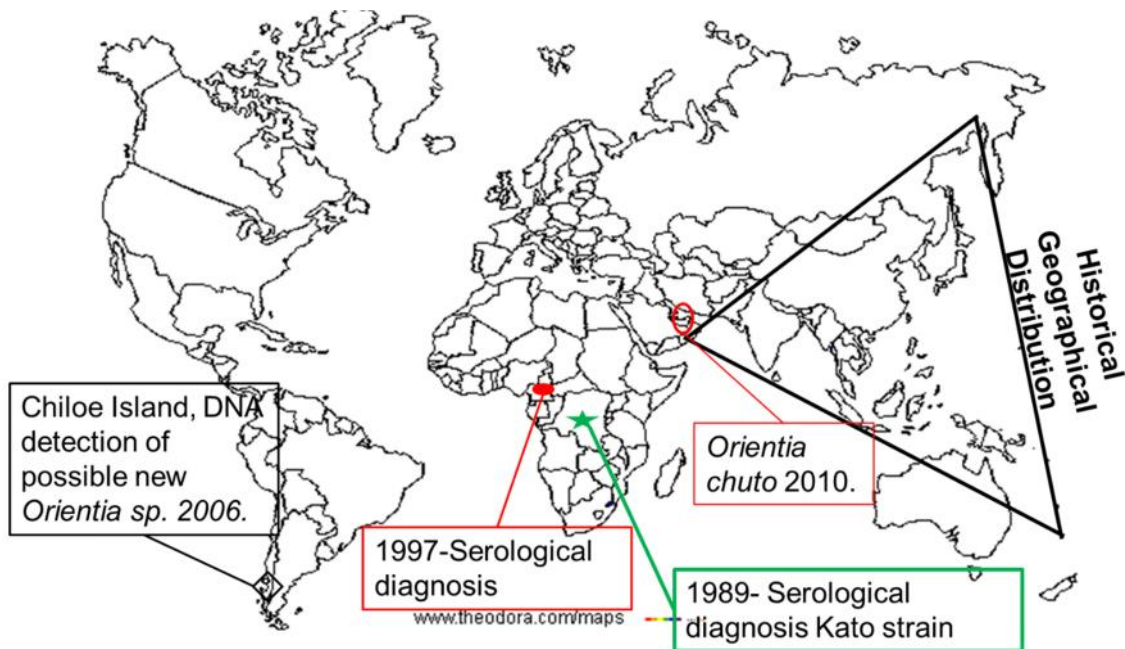


**Figure 1.2: Geographic distribution of *Orientia* and *Orientia*-like agents.**

In the last ten years, one definitive new species has been discovered with another possible new species well outside the historical distribution (Izzard 2010, Balcells 2011). It is not too farfetched to hypothesize that there are several species spread throughout the globe that cause scrub typhus-like illness.

### **Clinical manifestations**

*Orientia tsutsugamushi* is transmitted by the bite of the larval stage of trombiculid mites (chiggers). Humans are a dead-end host, but once the bacteria are transmitted, the initial signs of illness may begin after a 5-20 day incubation period (**Figure 1.3**) (Nagayo 1917 and 1939, Audy 1947). Scrub typhus presents initially as a flu-like syndrome with fever, headache, and malaise.

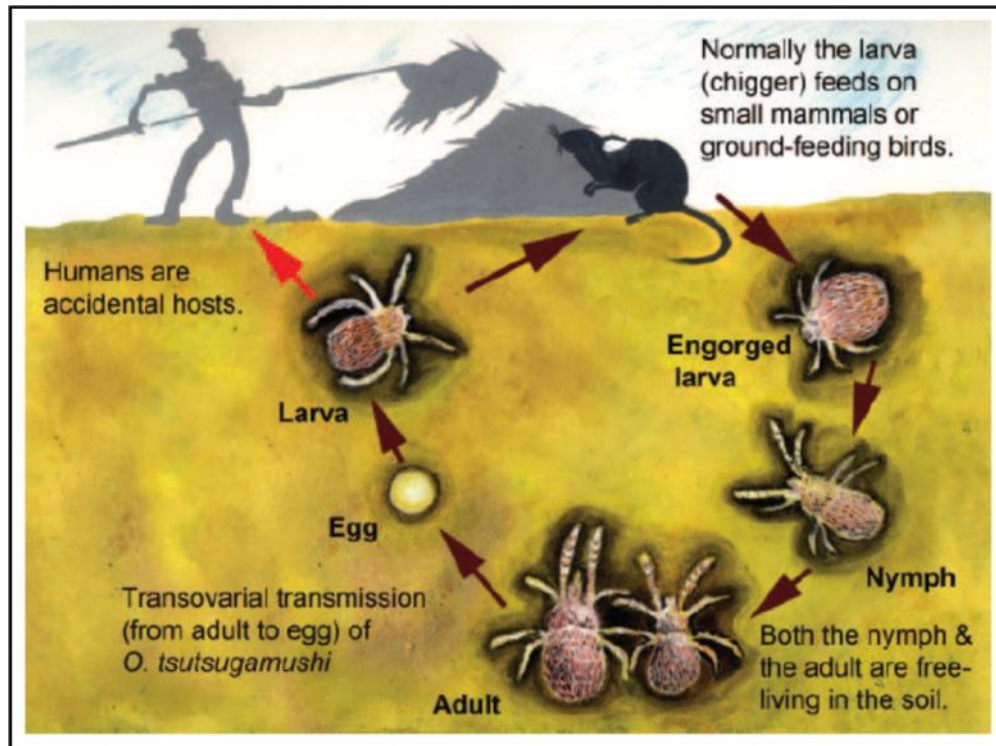


**Figure 1.3: Scrub typhus transmission cycle.<sup>2</sup>**

*Orientia* is maintained in a mite-cycle where vertebrates play an undetermined role. Larval mites are the only stage that feeds on vertebrates; therefore, maintenance of the bacteria occurs transovarially (Traub 1975).

Eschars develop at the site of mite attachment in 60-100% of scrub typhus infections, but may be as low as 7% or absent for unknown reasons (Kelly 2009). The severity of this disease is variable with some cases being mild and self-limiting, moderate, requiring hospitalization, or severe, resulting in multiple organ system failure, acute respiratory distress syndrome (ARDS), hepatosplenomegaly, encephalitis and a potential for coagulation disorders (Ben 1999). Lymphocytosis has been described in upwards of 70% of cases (Irons 1946, Sayen 1946, Berman and Kundin 1972). Scrub typhus is traditionally treated with particular antibiotics, but when severe cases are misdiagnosed or mistaken for

<sup>2</sup>Taken from Jeong *et al.* 2007 with permission.



another infection, such as dengue or Japanese encephalitis, the mortality can be as high as 30%. Individual host factors and bacterial strain variability are thought to be the underlying reasons behind this variable disease outcome. To date, it has only been suspected that disease severity in humans may be correlated with the oriental strain as evidenced in the various animal models that have been used to study scrub typhus.

During *Orientia* infection, the bacteria infect endothelial cells, macrophages, cardiac myocytes, and dendritic cells (Moron 2001, Paris 2012). Similar to most of the bacteria belonging to the family Rickettsiaceae, *Orientia* exhibits endothelial tropism. As such, scrub typhus is a disseminated endothelial infection that affects all organs. The main characteristics of fatal scrub typhus pathology include diffuse interstitial pneumonia (**Figure 1.4**), hepatic lesions, meningoencephalitis, and coagulation disorders (Allen and Spitz 1945, Moron 2001, Jeong 2007, Kim and Walker 2010).

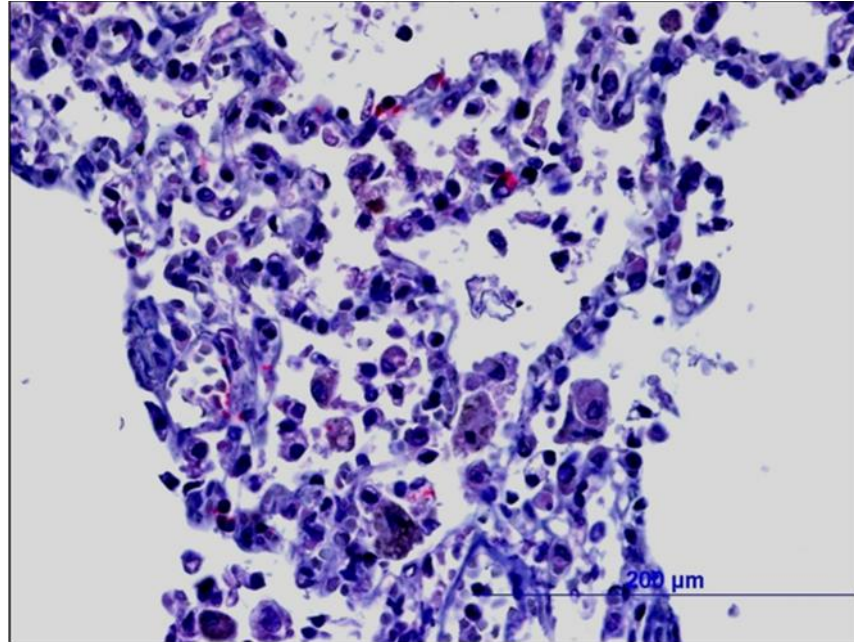


**Figure 1.4: Immunohistochemical staining of *Orientia* in human lung tissue.**

Archival human scrub typhus lung tissue stained by IHC. Oriental staining is indicated by the pink coloration located in the aveolar septa.

## Current research models

As referenced above (Kundin 1964), the majority of scrub typhus research has been conducted on various strains of mice infected via intraperitoneal inoculation (Kundin 1964, Osterman and Groves 1978). Osterman and Groves utilized ~40 cross-bred, inbred, and outbred mice strains to study *Orientia* infection. Using intraperitoneal (i.p.) route of infection, they tried to establish a disease model for scrub typhus; all combinations resulted in disease, but none that reproducibly resembled human scrub typhus pathology (Osterman and Groves 1978). Kundin *et al.* inoculated albino-Swiss mice via intracranial (i.c.), intramuscular (i.m.), i.p., and subcutaneous (s.q.) routes that resulted in route-specific disease development without exhibiting human scrub typhus-like pathology (Kundin 1964) (**Table 1.1**).

Throughout the century of scrub typhus research, various mammals, in addition to mice, have been utilized in the quest to understand this disease. In the early 1900s, rabbits and their tissues were used to study scrub typhus, but the lack of immunological reagents and variability between strains of rabbits and *O. tsutsugamushi* led to using them primarily for anti-sera production (Nagayo 1931, 1939). Two species of gerbils were studied by Zarafonetis using i.p. inoculation of *O. tsutsugamushi* that had been passaged through guinea pigs and rabbits. They found that i.p. inoculation of gerbils with *Orientia* resulted in severe peritonitis, which was usually 100% fatal (Zarafonetis 1945). Guinea pigs have been used for isolating and studying *Orientia* sp. (Kouwenaar and Esseveld 1948, Irons 1946) with strain-specific lethality and anti-sera production. Dogs were also studied (Shirai 1979a), but results were highly variable. Some strains produced an eschar and regional lymphadenopathy upon intradermal (i.d.) inoculation while others were lethal via



intravenous (i.v.) inoculation resulting in signs similar to human cases with Gilliam strain being more severe than Karp strain, which is the opposite the outcomes of the mouse studies. White rats were used to isolate bacteria from febrile patients. Rats were inoculated i.v., and when they became moribund, spleen and liver were collected, homogenized, and used to inoculate mice i.p. (Rights and Smadel 1948).

Silvered leaf monkeys were also studied but proved too difficult (high mortality) to maintain in captivity and often had preexisting antibodies against *Orientia* (Shirai 1979b). More recently, cynomolgus monkeys were studied for evaluating potential vaccine candidates as well as by intradermal inoculation with little disease development (Chattopadhyay 2005, 2007). Wild caught monkeys must be thoroughly screened for multiple pathogens including *Orientia*. Human volunteers have also been invaluable in the study of *Orientia* transmission and establishing clinical signs during known scrub typhus infections (Shirai 1982).

**Table 1.1. Mouse strains used in *Orientia* research and strain susceptibility.**

Mouse strain	Ref.	Breeding	Route of Inoc.	Response to Karp	Response to Gilliam
A/HeJ	Groves and Osterman 1978	Inbred mice	i.p.	Susceptible @ 10 <sup>3</sup> +	Susceptible
A/J	Groves and Osterman 1978	Inbred mice	i.p.	Susceptible @ 10 <sup>3</sup> +	Susceptible
C3H/HeDub	Groves and Osterman 1978	Inbred mice	i.p.	Susceptible @ 10 <sup>3</sup> +	Susceptible
C3H/HeJ	Groves and Osterman 1978	Inbred mice	i.p.	Susceptible @ 10 <sup>3</sup> +	Susceptible
C3H/HeN	Groves and Osterman 1978	Inbred mice	i.p.	Susceptible @ 10 <sup>3</sup> +	Susceptible
C3H/St	Groves and Osterman 1978	Inbred mice	i.p.	Susceptible @ 10 <sup>3</sup> +	Susceptible
CBA/J	Groves and Osterman 1978	Inbred mice	i.p.	Susceptible @ 10 <sup>3</sup> +	Susceptible
DBA/1J	Groves and Osterman 1978	Inbred mice	i.p.	Susceptible @ 10 <sup>3</sup> +	Susceptible
DBA/2J	Groves and Osterman 1978	Inbred mice	i.p.	Susceptible @ 10 <sup>3</sup> +	Susceptible
SJL/J	Groves and Osterman 1978	Inbred mice	i.p.	Susceptible @ 10 <sup>3</sup> +	Resistant
AKR/J	Groves and Osterman 1978	Inbred mice	i.p.	Susceptible @ 10 <sup>3</sup> +	Resistant
Balb/cDub	Groves and Osterman 1978	Inbred mice	i.p.	Susceptible @ 10 <sup>3</sup> +	Resistant
	Ewing et al 1978	Inbred mice	i.p.	Susceptible @ 10 <sup>3</sup> +	Resistant
	Murata et al 1985	Inbred mice	i.p., s.q.	Susceptible @ 10 <sup>3</sup> +	Resistant
	Fukuhara et al 2005	Inbred mice	i.p.	Susceptible @ 10 <sup>3</sup> +	NA
DDD mice	Murata et al 1985	Inbred mice	i.p.	Susceptible @ 10 <sup>3</sup> +	NA
Balb/cj	Groves and Osterman 1978	Inbred mice	i.p.	Susceptible @ 10 <sup>3</sup> +	Resistant
C57BL/6J	Groves and Osterman 1978	Inbred mice	i.p.	Susceptible @ 10 <sup>3</sup> +	Resistant
C57L/J	Groves and Osterman 1978	Inbred mice	i.p.	Susceptible @ 10 <sup>3</sup> +	Resistant
SWR/J	Groves and Osterman 1978	outbred mice	i.p.	Susceptible @ 10 <sup>3</sup> +	Resistant
Wrc:(ICR)	Groves and Osterman 1978	outbred mice	i.p.	Susceptible @ 10 <sup>3</sup> +	Selectively Resistant
Caw:CF1(albino)	Groves and Osterman 1978	outbred mice	i.p.	Susceptible @ 10 <sup>3</sup> +	Resistant
Caw:CFW(SW)	Groves and Osterman 1978	outbred mice	i.p.	Susceptible @ 10 <sup>3</sup> +	Selectively Resistant
CrI:COBS CD1 (ICR)	Groves and Osterman 1978	outbred mice	i.p.	Susceptible @ 10 <sup>3</sup> +	Resistant
Mai:(S)	Groves and Osterman 1978	outbred mice	i.p.	Susceptible @ 10 <sup>3</sup> +	Susceptible
Dub: (ICR)	Groves and Osterman 1978	outbred mice	i.p.	Susceptible @ 10 <sup>3</sup> +	Selectively Resistant
AKD2F1	Groves and Osterman 1978	hybrid mice	i.p.	Susceptible @ 10 <sup>3</sup> +	Resistant
B6D2F1	Groves and Osterman 1978	hybrid mice	i.p.	Susceptible @ 10 <sup>3</sup> +	Resistant

C3D2F1	Groves and Osterman 1978	hybrid mice	i.p.	Susceptible @ 10 <sup>3</sup> +	Susceptible
LAF1	Groves and Osterman 1978	hybrid mice	i.p.	Susceptible @ 10 <sup>3</sup> +	Resistant
C3CF1	Groves and Osterman 1978	C3H/He x Balb/c M	i.p.	Susceptible @ 10 <sup>3</sup> +	Resistant
CC3F1	Groves and Osterman 1978	Balb/c x C3H/He M	i.p.	Susceptible @ 10 <sup>3</sup> +	Resistant
F2	Groves and Osterman 1978	CC3F1 x CC3F1 C3CF1 x C3H/He	i.p.	Susceptible @ 10 <sup>3</sup> +	Selectively Resistant
C3H backcross	Groves and Osterman 1978	M	i.p.	Susceptible @ 10 <sup>3</sup> +	Resistant
Balb/c backcross	Groves and Osterman 1978	CC3F1 x Balb/c M	i.p.	Susceptible @ 10 <sup>3</sup> +	Resistant
Albino Swiss-suckling	Kundin et al 1964		i.p., s.q., i.c., i.m.	Susceptible @ 10 <sup>3</sup> +	days to death 10-14
Albino Swiss-weanling			i.p., s.q., i.c., i.m.	Susceptible @ 10 <sup>3</sup> +	days to death 11-21
Mouse strains that expired after infection are defined as susceptible; those strains for which a lethal dose was not determined were defined as resistant. Selectively resistant refers to a dose-dependent lethality.					

## Scrub typhus immunology

The immunological response to *Orientia* infection is not well characterized. Much like the studies concerning the pathology of scrub typhus, excluding those involving human cases, the majority of studies conducted on scrub typhus immunity have used the i.p. inoculation mouse model to garner what is inadequate understanding of the host's response to *Orientia tsutsugamushi*. Using the i.p. model, researchers have tried to extrapolate the events that occur in the peritoneal cavity of experimentally infected mice to the events that unfold during systemic scrub typhus infections in humans. Kundin and Ewing studied i.p. oriental infection, determining that they are capable of infecting macrophages and mesothelial cells lining the peritoneal surfaces of organs residing there (Kundin 1964, Ewing 1978). Kundin's study also investigated intracranial, intramuscular, and subcutaneous inoculations. They found the bacterial antigen to be distributed in an inoculation route-specific manner. All routes seemed to result in infection of multiple cell types, but few were fully characterized referring instead, for example, to the generic term of "infected connective tissue" (Kundin 1964). Macrophages were also observed to be infected, both in the peritoneal cavity and systemically, primarily macrophages located in the liver. Probably the most important observation from this study is that *Orientia* is capable of eventual dissemination, independent of route of infection (Kundin 1964). It has been suggested the peritoneal macrophages may have an impact on disease outcome, but *in vitro* comparisons of macrophages isolated from resistant and susceptible mouse strains resulted in little difference in the bacterial clearance or entry whereas *in vivo* macrophage activation was delayed and inconsistent in susceptible mice but robust in resistant mice indicating other unidentified host factors were involved (Nacy and Groves 1981). Jerrells

and Osterman demonstrated depletion of macrophages in susceptible C3H/He mice resulted in death at lower doses when challenged i.v. and i.p., but resistant C3H/Rv mice required radiation and macrophage depletion to result in death (Jerrells and Osterman 1982). While these studies provided some understanding of how macrophages respond to *Orientia* and how general immunosuppression can affect *Orientia* infection, they failed to establish any specific role of macrophages during scrub typhus. The increase in mortality for those mice that were challenged i.v. and had their macrophages inhibited may provide some evidence for a protective role for macrophages, but further characterization of these methods would be necessary to assure only macrophages were depleted.

T cells have been demonstrated as important to mouse survival, as athymic BALB/c mice are highly susceptible to i.p. challenge with Gilliam strain, where wild-type BALB/c mice are resistant and administration of T cells from wild-type BALB/c mice reconstituted the resistant phenotype (Jerrells and Eisemann 1982); furthermore, transfer of T cells from mice previously challenged with *Orientia* to naïve mice protected them from primary challenge (Jerrells and Osterman 1983). Rollwagen *et al.* demonstrated that cytotoxic T lymphocytes (CTLs) from *Orientia*-challenged mice are highly efficient at lysing *Orientia*-infected cells (Rollwagen 1986), and Carl *et al.* found that CTLs that kill cells infected with typhus group rickettsiae were unable to lyse cells infected with *Orientia* demonstrating that this aspect of cellular immunity was not cross-reactive (Carl 1988). Studies elucidating the cells involved in cellular immunity of humans are few, especially *ex vivo* characterization, but Ikeda *et al.* found patients infected with scrub typhus had significantly higher numbers of circulating CTL when compared to healthy and non-rickettsia infected controls (Ikeda 1994). Combined with the cellular response, there have

been few *in vivo* animal studies that have focused on the immune regulatory proteins, i.e., chemokines and cytokines that are produced during scrub typhus infection.

The effects of proinflammatory cytokines (TNF- $\alpha$  and IFN- $\gamma$ ) on the intracellular growth of *Orientia* have been shown to result in reduction of the oriental replicative ability in a cell type- and dose- dependent manner or to have little-to-no effect *in vitro* (Hanson 1991a; 1991b, Jerrells and Geng 1994, Geng and Jerrells 1994, Ge and Rikihisa 2011). Using the i.p. model, Yun *et al.* performed one of the first extensive cytokine analyses *in vivo* (Yun 2005). Not surprisingly, the results showed a strong pro-inflammatory response in both mouse strains studied, but susceptible C3H/HeN mice produced a significantly stronger response with little difference in TNF- $\alpha$  and IFN- $\gamma$  production between the resistant and susceptible mice (Koh 2004, Yun 2005). Serum levels of soluble cellular adhesion molecules (sCAM) indicate endothelial activation, and possible infection, and their release into the circulation activates and recruits white blood cells (WBCs) to the areas of infection (Paris 2008). Under normal conditions, WBCs use CAMs to migrate along the tissue surface, but when cells are injured they release sCAMs which the WBCs come in contact with. When this happens, WBCs become activated and begin to migrate toward the source of sCAM release in a concentration dependent manner. Serum cytokine levels of scrub typhus-infected patients during the acute phase (~5-12 days after initial symptoms) revealed elevated IFN- $\gamma$  and IL-10, but only detected an increase of TNF- $\alpha$  and IL-1 $\beta$  in a small portion of cases during the acute phase (Kramme 2009). The presence of both pro- and anti-inflammatory cytokines during acute *Orientia* infection is an example of the infected host trying to maintain homeostasis during infection, but how this affects the clinical outcome of scrub typhus has yet to be elucidated. Although there is a plethora

of immunologic data for scrub typhus, the physiological relevance can be questioned as the vast majority of the information has been acquired using an inadequate model system.

## CHAPTER 2

### Specific Aims

Scrub typhus is an often lethal infection that is caused by the obligately intracellular bacterium *Orientia tsutsugamushi*. Scrub typhus is a disseminated infection of endothelial cells. There is no vaccine for scrub typhus, and the mechanisms of protective immunity are poorly understood. Mechanistic studies of immunity have been performed primarily in intraperitoneally inoculated mice in which *O. tsutsugamushi* is largely confined to the peritoneal cavity and infects peritoneal macrophages and the mesothelial lining of the peritoneum (Kundin 1964) rather than causing disseminated endothelial infection and multifocal vasculitis affecting the brain, lungs, and other organs as occurs in scrub typhus in humans (Allen and Spitz 1945, Moron 2001, Smadel 1950). Immunity to rechallenge with the homologous strain of *O. tsutsugamushi* wanes over a few years in humans and is even shorter lived against heterologous strains. Most mechanistic research on immunity to scrub typhus was performed more than 25 years ago when many contemporary tools and concepts of immunology had not been developed. There is a critical need for a valid endothelial-target mouse model of scrub typhus to enable determination of the mechanisms of protective immunity against *O. tsutsugamushi*. Recent efforts toward scrub typhus vaccine development have been hampered by the failure to understand the critical, protective immune mechanisms and have resulted in a disappointing lack of progress. The **gap in knowledge** in this field is two-fold; the lack of an accurate disease model of scrub typhus and the subsequent lack of knowledge of the host immune response are fundamental impediments to the understanding of the mechanisms of immunity and pathogenesis in scrub typhus.

Our **long-term goals** are to determine the critical mechanisms of immunity and pathogenesis of *O. tsutsugamushi* and to identify immunogenic cross-protective antigens



of the diverse strains of *O. tsutsugamushi*. The objective of this research is to develop a valid disseminated endothelial-target mouse model of scrub typhus and to elucidate the major immune mechanisms of this disease. The **central hypothesis** of this project is that *Orientia* infection of endothelial cells activates the innate immune response resulting in increased vascular permeability, shock, and eventual death mediated by the host's immune response. These aims will address this hypothesis.

### **Specific aim 1**

**Develop and characterize a murine model of disseminated endothelial infection through intravenous inoculation of *O. tsutsugamushi*.** The working hypothesis for this aim is that inoculation of *Orientia* intravenously will cause a disseminated endothelial infection resulting in a valid murine model for severe scrub typhus. *Rationale:* Development of a disseminated endothelial disease model for scrub typhus through i.v. administration will allow elucidation of the relevant immune mechanisms for this disease as demonstrated by three murine models of human spotted fever rickettsiosis previously published from our laboratory (Feng 1993, 1994, Walker 1994, 2000).

**Sub-aim 1: Characterize and compare the course and histopathology of the classic intraperitoneally inoculated and novel intravenous inoculation mouse models of scrub typhus.** Previous studies have demonstrated that the route of inoculation produces route-dependent histopathology, but without producing a consistent endothelial tropic infection with resulting pathology paralleling human disease. The working hypothesis of this aim is that intravenous inoculation will result in a model that demonstrates endothelial tropism and has histopathology that parallels human disease.

**Sub-aim 2: Characterize the cytokine response during lethal scrub typhus using a hematogenously disseminated murine model of disease.** The cytokine response during scrub typhus has been studied only in piecemeal fashion using various cell models

and acute patient sera samples. The working hypothesis of this sub-aim is that the cytokine profile observed will strongly recruit neutrophils to the site of infection leading to the pathology observed in our i.v. inoculated mouse model.

## **Specific aim 2**

**Determine the effect of neutrophil depletion on disease progression using a hematogenously disseminated murine model of scrub typhus.** Neutrophils are important innate immune cells that have multiple functions during the course of an infection. Recent studies suggest that neutrophils may have a more complex role in infectious diseases than previously thought (Nathan 2006, Jaeger 2012). *Rationale:* Preliminary studies using this model demonstrated neutrophilia throughout the course of infection, and all case reports that included blood cell counts have described neutrophilia during acute scrub typhus. The working hypothesis of this sub-aim is that the neutrophilia observed in mice infected with *O. tsutsugamushi* is detrimental to disease outcome and depletion of neutrophils during infection will rescue lethally challenged mice.

## **Innovation, outcomes, and benefits**

The innovation of this proposal does not lie in the methods, but the application of established methods to the neglected field of scrub typhus research. Establishment of an animal model that parallels human disease will provide the opportunity to gain insight into the disease pathogenesis and will provide a tool which researchers can exploit to develop better diagnostics and prevention strategies such as vaccine development. As scrub typhus is characterized by disseminated endothelial infection, development of an animal model that also shares this characteristic will revolutionize the scrub typhus field. Also, understanding of how *O. tsutsugamushi* is able to spread from the initial site of infection

(skin) and disseminate, infecting the endothelium systemically, will be crucial to the evaluation of appropriate vaccine candidates, but these goals are beyond the scope of the current proposal.

### **Expected outcomes**

The completion of Specific Aim 1 will reiterate that the traditional i.p. model lacks the pathology of scrub typhus and will establish a disseminated endothelial infection model via i.v. inoculation, providing a model for studying the events of systemic *Orientia* infection. Completion of this aim will provide an effective method to study the disease progression and the pathology of both lethal and sublethal infections and will illustrate the importance of cytokine expression and regulation in the disease outcome of scrub typhus by regulating the activation and function of innate immune cells. Completion of Specific Aim 2 will determine that innate immunity is crucial to both the host's ability to clear the infection (mild-to-moderate infections) as well as the development of scrub typhus pathology with subsequent mortality (severe-to-fatal infections), demonstrating the importance of neutrophils in determining the outcome of severe scrub typhus and their contribution to vasculitis and cellular infiltration of the aveolar septa leading to ARDS.

### **Significance**

Completion of these aims will have the cumulative impact of generating a relevant animal model for human scrub typhus and will produce a greater understanding of the disease progression, providing a solid foundation for the development of efficacious vaccines for this seriously understudied disease of millions.

## CHAPTER 3

### Materials and Methods

#### Bacterial culture

*Orientia tsutsugamushi* Karp strain was cultivated in Vero E6 cells or serially passaged in 8-12 week old female C57BL/6 mice (Harlan Laboratories, Houston, TX). For cultivation in Vero cells, bacteria were inoculated onto confluent monolayers in T150 cell culture flasks and gently rocked for two hours at 34°C, at the end of which 25 mL of Dulbecco's Modified Eagle Medium (DMEM) with 1% fetal bovine serum (FBS) and 1% HEPES buffer were added. Cells were observed for cytopathic effect, which usually occurred at 14-21 days. When areas of rounded or floating cells were observed throughout the flask, a smear was prepared, and the level of infection was assessed either by Dif-Quik (Fisher Scientific, Kalamazoo, MI) or immunofluorescence staining. When the flask reached 80-90% of cells infected, the cells were removed and seeded onto fresh Vero cell monolayers. This process was repeated for a total of six passages. Infected flasks were harvested by scraping, and cell suspensions were collected in 250 mL Oakridge high speed centrifugation bottles and centrifuged at 22,000 x g for 45 minutes at 4°C. The pellet was resuspended in 10 mL of sucrose-phosphate-glutamate (SPG) buffer (0.218 M sucrose, 3.8 mM KH<sub>2</sub>PO<sub>4</sub>, 7.2 mM KH<sub>2</sub>PO<sub>4</sub>, 4.9 mM monosodium L-glutamic acid, pH 7.0) per T150 flask and then transferred to a 50 mL conical tube containing 5 mL of sterile glass beads. The conical tubes were gently vortexed at 10 sec intervals to release the intracellular bacteria and placed on ice. The tubes were then centrifuged at 700 x g to pellet cell debris and the supernatant collected in 50 mL Oakridge tubes on ice. The tubes were then centrifuged at 22,000 x g for 45 minutes to pellet cell-free bacteria. Pellets were

resuspended in 1 mL of SPG buffer per Oakridge tube, placed in 2 mL Sarsted tubes in 200  $\mu$ L aliquots, and stored at -80°C until used. Preliminary studies were conducted using cell cultured orientiae. Animal passages were performed to rapidly produce high titer oriental stocks from infected tissues. Two groups of four 8-12 week old female C57BL/6 mice were inoculated intravenously (i.v.) with  $1.25 \times 10^6$  focus forming units (FFU) of *Orientia* cultivated in Vero E6 cells. When the animals exhibited signs of illness, i.e., hunched posture, lethargy, and ruffled fur, usually at six days post infection, they were euthanized, and the liver and lungs aseptically collected and placed in DMEM. Organ-specific pools were homogenized using a 7 mL glass Dounce apparatus. Homogenized samples were then rinsed with cold SPG buffer and placed in a 50 mL conical tube and centrifuged at 700 x g for 10 minutes at 4°C to pellet the tissue debris. Supernatant fluid was collected and placed on ice. The tissue pellets were resuspended in 5 mL of SPG buffer, homogenized and centrifuged as above. Organ-specific supernatants were pooled on ice and then centrifuged at 22,000 x g for 45 minutes at 4° C in a Beckman high speed centrifuge. The pellets were resuspended in 10 mL of SPG buffer, aliquoted, and stored at -80°C.

### **Focus forming assays (FFA)**

It takes greater than 15 days for plaques to form in *O. tsutsugamushi*-infected monolayers (McDade 1970, personal observation). Thus, in order to quantitate the number of viable bacteria in a timely manner, a focus forming assay was used (Payne 2006). Vero E6 cells in DMEM with 1% FBS and 1% HEPES were seeded onto 12-well plates and allowed to attach overnight at 37°C in a 5% CO<sub>2</sub> atmosphere. Once the cells were confluent, serial 10-fold dilutions of oriental stocks were prepared, and 200  $\mu$ L aliquots

were seeded onto the confluent monolayers in triplicate. The infected plates were centrifuged for 5 minutes at 700 x g to facilitate bacterial attachment and then incubated for two hours at 37°C in 5% CO<sub>2</sub>. After two hours, the wells were rinsed three times with warm Dulbecco's PBS (DPBS) with calcium and magnesium to remove extracellular non-viable bacteria. The wells were then overlaid with DMEM containing 1% FBS, 0.5% sterile methylcellulose, and 2 µg cyclohexamide and incubated at 34°C for 5 days. After 5 days, the overlay was aspirated and the monolayers gently rinsed as above. The monolayers were fixed in methanol for 30 minutes at 4°C, after which the methanol was removed and the wells rinsed as above. Wells were blocked using PBS with 1% BSA for 30 minutes at room temperature. Blocking buffer was then removed and the wells washed with 0.5% Tween-20 in PBS three times. Primary polyclonal rabbit anti-*O. tsutsugamushi* Karp strain antibody diluted 1:500 was added to each well and incubated at room temperature for 30 minutes. The primary antibody was removed and wells washed as above. Alexa 594-labeled goat anti-rabbit IgG (Invitrogen, Carlsbad CA) diluted 1:1,000 was added to each well, incubated for 30 minutes and then washed as above. Wells were examined using an inverted-fluorescent microscope. Wells containing 10-100 foci of cells infected with *Orientia* were counted, and the concentration of focus-forming units was calculated.

### **Quantitative oriential viability assay**

In order to quantitate the number of viable bacteria quickly, an *Orientia* viability assay was developed. Vero E6 cells in DMEM with 1% FBS and 1% HEPES were seeded onto 12-well plates and allowed to attach overnight at 37°C with 5% CO<sub>2</sub>. Once the cells were confluent, oriential stocks were diluted in serial 10-fold serial dilutions, and a 200 µL

aliquot was seeded onto the confluent monolayers in triplicate. The infected plates were centrifuged for 5 minutes at 700 x g to facilitate attachment and then incubated for two hours at 37°C with 5% CO<sub>2</sub>. After one hour, the wells were rinsed 3 times with warm DPBS with calcium and magnesium to remove any extracellular bacteria, i.e., non-viable bacteria. DNA was extracted from each well using a DNeasy Kit (Qiagen), and the bacterial load determined by real-time quantitative PCR (Jiang 2004).

## **Mice**

C57BL/6 (B6) or C57BL/6J and C3H/HeN (C3H) mice were purchased from Harlan Laboratories, Houston, TX or Jackson Laboratories, Bar Harbor, ME. Age- and gender-matched, 8-12 week old mice were used in all studies. Experimentally infected mice were housed in a biosafety level 3 facility, and all experiments and procedures were approved by the Animal Care and Use Committee of the University of Texas Medical Branch, Galveston.

## **Mouse strain comparison**

A multitude of mice strains have been shown to be susceptible to intraperitoneal inoculation of *O. tsutsugamushi* Karp strain including C57BL/6 and C3H/HeN mice, but very few data exist describing susceptibility via i.v. challenge. These mouse strains were compared for susceptibility to *Orientia* infection via intravenous challenge. To determine the infectivity of the cell culture stock, intraperitoneal (i.p.) inoculated animals were studied in parallel with i.v. inoculated animals to ensure viability. Animals were challenged with  $2.5 \times 10^6$ ,  $1.25 \times 10^6$ ,  $1.25 \times 10^5$ ,  $1.25 \times 10^4$ , and  $1.25 \times 10^3$  organisms and were

observed daily for signs of illness for 28 days post infection (dpi) or until animals became moribund.

### **Characterization of lethal and sublethal mouse models of *Orientia tsutsugamushi* infections**

*Orientia tsutsugamushi* Karp strain, passaged and maintained as described above was diluted in PBS, and the bacteria were injected i.v. through the tail vein or i.p. in a volume of 200  $\mu$ L. Control mice were inoculated with 200  $\mu$ L of similarly prepared material from uninfected cells or tissue diluted in PBS. Animals were challenged i.p. or i.v. with  $1.25 \times 10^6$ ,  $1.25 \times 10^5$ , or  $1.25 \times 10^4$  organisms. All infected and non-infected animals were monitored for signs of illness and body weight measured daily. Mice were necropsied at 3, 6, 9, and 12 dpi or when moribund for lethally challenged animals and 15 dpi for sublethal i.v. challenge. Four randomized i.p. and four i.v. inoculated animals were euthanized, and blood, brain, heart, kidney, liver, lung, lymph nodes, and spleen were collected for histopathology and blood, brain, liver, lung, and spleen for bacterial load determination. Mice were monitored daily for signs of illness until day 21.

### **Histopathology and immunohistochemistry**

All tissues were fixed in 10% neutral buffered formalin and embedded in paraffin. Tissue sections (5  $\mu$ m thickness) were stained with hematoxylin and eosin or processed for immunohistochemistry. Immunohistochemical staining was used to assess cellular distribution and intensity of *Orientia* infection in the organs of experimental animals. Sections were deparaffinized and rehydrated. The sections were placed on poly-L-lysine, silane-coated slides and incubated at 70°C for 20 minutes, then rehydrated in water and digested with antigen retrieval solution. Antigens were retrieved in citrate buffer (pH = 6)



at 98°C for 20 minutes followed by casein endogenous IgG blocking for 15 minutes. Endogenous alkaline phosphatase activity was quenched by incubation with Levamisole for 15 minutes and slides rinsed in deionized water. Nonspecific binding of antibody was blocked by incubating sections with normal goat serum and avidin blocking reagent (Vector Laboratories, Burlingame, CA) mixture (1:10) for 30 minutes. Sections then were incubated for 2 hours with polyclonal rabbit anti-*O. tsutsugamushi* Karp strain antibody (dilution: 1:500), followed by incubation for 30 minutes with biotinylated anti-rabbit IgG (1:2000, catalog number BA-1000, Vector Laboratories, Burlingame, CA). Signals were detected by the labeled streptavidin-biotin method with a UltraVision Alk-Phos kit (catalog number: TS-060-AP, Thermo Scientific, Waltham, MA). Vector Red Alkaline Phosphatase substrate (catalog number: SK-5100, Vector Laboratories, Burlingame, CA) was used as chromogen, and counterstaining was performed with hematoxylin. Reagent negative controls consisted of samples in which primary antibody was replaced with normal rabbit IgG. Sections were dehydrated and mounted in Permount. For identification of neutrophils (PMN) and myeloperoxidase (MPO), sections were incubated for 2 hours at room temperature with primary antibodies including rat monoclonal antibody to mouse neutrophil (clone 7/4, Caltag Laboratories) (1:25 dilution) and polyclonal rabbit anti-MPO (Abcam) (1:25 dilution). Biotinylated goat anti-rat or anti-rabbit secondary Ab (Vector Laboratories) (1:200) was applied to the sections for 30 minutes at room temperature, followed by AP-conjugated streptavidin (Vector Laboratories) (1:200).

### **Bacterial load determination**

Bacterial loads were assessed by quantitative real-time polymerase chain reaction (PCR) (Jiang 2004). DNA was extracted using a DNeasy Kit (Qiagen, Gaithersburg, MD) from the tissue samples, and the bacterial load at each time point and for each organ sampled was determined by quantitative real-time PCR (Jiang 2004). The 47 kDa gene was amplified using OtsuF630-5 -AACTGATTTTATTCAAATAATGCTGCT and OtsuR747-5 -TATGCCTGAGTAAGATACGTGAATGGAATT primers (IDT, Coralville, IA) and detected using probe OtsuPr665-5 -6FAM-TGGGTAGCTTTGGTGGACCGATGTTTAATCT-TAMRA (Applied Biosystems, Foster City, CA). Bacterial loads were normalized to total nanogram (ng) of DNA per  $\mu$ L for the same sample and expressed as the number of 47 kDa gene copies per picogram (pg) of DNA. Bacterial loads were normalized in this manner because an efficient plasmid for our mouse housekeeping gene was not available.

### **Blood cell counts**

At the time points that animals were euthanized, blood samples were collected in K<sub>2</sub>EDTA coated-BD microtainer tubes (Becton Dickinson, Franklin Lakes, NJ) and blood cell counts performed using a 950FS HemaVet™ apparatus (Drew Scientific Inc., Waterbury, CT) that differentiates cell types by size and granularity in a 20  $\mu$ L sample of whole blood.

## Transmission electron microscopy

Lung tissue from lethally infected animals was collected at 6 dpi and prepared for transmission electron microscopy. For ultrastructural analysis in ultrathin sections small pieces (~ 1 mm<sup>3</sup>) of tissues were fixed for at least 1 hour in a mixture of 2.5% formaldehyde prepared from paraformaldehyde powder, and 0.1% glutaraldehyde in 0.05 M cacodylate buffer, pH 7.3, to which 0.03% picric acid and 0.03% CaCl<sub>2</sub> were added. Then they were washed in 0.1 M cacodylate buffer and post-fixed in 1% OsO<sub>4</sub> in 0.1 M cacodylate buffer, pH 7.3, for 1 hour, washed with distilled water and *en bloc* stained with 2% aqueous uranyl acetate for 20 minutes at 60°C. The samples were dehydrated in ethanol, processed through propylene oxide and embedded in Poly/Bed 812 (Polysciences, Warrington, PA). Semi-thin sections 1 µm thick were cut and stained with toluidine blue. Ultrathin sections were cut on Leica EM UC7 ultramicrotome (Leica Microsystems, Buffalo Grove, IL), stained with lead citrate and examined in a Philips 201 transmission electron microscope at 60 kV.

## Serum chemokine/cytokine measurements

Serum was collected for cytokine/chemokine assays and tested for seroconversion, Quantibody array (**Table 3.1**) (Raybiotech, Norcross, GA) and enzyme-linked immunosorbent assay (ELISA), respectively, (<http://www.raybiotech.com/quantitative/quantibody datasheet.pdf>, Dasch GA 1979).

<b>Table 3.1. Selected secreted endothelial proteins and chemokines/cytokines.</b>				
<b>Endothelial secreted/surface proteins</b>		<b>Chemokine/Cytokine</b>		
sE-cadherin	sMadCAM-1	Fas ligand	IL-15	MCP-5
sE-selectin	sP-selectin	IFN-	IL-17	RANTES
sICAM-1	sVECAM-1	IL-10	IL-1	TNF-
sL-selectin		IL-12p40/p70	IL-2	VEGF

### **Quantitative reverse transcriptase PCR (qRT-PCR) analysis**

Total RNA was extracted from liver, lung, kidney and spleen tissues using RNeasy Mini kit (Qiagen) and digested with Rnase-Free Dnase set (Qiagen). cDNA was synthesized using the iScript™ cDNA synthesis kit (Bio-Rad, Hercules, CA). The abundance of target genes was measured by quantitative PCR (qPCR) using Bio-Rad CFX96 real-time PCR apparatus (Bio-Rad Laboratories, Hercules, CA), and SYBR Green Master Mix (Bio-Rad Laboratories) was used for all PCR reactions. The qRT-PCR conditions were, 95°C for 3 minutes, and 39 cycles of 95° C for 10 seconds, 60° C for 10 seconds and elongation step at 72° C for 10 seconds. Dissociation melting curves were obtained after each reaction to confirm the purity of PCR products. Relative abundance of mRNA expression was calculated using the 2<sup>-CT</sup> method. Glyceraldehyde-3-phosphate dehydrogenase (GAPDH) and  $\alpha$ -actin were used as the housekeeping genes. Primer sequences are listed in **Table 3.2**.

---

**Table 3.2. Primers of murine genes for real time PCR**

---

GAPDH	Forward 5'-TGGAAAGCTGTGGCGTGAT-3'	Reverse 5'-TGCTTCACCACCTTCTTGAT-3'
IFN-	Forward 5'-ATGAACGCTACACACTGCATC-3'	Reverse 5'-CCATCCTTTTGCCAGTTCCTC-3'
TNF-	Forward 5'-ATAGCTCCCAGAAAAGCAAGC-3'	Reverse 5'-TTGGTCCTTAGCCACTCCTTC-3'
IL-1	Forward 5'-GCAACTGTTCTCTGAACCTCAACT-3'	Reverse 5'-ATCTTTTGGGGTCCGTCAACT-3'
IL-4	Forward 5'-GGTCTCAACCCCCAGCTAGT-3'	Reverse 5'-GCCGATGATCTCTCTCAAGTGAT-3'
IL-5	Forward 5'-CTCTGTTGACAAGCAATGAGACG-3'	Reverse 5'-TCTTCAGTATGTCTAGCCCCTG-3'
IL-6	Forward 5'-TAGTCCTTCCTACCCCAATTTCC-3'	Reverse 5'-TTGGTCCTTAGCCACTCCTTC-3'
IL-10	Forward 5'-GCTCTTACTGACTGGCATGAG-3'	Reverse 5'-CGCAGCTCTAGGAGCATGTG-3'
IL-13	Forward 5'-CCTGGCTCTTGCTTGCCTT-3'	Reverse 5'-GGTCTTGTGTGATGTTGCTCA-3'
IL-33	Forward 5'-TCCAACCTCCAAGATTTCCCCG-3'	Reverse 5'-CATGCAGTAGACATGGCAGAA-3'
CXCL9	Forward 5'-GGAGTTCGAGGAACCCTAGTG-3'	Reverse 5'-GGGATTTGTAGTGGATCGTGC-3'
CXCL10	Forward 5'-CCAAGTGCTGCCGTCATTTTC-3'	Reverse 5'-GGCTCGCAGGGATGATTTCAA-3'
CXCL11	Forward 5'-GGCTTCCTTATGTTCAAACAGGG-3'	Reverse 5'-GCCGTTACTCGGGTAAATTACA-3'
ST2	Forward 5'-TGTATTTGACAGTTACGGAGGGC-3'	Reverse 5'-ACTTCAGACGATCTCTTGAGACA-3'
T-bet	Forward 5'-CCACTGGATGCGCCAGGAAGTT-3'	Reverse 5'-TTCACCTCCACGATGTGCAGCC-3'
ROR t	Forward 5'-TGTCCTGGGCTACCCTACTGA-3'	Reverse 5'-CACATTACACTGCTGGCTGC-3'
GATA3	Forward 5'-GGGGCCTCTGTCCGTTTACCCT-3'	Reverse 5'-GTCTGGGGAGACGTCTTTCGGC-3'
TGF-	Forward 5'-CACCGGAGAGCCCTGGATA-3'	Reverse 5'-TGTACAGCTGCCGCACACA-3'

---

## CHAPTER 4

### **Development of a hematogenously disseminated mouse model for scrub typhus.<sup>3</sup>**

**Specific aim 1:** *Develop and characterize a murine model of disseminated endothelial infection through intravenous inoculation of *O. tsutsugamushi*.*

**Hypothesis:** Inoculation of *Orientia* intravenously will result in a disseminated endothelial infection resulting in a valid murine model for severe scrub typhus.

**Rationale:** Animal model development is important for understanding disease progression and pathology. Models that are not similar to the human disease may provide misleading information about the disease of interest. In the case of scrub typhus, the historic mouse model presents with severe and lethal oriental peritonitis that has not been reported in human cases. That model utilizes an intraperitoneal route of inoculation that results in extensive infection of the mesothelial cells on the surface of the peritoneal organs. Development of a disseminated endothelial disease model for scrub typhus through i.v. administration will allow elucidation of the relevant immune mechanisms for this disease as demonstrated by three murine models of human spotted fever rickettsiosis previously published from our laboratory (Feng 1993; 1994, Walker 1994, 2000).

**Sub-aim 1: Characterize and compare the course and histopathology of the classic intraperitoneally inoculated and novel intravenous inoculation mouse models of scrub typhus.** Previous studies have demonstrated that the route of inoculation produces route-dependent histopathology, but without producing a consistent endothelial

---

<sup>3</sup> Parts of this chapter have been submitted for publication.

tropic infection with resulting pathology paralleling human disease. The working hypothesis of this aim is that intravenous inoculation will result in a model that demonstrates endothelial tropism and has histopathology that parallels human disease.

***Results:***

**Mouse strain comparison**

B6 and C3H mice were compared for susceptibility. To determine the infectivity of the cell culture stock, i.p. inoculated animals were studied in parallel with i.v. inoculated animals. Inoculation of  $10^3$  *Orientia* resulted in clinical illness in i.p. inoculated animals at 12-15 days post infection with only mild signs of illness in i.v.-inoculated animals. Histopathologic examination demonstrated systemic lesions most prominently in the lungs and liver of animals inoculated i.v. with this dose of *O. tsutsugamushi*. Lethal i.v. challenge was observed using  $2.5 \times 10^6$  and  $1.25 \times 10^6$  organisms with animals becoming moribund at 7-8 days post-inoculation (dpi) for C3H mice with both doses and at 9-11 dpi for B6 mice receiving  $2.5 \times 10^6$  organisms and 12-13 dpi for those animals that received  $1.25 \times 10^6$  organisms. Animals inoculated i.p. with the same doses expired at 7-8 dpi. Both C3H and B6 mouse strains developed similar illness with a fatal outcome with these doses inoculated i.p. I.p. and i.v. inoculation of  $10^3$ - $10^6$  *Orientia* was uniformly lethal for C3H/HeN mice with higher dose animals expiring earlier than lower dose animals. Further characterization of *Orientia* infection in C3H/HeN mice was not done. B6 mice were used exclusively thereafter as the abundance of knockout strains on a B6 background allows for extensive immunological studies and the longer course of disease more closely resembles scrub typhus in humans.

### Characterization of lethal i.v. and same dose i.p. *Orientia* infection in C57BL/6 mice

Mice challenged i.v. with  $1.25 \times 10^6$  bacteria all expired by 13 dpi (**Figure 4.1A**), approximately half of the animals inoculated i.v. with  $10^5$  *Orientia* expired between 13 and 15 dpi (data not shown), and 10% of mice challenged with  $10^4$  orientiae expired by 15 dpi (**Figure 4.1B**). Intraperitoneal inoculations of all doses were uniformly lethal (**Figure 4.1**).

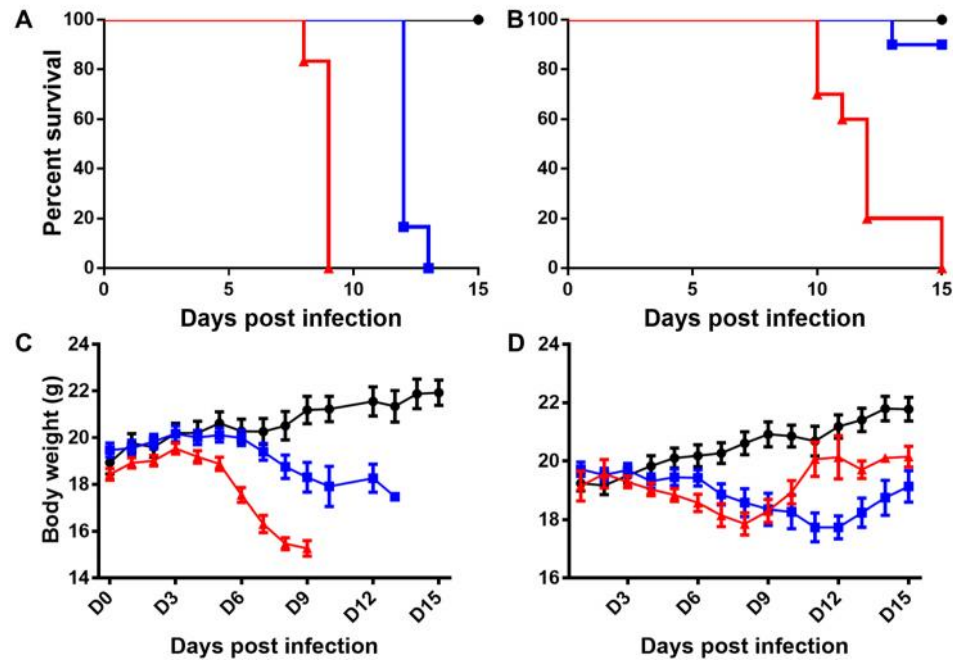


**Figure 4.1: Survival and body weight change of mice inoculated intraperitoneally or intravenously with *O. tsutsugamushi*.**

Animals inoculated intraperitoneally with  $1.25 \times 10^6$  organisms (**A and C- red triangles**) expired by 9 dpi and began losing weight at 4 dpi that continued until death. Intravenously inoculated animals expired by 13 dpi with weight loss starting at 7 dpi and continuing until death (**A and C- blue boxes**). Animals inoculated i.p. with  $1.25 \times 10^4$  organisms expired by 15 dpi losing weight until day 9 when most animals began to increase in body weight (**B and D- red triangles**). This late increase in body weight corresponded with an increase in peritoneal fluid accumulation. Animals inoculated i.v. with the same dose became ill at 6-7 dpi, but only 1 of 10 animals expired with all animals losing weight until 12 dpi when signs of illness began to abate and animals appeared to be recovering (**B and D- blue boxes**). Uninfected controls are represented as solid black circles in all panels.



*DISEASE PROGRESSION OF INTRAPERITONEALLY INOCULATED MICE:* On 3 dpi there were no signs of illness except mild abdominal swelling. Overall activity was unchanged, and there was no weight change (**Figure 4.1 C**). Mice manifested mesenteric lymphadenopathy and mild accumulation of fibrin-containing proteineaceous fluid in the peritoneal cavity causing the lobes of the liver to adhere to one another. Portions of the gastrointestinal tract were edematous and discolored. Neither histopathologic lesions nor *Orientia* antigen was detected on day 3 in mice inoculated i.p. At 6 dpi, mice inoculated i.p. had begun to lose weight (**Figure 4.1 C-red triangles**) with narrowed eyes, severely hunched posture, and swollen abdomen. The animals' activity was diminished compared to uninfected controls. *Orientia* antigen was detected in endothelial locations in the lungs of these animals, but with minimal cellular response. Of particular interest were the moderate accumulation of peritoneal exudate and the extensive distribution of oriental antigen in cells on the peritoneal surfaces of all abdominal organs and mild-to-severe mesothelial hyperplasia (**Figure 4.2 A and B**). All animals were moribund or had expired by day 9. Severe peritonitis was observed with accumulation of 2-4 mL of peritoneal exudate. *Orientia* antigen was detected in the lungs terminally in association with vasculitis and interstitial pneumonia. These findings indicate that *Orientia* had eventually disseminated from the peritoneal cavity, but the most striking findings at this time were the mesothelial hyperplasia and inflammation on the peritoneal surface of liver (**Figure 4.2 D**) and spleen (**Figure 4.2 E**) and the extensive *Orientia* infection of these cells. The mesothelial cells overlying the kidney capsule (**Figure 4.2 C**) were also infected.

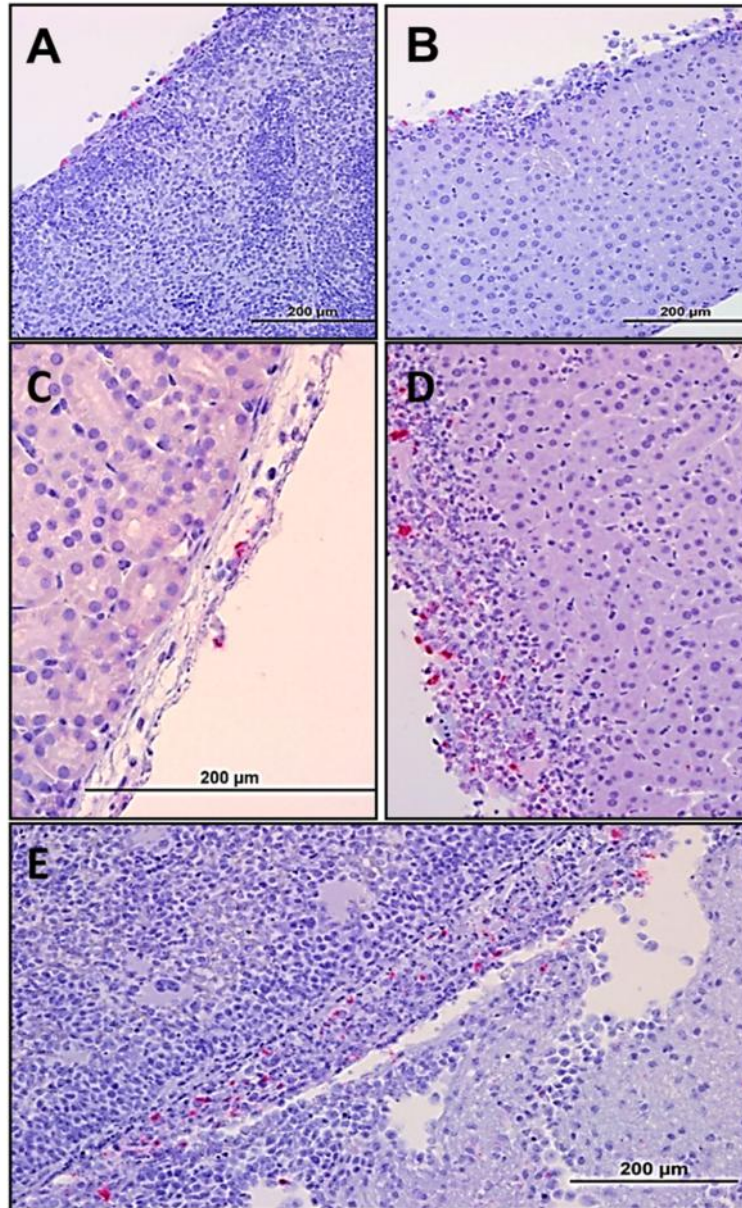


**Figure 4.2: Histopathology in mice following  $1.25 \times 10^6$  *Orientia* intraperitoneal challenge at days 6 and 9 pi.**

On 6 dpi *Orientia* antigen was detected on the surface of the peritoneal organs (A, B; 20x). The spleen at this time was slightly enlarged with no other gross pathology (A). The surface of the liver at this time revealed detectable *Orientia* antigen and mesothelial hyperplasia. By 9 dpi bacterial antigen was detected on the surface of the renal capsule (C-40x) and the hyperplastic inflamed surfaces of the liver (D-20x) and the spleen (E-20x).

*DISEASE PROGRESSION OF INTRAVENOUSLY INOCULATED MICE:* At necropsy 3 dpi, i.v. inoculated mice had generalized lymphadenopathy but no other gross lesions. The mice had perivascular lymphohistiocytic infiltrates in the meninges, and *Orientia* antigen was detected in the liver and lung with associated cellular infiltrates in both organs. The kidneys were unremarkable. At 6 dpi, the animals had a slight decrease in body weight (**Figure 4.1 C-blue boxes**) and generally appeared healthy although some animals exhibited decreased activity and slightly hunched posture. At this time, immunohistochemistry demonstrated that systemic infection was established with most of the *Orientia* observed in endothelial locations (**Figure 4.3**) as confirmed by electron microscopy of lung of i.v infected mice (**Figure 4.4**).

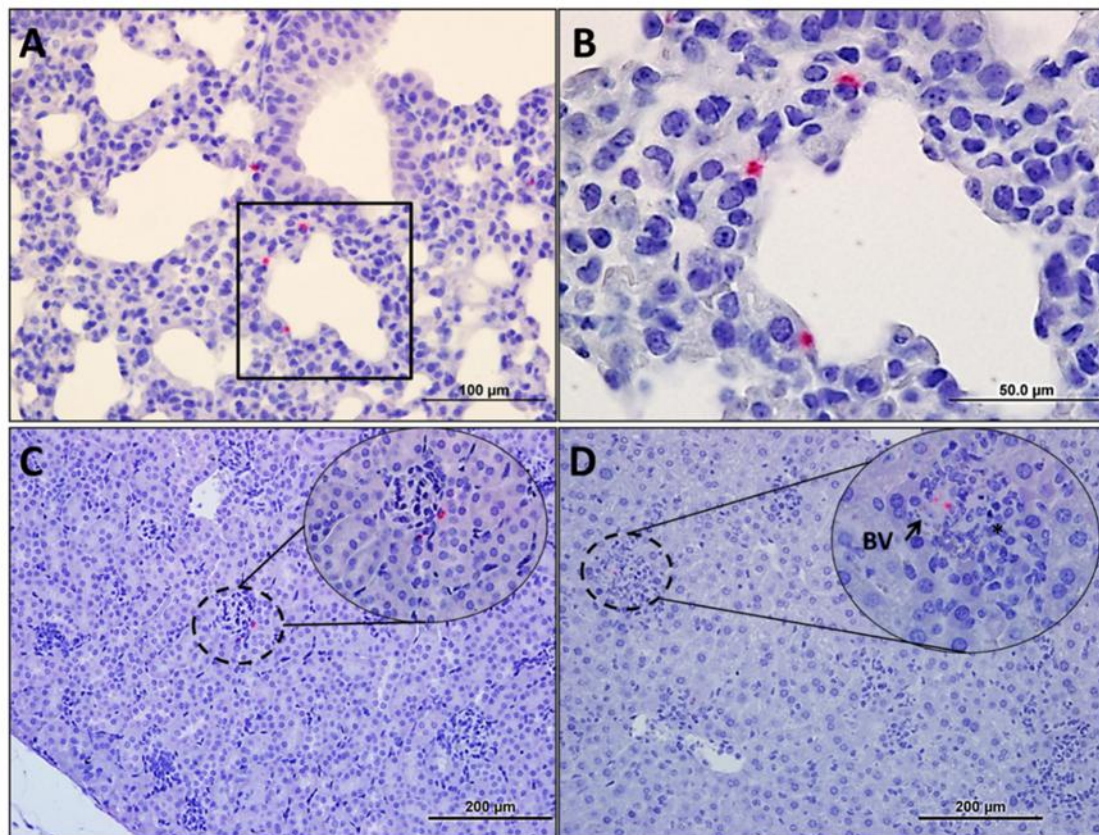




**Figure 4.3: Histopathology in mice following  $1.25 \times 10^6$  *Orientia* intravenous challenge at 6 dpi.**

All organs, except brain, had detectable *Orientia* antigen (**hashed circles and insets B-D**). *Orientia* antigen in the lung (**A- 40x**), (**B-100x**) was associated with vasculitis and interstitial pneumonia. Although antigen was detected in the kidney (**C-20x; inset-40x**) and spleen, no lesions were observed. Hepatic (**D-20x; inset-40x**) lesions increased in number and relative size and were often associated with blood vessels (**BV**). At this time, it was evident that systemic infection had been established with the majority of *Orientia* antigen present in endothelial locations.

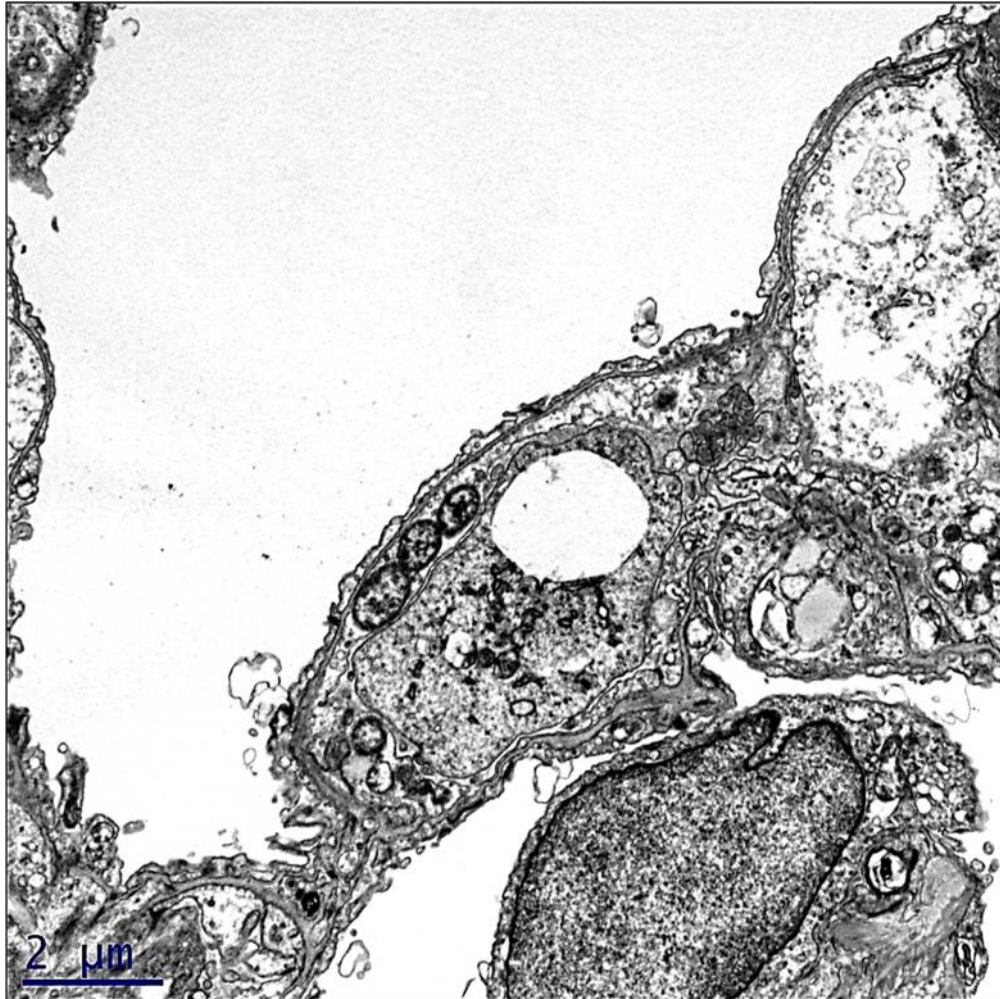


**Figure 4.4: Pulmonary endothelial infection by *Orientia*.**

Electron micrograph of mouse lung at 6 dpi, demonstrating alveolar septal endothelial infection by *Orientia*.

Cellular infiltration had become more evident at days 9 and 12 (**Figure 4.5**). Meningitis and cerebral perivascular infiltrates (**Figure 4.5 A-C**) were observed on both days, and focal cerebral hemorrhage was observed at 12 dpi (**Figure 4.5 D**). Cerebral microvascular endothelial cell infection was also evident (**Figure 4.5 E**). Pulmonary (**Figure 4.5 F, G**) vasculitis and interstitial pneumonia became more severe as the infection progressed. Hepatic (**Figure 4.5 H, I**) vasculitis became more pronounced, and multifocal mononuclear infiltrates were numerous. Cellular infiltrates between the tubules of the kidney (**Figure 4.5 J**) were evident at 9 days post inoculation with renal vasculitis observed at 12 days (**Figure 4.5 K**). The pathologic lesions of mice inoculated i.v. became progressively more severe through the course of infection with animals expiring on days 12-13 (**Figure 4.1 A**).

At this dose, the tissue bacterial loads of both i.p. and i.v. inoculated animals had similar kinetics in the lung throughout the course of disease (**Table 4.1**). The bacterial load in the lung of i.p. and i.v. inoculated mice increased until 9 dpi, the time of death for i.p. animals, but decreased at time of death for i.v. inoculated animals (12 dpi). This decrease in bacterial load coincided with an increased cellular infiltrate in the lungs of i.v. inoculated animals (**Figure 4.5 G**). Although i.p. inoculated animals had considerable numbers of bacteria detected in the lung with occasional staining on the pleura (**Table 4.1**), the cellular infiltration was minimal compared to i.v. inoculated animals. Interestingly, the liver of 6 and 9 dpi i.p. mice had very little antigen by IHC in the deep tissue, but considerable orientiae on the surface as did the spleen (**Figure 4.2**).



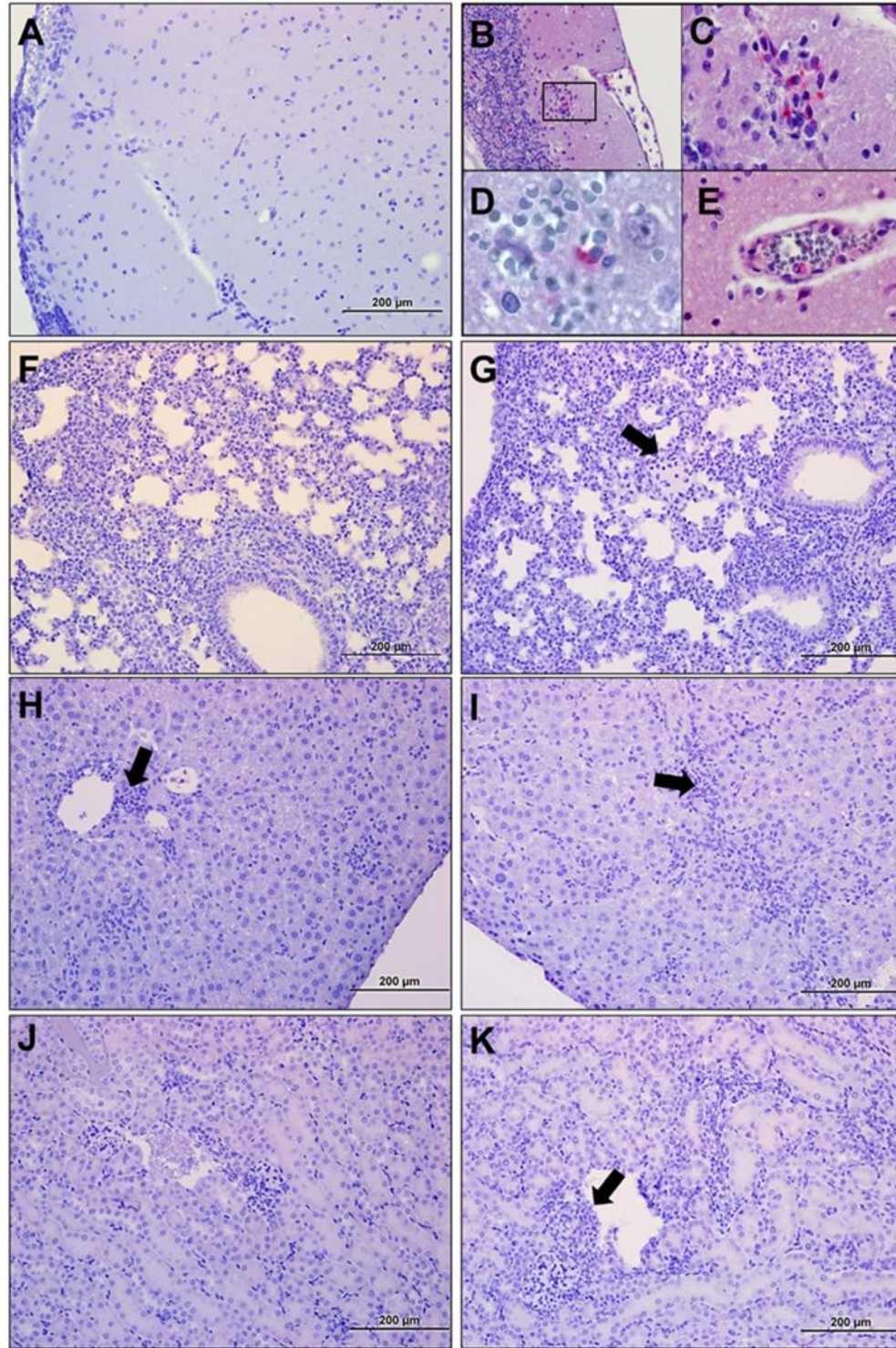


**Figure 4.5: Histopathology of mice following lethal *Orientia* intravenous challenge at days 9 and 12 pi.**

Immunohistochemical staining of orientiae in tissues from animals 9 and 12 dpi. At these times, oriential antigen was sparse, but cellular infiltrations were prominent. Meningoencephalitis (**A-20x**) was observed in the majority of animals on 9 dpi with cerebral and meningeal perivascular, lymphohistiocytic infiltrates (**B-inset; 40x, C-100x**); cerebral hemorrhage (**D-100x**) and endothelial infection (**E-100x**) occurred in moribund animals at 11 dpi. Because this is IHC staining without eosin, red blood cells appear gray in **D**. Pulmonary cellular infiltrates were marked on 9 dpi resulting in interstitial pneumonia (**F-20x**). At 12 dpi (**G-20x**), peribronchial and perivascular infiltration, interstitial pneumonia, and edema (**G-arrow**) were observed in all animals. Portal triaditis (**H-arrow; 20x**) was prominent at 9 dpi, and at 12 dpi perivascular cellular infiltrates were observed in the hepatic sinusoids (**I-arrow; 20x**). Mild perivascular infiltrates were observed in the kidney at 9 dpi (**J-20x**), and at 12 dpi (**K-arrow; 20x**) cellular infiltrates were observed throughout the kidney, particularly as peritubular infiltrates.

### **Circulating blood cell counts**

Both i.p and i.v. inoculated animals were compared to uninfected controls and published normal ranges for B6 mice. At 3 dpi mice all showed slightly elevated WBC counts, mainly neutrophils, compared to uninfected controls, but within the normal range. At day 6, both i.p. and i.v. inoculated animals manifested leukocytosis with lymphopenia, with i.v. inoculated animals having marginally greater elevation of WBC counts than i.p. inoculated animals. Intravenously inoculated animals had neutrophil concentrations three times greater than uninfected controls. At 9 days, i.v. inoculated animals had leukocytosis, mostly neutrophils but less than on day 6, as well as lymphopenia. Intraperitoneally inoculated animals had lymphopenia and neutrophilia that was less severe than that of i.v. inoculated animals. At 12 days, leukocytosis persisted with neutrophil concentrations being five times greater than uninfected controls. At this time, all i.p. inoculated animals had expired (9 dpi), and all i.v. inoculated animals were moribund.

**Table 4.1. Bacterial load (47 kDa gene copies/pg of DNA or  $\mu$ L of blood) kinetics of  $1.25 \times 10^6$  FFU-challenged C57BL/6 mice.**

	<b>3 dpi</b>		<b>6 dpi</b>	
	i.v. Mean (Range)	i.p. Mean (Range)	i.v. Mean (Range)	i.p. Mean (Range)
<b>Blood</b>	27 (ND <sup>a</sup> -61)	11 (ND <sup>a</sup> -16)	51 (10-110)	71 (51-88)
<b>Liver</b>	23,400 (1,290-70,000)	25,470 (2,720-56,800)	9,400 (2,600-21,300)	294,595 (1,270-702,000)
<b>Lung</b>	255 (12-823)	360 (40-604)	19,447 (925-14,500)	21,515 (1,130-56,500)
<b>Spleen</b>	60,043 (490-219,000)	74,839 (2,260-182,000)	18,925 (1,050-60,200)	12,907 (1,130-44,700)
	<b>9 dpi</b>		<b>12 dpi</b>	
	i.v.	i.p.	i.v.	i.p.
<b>Blood</b>	21 (6-35)	27 (ND <sup>a</sup> -48)	11 (8-23)	-
<b>Liver</b>	54,566 (942-216,000)	3,854 (168-13,900)	73 (3-197)	-
<b>Lung</b>	125,129 (437-45,4000)	267,811 (14,200-1,310,000)	17,323 (3,470-31,200)	-
<b>Spleen</b>	31 (11-63)	383,950 (25,800-706,000)	69,096 (185-236,00)	-

a, ND- not detected.



### **Characterization of the sublethal i.v. and same dose i.p. *Orientia* infection in C57BL/6 mice**

Disease progression of animals inoculated i.v. with  $1.25 \times 10^4$  organisms resulted in modified disease progression compared to lethally challenged animals with signs of illness typically 2-3 days later than in lethally infected animals (**Table 4.2**), with sublethally infected animals becoming lethargic and developing severely hunched posture at 12-13 days. With this dose, 10 % of animals were moribund at 13 days, with the remaining animals recovering between 15 and 21 days. Histopathologic observations at the various time points revealed that the lesions progressed similarly to those in the lethally infected animals, but with delayed appearance of hepatic lesions and mild pulmonary cellular infiltration and *Orientia* being observed in some but not all sections at 6 days and interstitial pneumonia developing between 9 and 12 days. On day 15, multifocal cellular infiltrates were observed in the lungs (**Figure 4.6**), kidneys, and liver. Similarly to i.v.-inoculated mice, animals inoculated i.p. with  $1.25 \times 10^4$  *Orientia* organisms had an incubation period two days longer before signs of illness, but, unlike the i.v.-inoculated animals, this dose was uniformly lethal by day 15 (**Figure 4.1B**). Severe peritonitis was observed with accumulation of peritoneal exudate in excess of 2 mL. *Orientia* antigen was detected focally in the lungs in association with vasculitis and interstitial pneumonia on day 15. At this time point, animals' body weights had increased, owing to the accumulation of exudate in the peritoneal cavity (**Figure 4.1 D**).

**Table 4.2. Summary of disease manifestations**

	<b>1.25E+06</b>		<b>1.25E+04</b>	
<b>Pathology/Route of Inoculation</b>	<b>IV</b>	<b>IP</b>	<b>IV</b>	<b>IP</b>
Survival	0/10	0/10	9/10	0/10
Onset of illness *	6 dpi	5 dpi	8 dpi	7 dpi
Day of death	10-13 dpi	8-9 dpi	13 dpi	10-15 dpi
Abdominal swelling	0/10	7**/10	3***/10	10**/10
Peritonitis	0/10	10 /10	0/10	10/10
Pleural effusion	7/10	0/10	10/10	3/10
Hepatomegaly	10/10	10 /10	10/10	10 /10
Splenomegaly	10/10	10 /10	10/10	10 /10
Peripheral lymphadenopathy	10/10	8/10	10/10	10/10
Mesenteric lymphadenopathy	2/10	10/10	5/10	10/10
<p>*, mice began exhibiting hunched posture, lethargy, ruffled fur, and rapid breathing. **, Animals had accumulation of turbid, peritoneal exudate. ***, Animals had accumulation of clear ascites fluid. , proteinaceous exudate was absent in three animals, but histopathology revealed mesothelial hyperplasia. , Hepatosplenomegaly was less severe than i.v. inoculated animals.</p>				

At this dose, the tissue bacterial loads of both i.p. and i.v. inoculated animals had more route-specific bacterial kinetics than at the higher dose (**Table 4.3**). The bacterial loads in the lung of i.p. and i.v. inoculated mice increased until 9 dpi, with the bacterial loads of i.v. animals being consistently higher throughout the time course. I.p. inoculated animals had greater bacterial loads in the liver and spleen throughout most of the time course with i.v. inoculated animals having a higher splenic bacterial load at 15 dpi (**Table 4.3**). At this challenge dose, i.v. and i.p. inoculated animals had detectable bacterial loads in liver, lung, and spleen throughout the disease course (**Table 4.3**), but *Orientia* in the blood was not detected consistently until 6 dpi for i.v. inoculated animals and 9 dpi for i.p. inoculated animals.

**Table 4.3 Bacterial load (47 kDa gene copies/pg of DNA or  $\mu$ L of blood) kinetics of  $1.25 \times 10^4$  FFU-challenged C57BL/6 mice.**

	<b>3 dpi</b>		<b>6 dpi</b>	
	i.v. Mean (Range)	i.p. Mean (Range)	i.v. Mean (Range)	i.p. Mean (Range)
<b>Blood</b>	3 (ND <sup>a</sup> -4)	ND <sup>a</sup>	92 (ND <sup>a</sup> -170)	6 (ND <sup>a</sup> -11)
<b>Liver</b>	32 (4-67)	28 (ND <sup>a</sup> -47)	558 (61-1,380)	2,934 (80-6,530)
<b>Lung</b>	18,140 (4,120-48,700)	671 (ND <sup>a</sup> -2,100)	446,975 (18,100-1,220,000)	46,005 (1,610-115,000)
<b>Spleen</b>	1,466 (199-3,470)	16,275 (ND <sup>a</sup> -24,000)	9,875 (1,400-27,500)	26,375 (9,400-41,400)
	<b>9 dpi</b>		<b>12 dpi</b>	
	i.v.	i.p.	i.v.	i.p.
<b>Blood</b>	408 (ND <sup>a</sup> -779)	15 (5-23)	13 (ND <sup>a</sup> -43)	88 (12-158)
<b>Liver</b>	1,501 (124-2,860)	14,400 (421-46,200)	70 (18-190)	1,716 (334-3,590)
<b>Lung</b>	525,625 (28,500-1,020,000)	133,425 (21,400-275,000)	24,215 (4,380-64,600)	97,593 (2,290-340,000)
<b>Spleen</b>	7,100 (4,360-11,300)	66,008 (5,530-165,000)	2,601 (422-5,770)	38,720 (3,680-66,900)
	<b>15 dpi</b>			
	i.v.	i.p.*		
<b>Blood</b>	ND <sup>a</sup>	ND <sup>a</sup>		
<b>Liver</b>	92 (ND <sup>a</sup> -348)	4 (3.48-3.53)		
<b>Lung</b>	5,398 (141-18,000)	846 (561-1,130)		
<b>Spleen</b>	8,149 (107-30,300)	169 (109-228)		

a, ND- not detected. \*, only two animals remained.

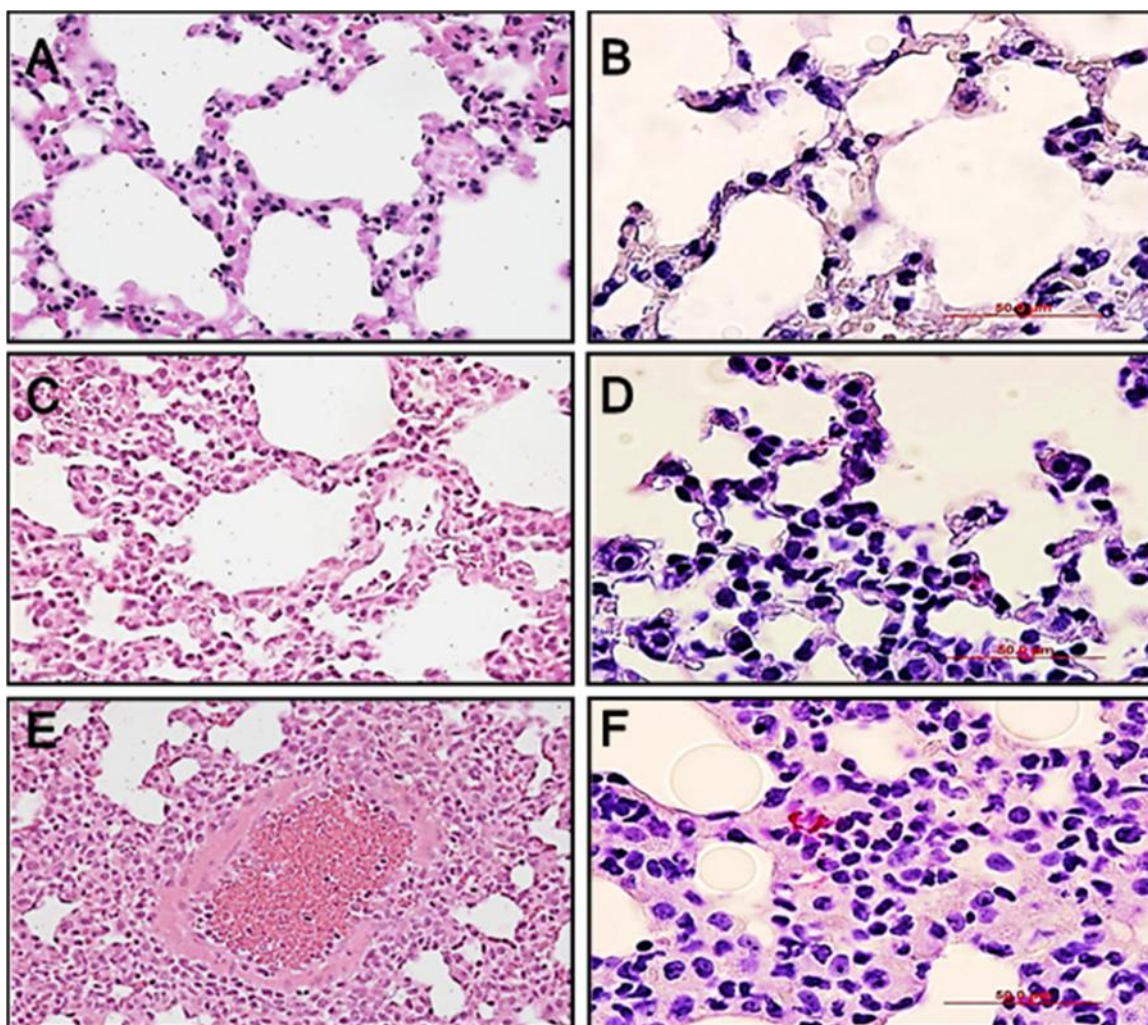


**Figure 4.6: Histopathology of the lung following  $1.25 \times 10^4$  *Orientia* challenge.**

H & E stained uninfected lung tissue (A-20x) and IHC of uninfected lung (B-40x) compared with lung from i.p. inoculated mice 12 dpi (C-20x, D-40x), and lung from i.v. inoculated 15 dpi (E-20x, F-40x). All i.p. infections were lethal with less severe pulmonary cellular infiltrates when compared to that of i.v. infected mice with capillary endothelial cell infection of the alveolar septa. Panels D and E demonstrate *O. tsutsugamushi* by IHC.

## Discussion

Human scrub typhus has been described as one of most severely neglected tropical diseases, but has potentially more fatal cases annually than dengue (Paris 2013). It was first described in China in 84 B.C. and made its presence felt during the wars that took place in the region during the last century.

The lack of an appropriate animal model for scrub typhus has been a major impediment to increasing the understanding of scrub typhus pathogenesis and immunity. The i.v. inoculation of *O. tsutsugamushi* Karp strain resulted in a hematogenously disseminated scrub typhus model that reliably resulted in pathology and target cell tropism similar to scrub typhus in humans. Similar to other members of the Rickettsiaceae family, *Orientia* predominantly infects endothelial cells after dissemination from the site of mite feeding (Moron 2001). The intravenously infected animals developed disseminated endothelial infection as occurs in human scrub typhus, unlike the intraperitoneal model that resulted in the infection of mainly mesothelial cells and macrophages of the peritoneum.

The pathology of scrub typhus is characterized by multifocal cellular infiltrates around the blood vessels of all organs, particularly the brain, lungs, and liver. The central nervous system (CNS) is frequently involved in scrub typhus infection. Headache, nausea, vomiting, transient hearing loss, confusion, neck stiffness, delirium, and mental changes may be observed, and in severe cases convulsions and coma may occur (Ben RJ 1999). Glial nodules consisting of perivascular infiltration by lymphocytes and macrophages as well as hemorrhage were observed in our lethal model that strongly resemble the lesions and cell tropism described by Allen and Spitz (1945) and Moron *et al.* (2001), respectively (**Figure 4.5 C**).

Respiratory involvement is common in severe scrub typhus infections. Approximately 40% of scrub typhus patients manifest cough at the time of admission (Wang 2007). Interstitial pneumonia, pulmonary edema, pleural effusions, cardiomegaly, and/or focal atelectasis are observed by chest radiography in those patients (Song 2004, Jeong 2007). The presence of respiratory symptoms is closely associated with severity of

scrub typhus (Lee 2008). Pulmonary pathology observed in humans comprises interstitial pneumonia with mononuclear cell infiltrates (Hsu 2008, Moron 2001, Allen and Spitz 1945). The intravenously infected animals developed similar lesions (**Figure 4.5 F, G**).

Hepatomegaly and modest elevations of aminotransferases have been documented and may be associated with the liver pathology observed in fatal scrub typhus (Tsay 1998, Moron 2001, Allen and Spitz 1945) (**Figure 4.5 H, I**). Severe scrub typhus frequently results in acute renal failure (Yen 2003). Cellular infiltrates around the microvasculature of the kidney, particularly between the tubules, were observed by Allen and Spitz (1945) and were prominent during the later time points in infected mice (**Figure 4.5 J, K**).

Intravenous inoculation of  $1.25 \times 10^4$  *Orientia* resulted in a delayed onset with signs being observed ~2 days later than in lethally challenged mice. Development of lesions in the liver were first observed at 6 dpi in sublethally infected mice compared to 3 dpi in lethally challenged animals. Cellular infiltrates in the other tissues were also delayed by 3 days when compared to lethally challenged mice. This delay in cellular immune response may explain why animals that have similar pathology and signs have dose dependent mortality. Bacterial distribution was similar in both routes of infection, indicating the resulting pathology was dependent on the route of inoculation rather than the doses given. Further characterization of the immune response to scrub typhus is needed to elucidate this fully.

The model characterized in this study closely parallels the disease pathology described for lethal scrub typhus in humans. Intravenous inoculation of  $1.25 \times 10^6$  *Orientia* resulted in an acute infection that culminated in death on 12-13 dpi. Pathological progression was observed in animals euthanized at selected time points. These changes

will be useful for pinpointing the factors that result in the disease manifestations as well as provide a powerful tool to study the immunology of scrub typhus infection.

**Sub-aim 2: Characterize the cytokine response during lethal scrub typhus using a hematogenously disseminated murine model of disease.** The cytokine response during scrub typhus has been studied only in a piecemeal fashion using various cell models and acute patient sera samples. The working hypothesis of this sub-aim is that the cytokines observed would strongly recruit neutrophils to the site of infection leading to the pathology observed in our intravenously inoculated mouse model.

Using the serum collected at necropsy during the characterization of the histopathology of the i.v. model, I screened the lethally challenged animals for cellular activation markers and cytokines listed in **Table 3.1** of **Chapter 3** with the Quantibody Custom array (Raybiotech, Norcross, GA). As expected, the serum cytokine levels had a pro-inflammatory pattern with IL-12 p40/p70, tumor necrosis factor- $\alpha$  (TNF- $\alpha$ ), and interferon- $\gamma$  (IFN- $\gamma$ ) having at least a 2-fold increase greater than uninfected animals (**Figure 4.7**). The most strongly up-regulated analyte observed in the serum was Fas ligand, which had a 100-fold increase at 9 dpi and the time of death (**Figure 4.7**). Although not strongly up-regulated (0.5 fold increase), lungkine (chemokine [C-X-C motif] ligand 15 [CXCL-15], which is a potent neutrophil-recruiting cytokine, was present at every sampling point after 6 dpi, which correlates with the increase in circulating neutrophils described earlier.

Many cellular markers are shed when cells are activated or infected. In the preliminary analysis fluctuations were observed in endothelial markers in the serum, namely sE-selectin (**Figure 4.8**), which paralleled the bacterial burden observed in the lung at the same



time points (**Table 4.1**). sP-selectin was consistently up-regulated throughout the course of infection. Soluble vascular cellular adhesion molecule (sVCAM) concentration was increased at 6 dpi, but returned to near normal levels at the later time points. Soluble mucosal vascular addressin cell adhesion molecule 1 (sMadCAM) concentration increased at the later time points indicating an increased activation of the endothelium, which results in increased recruitment of inflammatory cells to sites of infection. Soluble CAMs (sCAM) are also observed in human scrub typhus infection (Paris 2008).

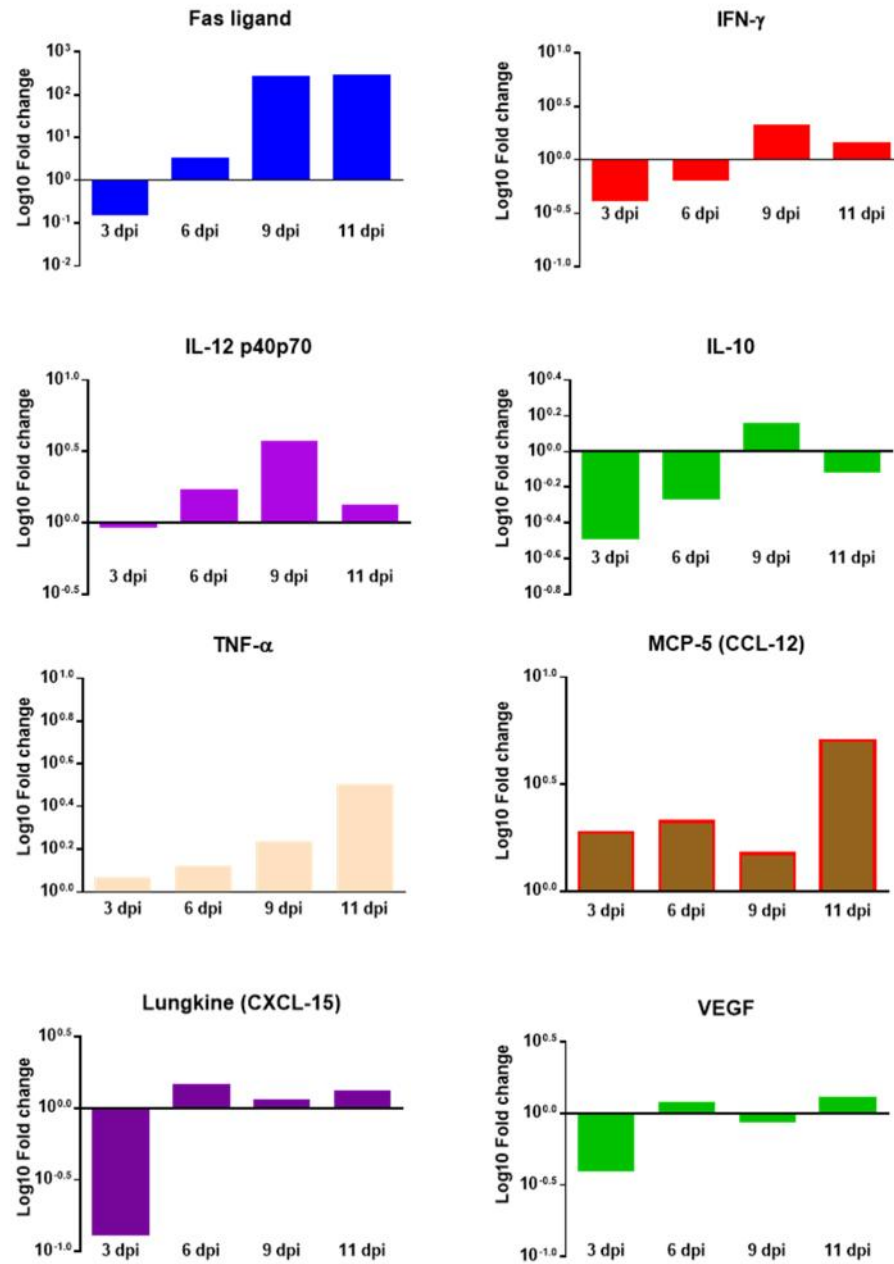


**Figure 4.7: Serum cytokine levels during lethal *Orientia* infection.**

Preliminary analysis using an immunofluorescent Quantibody Custom array revealed circulating pro-inflammatory cytokines throughout the course of infection. Values are represented as fold-change compared to non-infected controls.

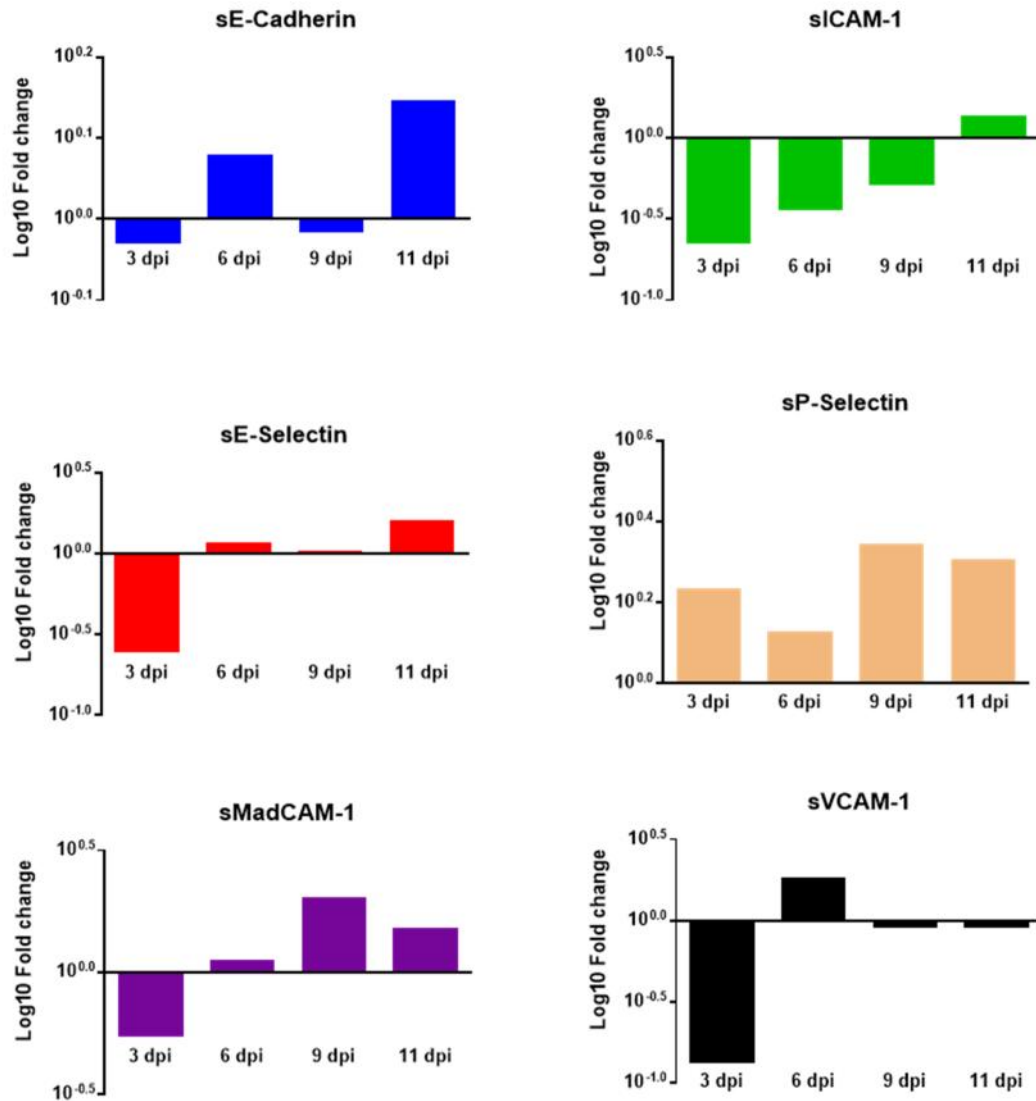


**FIGURE 4.8: Soluble cellular adhesion molecules in serum during lethal *Orientia* infection.**

Preliminary analysis using an immunofluorescent Quantibody Custom array revealed various soluble adhesion molecules in the serum. The presence of these molecules in the serum indicates the activation of endothelial cells.

*Sub-aim 2 experimental design:* In order to further evaluate the inflammatory kinetics during lethal *Orientia* infection, an experiment was designed evaluate to the cytokine profile at early (2 dpi), mid- (6 dpi), and late (10 dpi) intervals in the infection in the serum and tissues. Female 8-12 week old C57/BL6J mice (Jackson Laboratories, Bar Harbor, ME) were sacrificed at 2, 6, and 10 dpi (**Figure 4.9**), and kidney, liver, lung, and spleen were collected in RNA Later™, in order to measure cytokine expression at the mRNA level. An additional portion of tissue was collected for extraction of DNA for bacterial load determination, as described in **Chapter 3**. Remaining tissue was fixed in 10% buffered formalin for IHC staining. Animals were monitored daily for signs of illness, and body weights were measured to quantify disease progression.

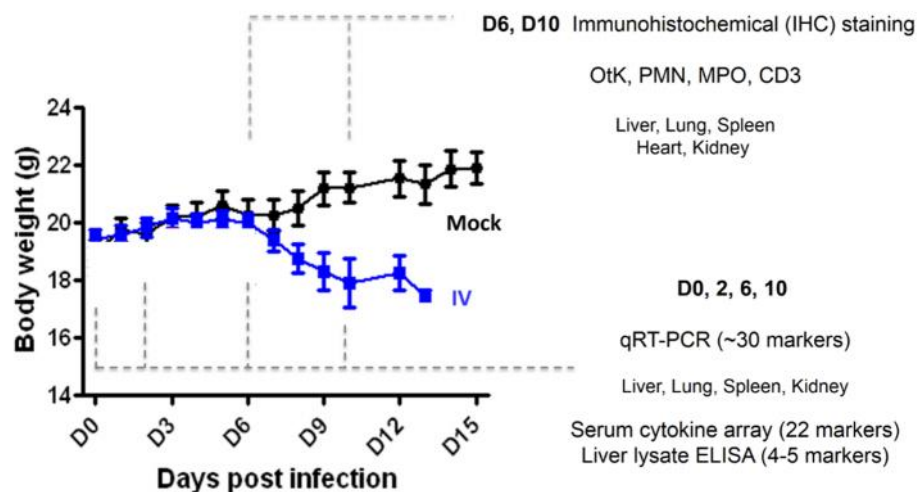


**Figure 4.9: Experimental design for cytokine analysis.**

## Results-Sub-aim 2

*DISEASE PROGRESSION:* Animals began to lose weight 6 dpi and continued to lose weight until the end of the experiment. At 2 dpi, there was no observed pathology and animals appeared normal. At 6 dpi, animals began to show signs of illness, namely hunched posture and mildly ruffled fur. Spleens were enlarged as described previously and oriental antigen was observed in liver and lung (**Figure 4.10**). Oriental staining was focal at 6 dpi and became more extensive by 10 dpi (**Figure 4.10**). Signs of illness and weight loss continued to worsen with the animals being moribund 10 dpi.

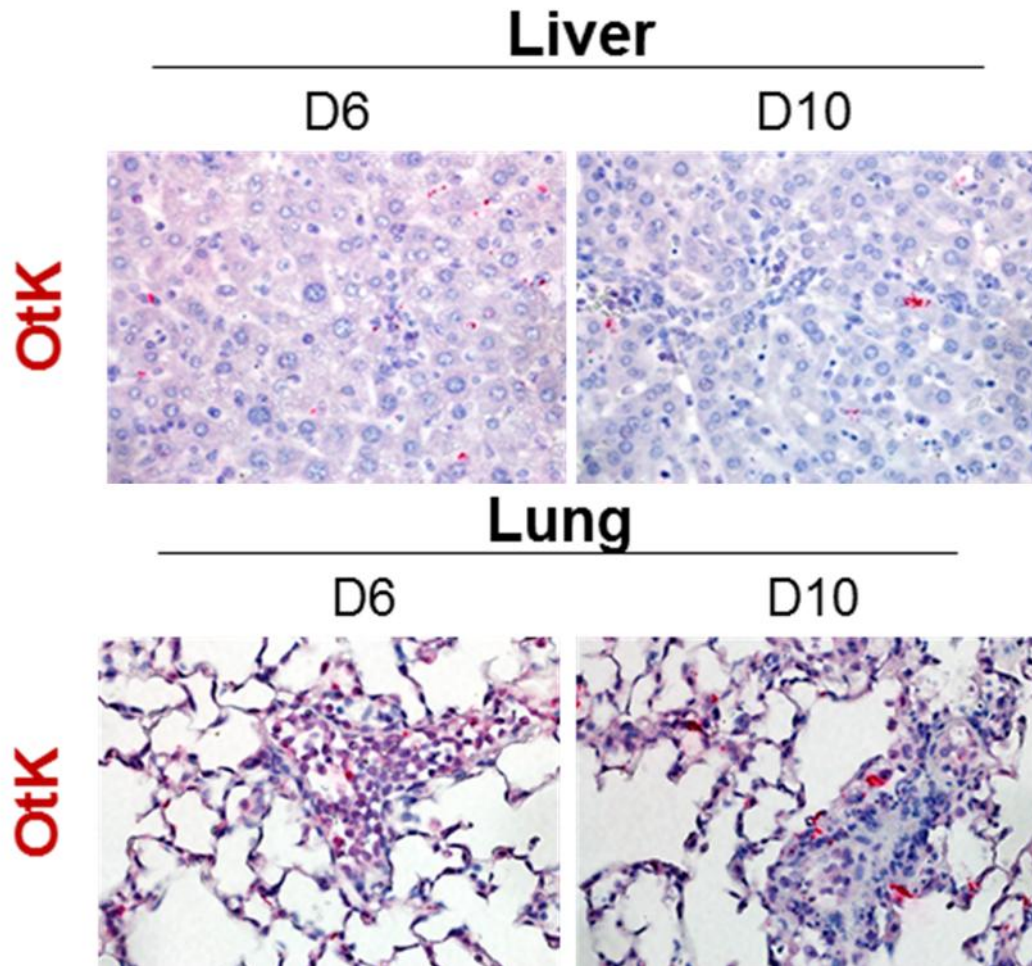


**Figure 4.10: IHC staining of liver and lung from mice lethally challenged with *Orientia*.**

Oriental antigen was detected in the liver and lung 6 dpi and 10 dpi (top panels 20x, bottom panels 40x).

*CYTOKINE EXPRESSION DURING ORIENTIA INFECTION:* mRNA concentrations of cytokines in specific tissues were normalized to housekeeping genes resulting in the relative mRNA expression reported here and statistically compared to naïve animals' tissue expression.

At 2 dpi, the kidney was relatively normal as compared to the liver, lung, and spleen (data not shown). Liver and lung had a significant or moderate increases in IL-1 and all three tissues had an increased level of expression of IFN- indicating a pro-inflammatory environment was being established (**Figure 4.11**). In the liver, IL-10 was also strongly up-regulated as compared to the uninfected animals. Also at this time IL-6, that plays both pro- and anti-inflammatory functions, was up-regulated in the liver. The lung shared a similar pattern of expression but not as robust as in the liver. The spleen at 2 dpi was not significantly different than the uninfected animals except for IFN- . There also was no significant difference in upstream promoters of Th-2, Th-1, or T-regulatory pathways such as transcription factors, GATA-binding protein (GATA-3), retinoic acid receptor-related orphan receptor- t (ROR- t), or Th-1 cell-associated transcription factor (T-bet).

The tissue specific cytokine profiles were dramatically different at 6 dpi (**Figures 4.12 and 4.13**). Pro-inflammatory cytokines were significantly up-regulated in the liver and lung (**Figure 4.14**). This pro-inflammatory response coincided with the onset of disease in these animals and the observation of lesions in the tissues.

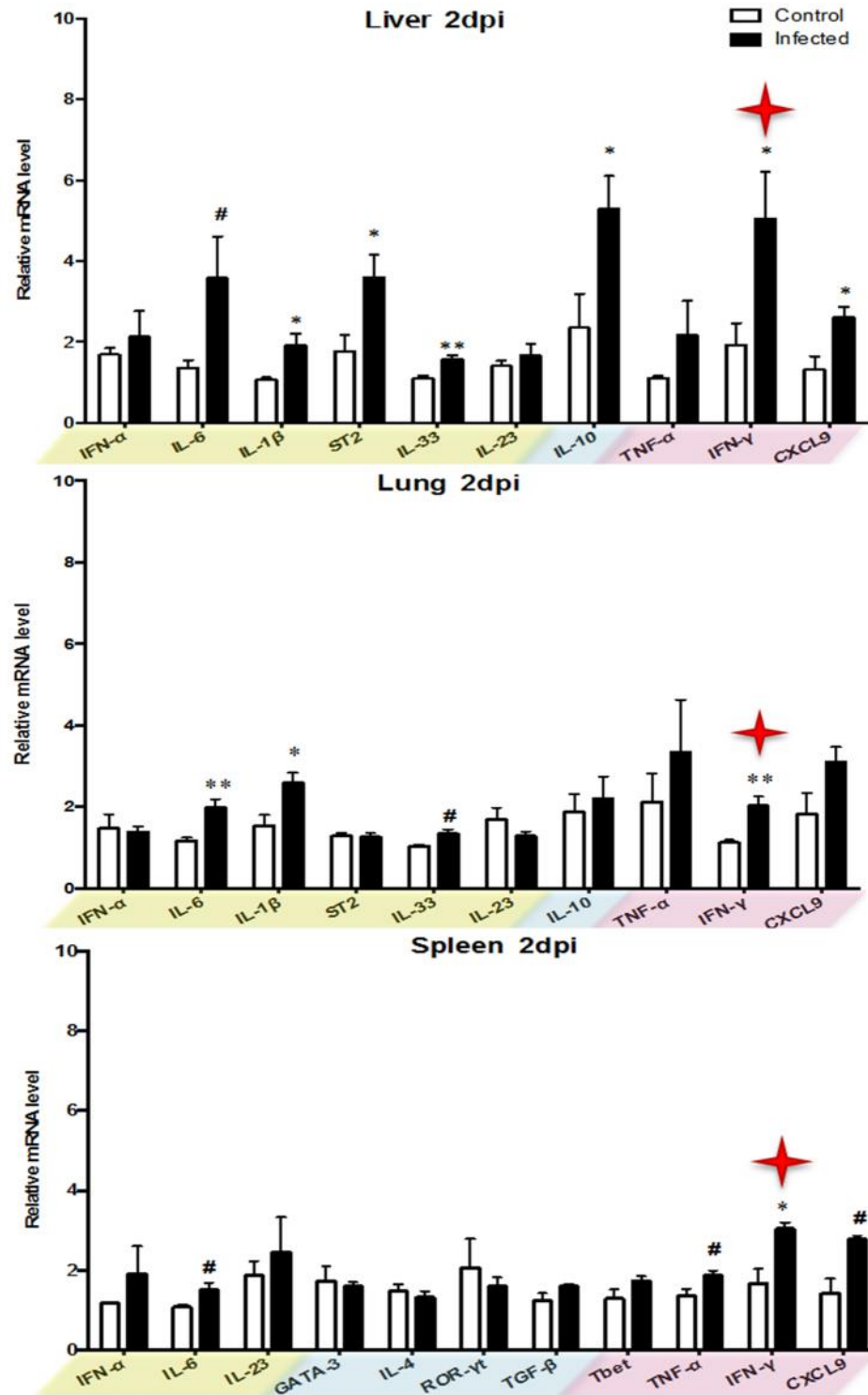


**Figure 4.11: Relative mRNA levels of selected cytokines and chemokines at 2 dpi with *Orientia*.**

Cytokine and chemokines are divided into pro-inflammatory Th-1 signature (pink), immune modulatory (blue), and those that have anti-inflammatory functions (olive). A red star indicates strongly significant up-regulation of IFN- $\gamma$ . (\* indicates  $p < 0.05$ ; \*\*  $p < 0.01$ , #  $p < 0.1$ )

In the liver, the receptor of IL-33, ST-2, was significantly up-regulated, but IL-33 was not. Significant up-regulation of IL-6 and IL-10 were also observed (**Figure 4.12**). The lung at this time point also exhibited a strong Th-1 signature as demonstrated by the high levels of TNF- $\alpha$ , IFN- $\gamma$ , and CXCL-9 as well as a pro-inflammatory profile. The lung exhibited down-regulated immune modulatory cytokines IL-33 and IL-13, but had a significant level of IL-10 expression (**Figure 4.12**).

At 6 dpi, the kidney profile changed dramatically when compared to 2 dpi. Aside from the modest up-regulation of TGF- $\beta$ , cytokine expression demonstrated a pro-inflammatory Th-1 signature (**Figure 4.13**). The spleen continued to have significant expression of Th-1 cytokines, but also had significant down-regulation of Th-2 and T regulatory transcription factors GATA-3 and ROR- $\gamma$  t (**Figure 4.13**). At this time, I also observed a down-regulation of IL-4 and IL-13, further supporting the pro-inflammatory Th-1 signature.

The cytokine profile at 10 dpi was very similar to the expression levels seen at 6 dpi for the respective tissues (**Figure 4.14 A-D**). Basically, a pro-inflammatory environment was established with a corresponding down-regulation of immune modulatory cytokines.

To confirm that the mRNA expression resulted in protein production, ELISAs for IL-6, IL-10, IFN- $\gamma$ , and TNF- $\alpha$  were performed on liver tissue homogenate and cell-free supernatants. This assay demonstrated that the protein expression and mRNA were similar except in the case of IL-10 where the mRNA levels were significantly up-regulated in the liver, but the actual cytokine was not significantly different than uninfected controls (**Figure 4.15**).



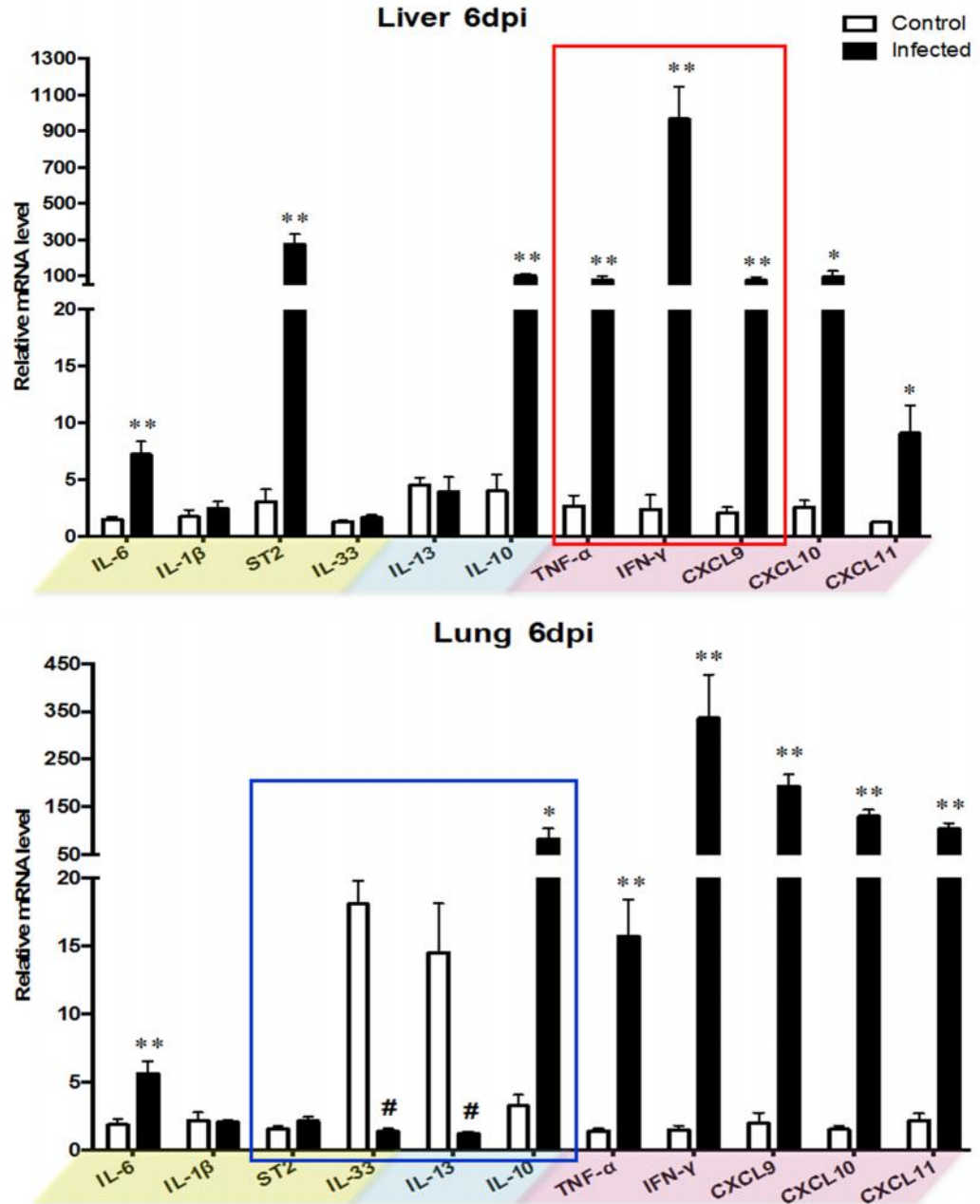


**Figure 4.12: Relative mRNA levels of selected cytokines and chemokines in the liver and lung at 6 dpi with *Orientia*.**

Cytokines and chemokines are divided into pro-inflammatory Th-1 signature (pink), immune modulatory (blue), and those that have anti-inflammatory functions (olive). At 6 dpi, the tissues investigated began to have distinct profiles. The liver at this time had a predominantly pro-inflammatory profile (red box) while the lung shared this profile, and down regulation of anti-inflammatory IL-13 and Th-2 promoting IL-33 was considerable (blue box). (\* indicates  $p < 0.05$ ; \*\*  $p < 0.01$ , #  $p < 0.1$ )

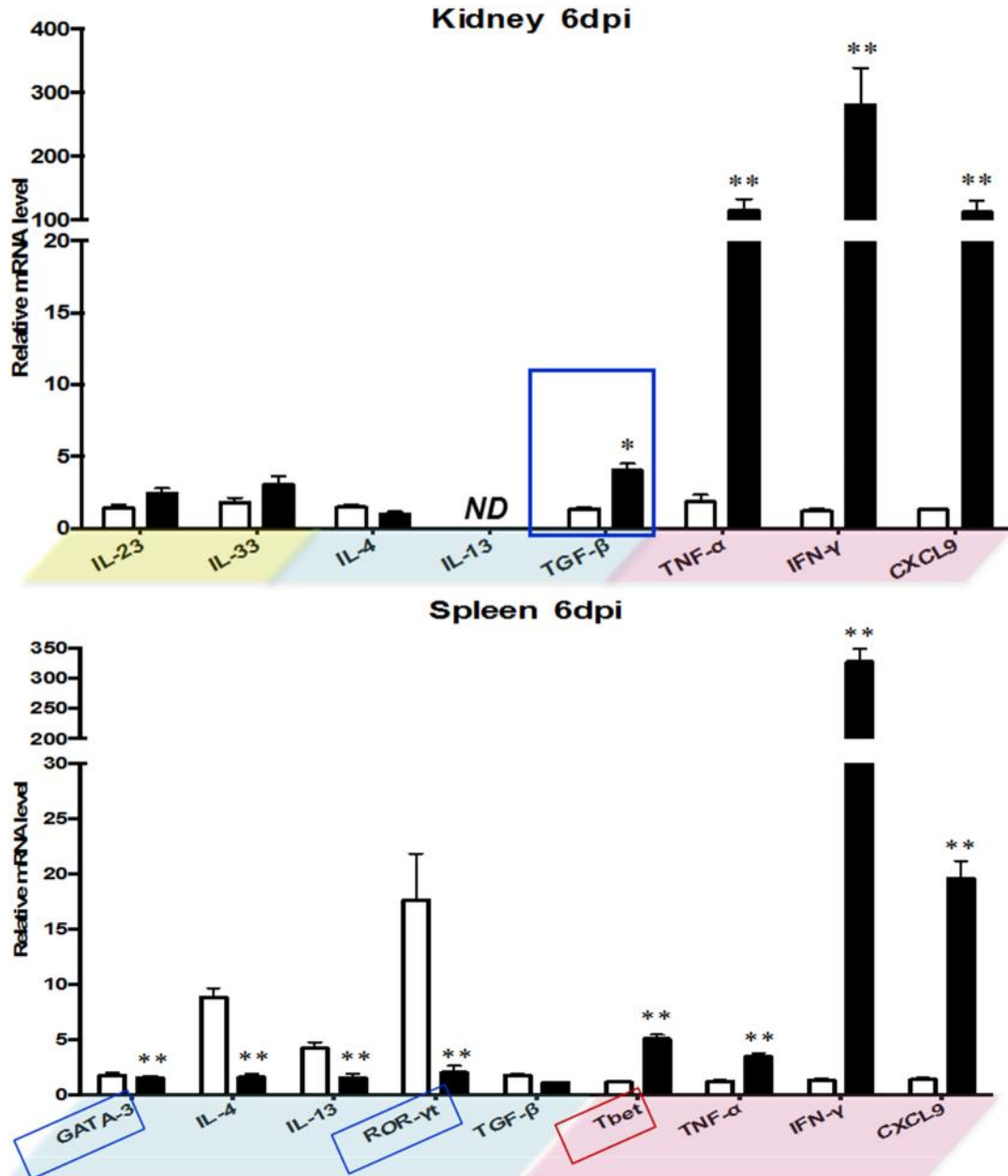


**Figure 4.13: Relative mRNA levels of selected cytokines and chemokines in the kidney and spleen at 6 dpi with *Orientia*.**

Cytokines and chemokines are divided into pro-inflammatory Th-1 signature (pink), immune modulatory (blue), and those that have anti-inflammatory functions (olive). At 6 dpi, the tissues investigated began to have distinct profiles. The kidney had a pro-inflammatory profile with the exception of the potent anti-inflammatory TGF-β (blue box) that was significantly up-regulated. The spleen also had a pro-inflammatory profile as well as the down-regulation of GATA-3 and ROR-γt (blue boxes). (\* indicates  $p < 0.05$ ; \*\*  $p < 0.01$ , #  $p < 0.1$ )

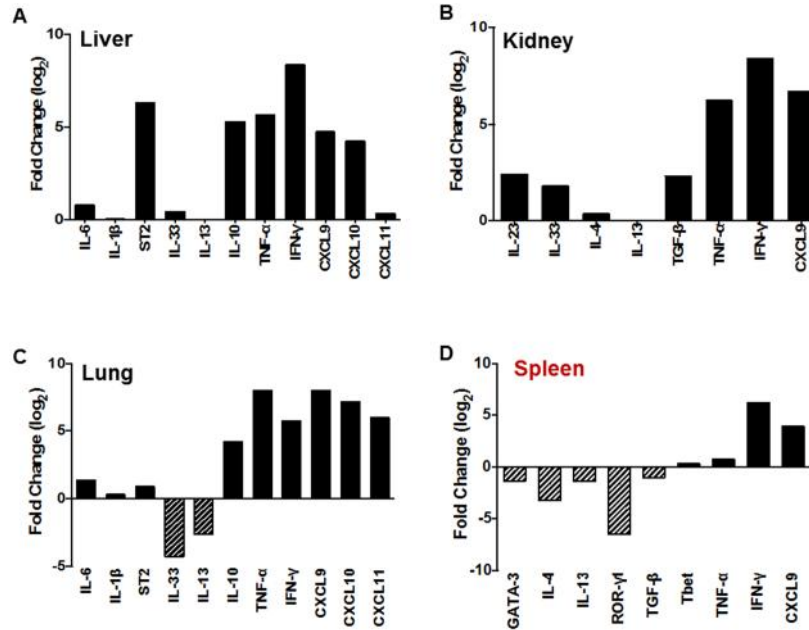


**Figure 4.14: Distinct repression of type 2 responses and activation of type 1 responses at 10 dpi with *Orientia*.**

qRT-PCR analyses were performed for the expression of ~30 markers. Data were analyzed and normalized to housekeeping genes. Data are presented as the “fold change (log<sub>2</sub>)” in comparison to the levels of corresponding controls.

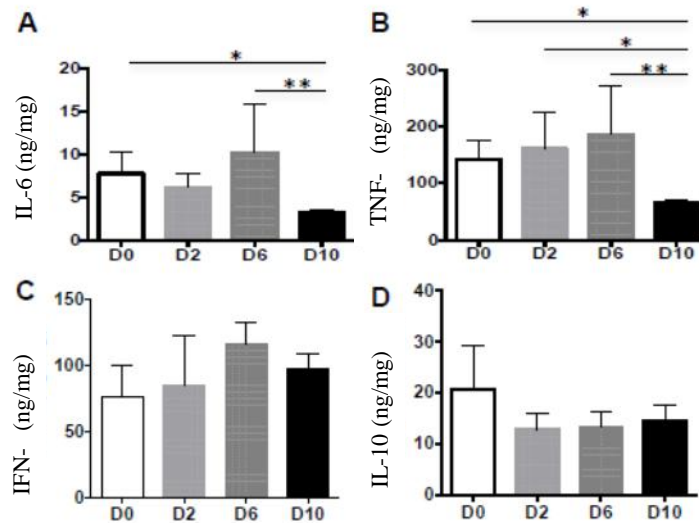


**Figure 4.15: Liver cytokine levels during *Orientia* infection.**

Liver tissue homogenate and cell-free supernatants were prepared, and total protein concentrations were determined by ELISA assay. \*  $p < 0.05$ ; \*\*  $p < 0.01$ .

*SERUM CYTOKINE AND CHEMOKINE LEVELS:* Serum levels were measured using Quantibody Cytokine 1 array (Raybiotech, Norcross, GA). As the serum samples were pooled for this analysis, statistical comparisons could not be done, but direct comparisons can be made. The serum cytokine levels were divided into low, intermediate, and high relative intensity to make it easier to see the trends of all cytokines measured (**Figure 4.16 A-C**). IL-4, a prominent driver of Th-2 differentiation, was high at 2 and 6 dpi, but steadily decreased until 10 dpi when it was lower than in uninfected animals. IL-13, another promoter of the Th-2 response, was also up-regulated at 2 dpi, but not during the rest of the time points. VEGF and TNF- were modestly up-regulated in the serum throughout the course of infection. Interestingly, IL-10 levels in the serum were not elevated and appeared to decrease over the course of infection (**Figure 4.16 A blue box**).

The intermediate intensity serum cytokines were highly elevated and predominantly pro-inflammatory (**Figure 4.16 B red boxes**). As with the mRNA levels, on 6 dpi serum cytokines were increased with many of these proteins remaining so through 10 dpi. The presence of granulocyte-colony stimulating factor (G-CSF), CCL5 or regulated on activation, normal T cell expressed and secreted (RANTES), CCL12 or monocyte chemoattractant protein-5 (MCP-5), and tissue inhibitor of metalloproteinase-1 (TIMP1) supports the pro-inflammatory environment by recruiting more inflammatory cells to the sites of infection. The most intensely elevated cytokine levels were also pro-inflammatory with both forms of IL-12 being up-regulated (**Figure 4.16 C red box**). This is important as IL-12 signaling also modulates other pro-inflammatory cytokines.

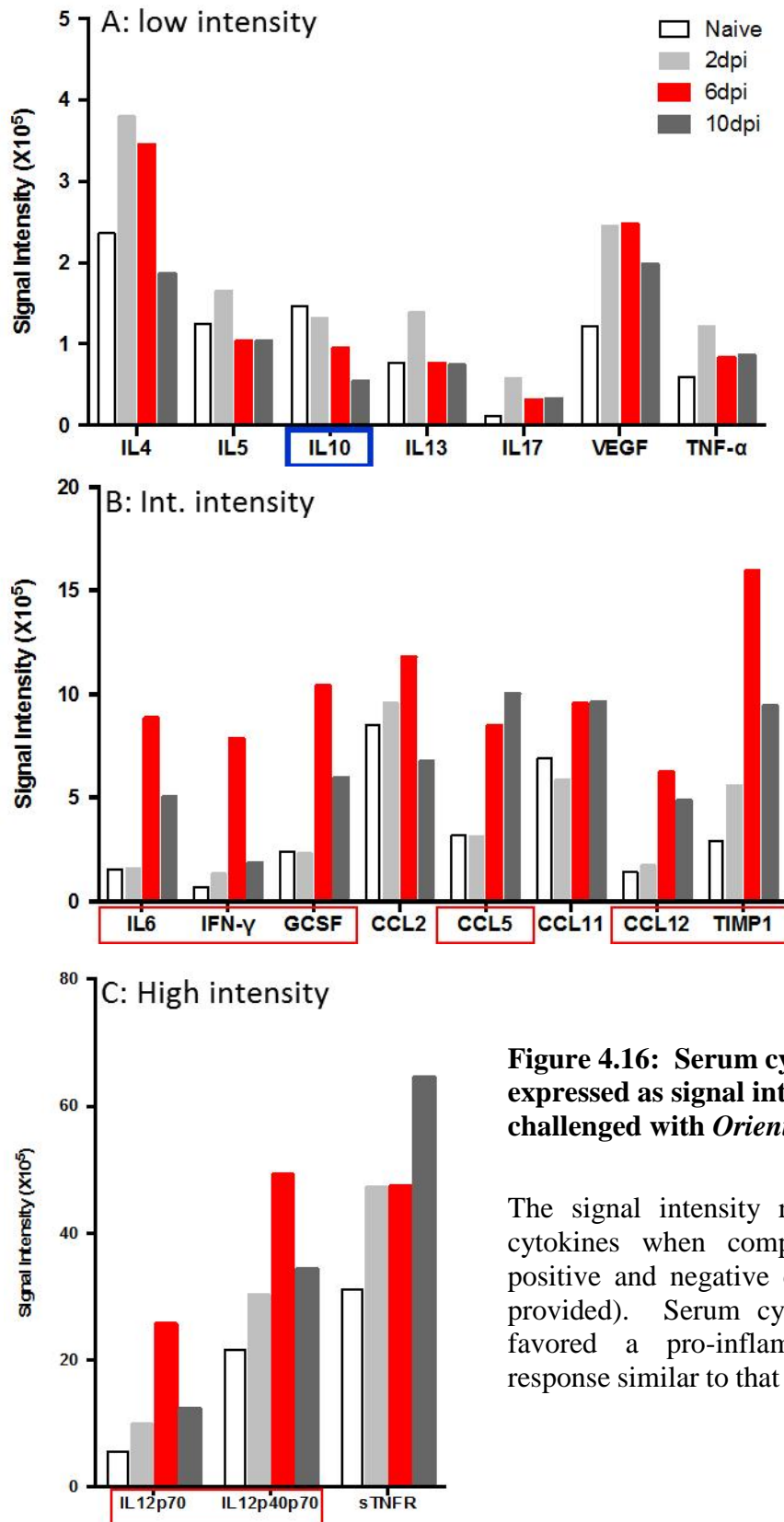


**Figure 4.16: Serum cytokine levels expressed as signal intensity in mice challenged with *Orientia*.**

The signal intensity refers to the level of cytokines when compared to the internal positive and negative controls (manufacturer provided). Serum cytokine levels strongly favored a pro-inflammatory (red boxes) response similar to that observed in the tissues.

## Discussion

Understanding the role that the immune system plays in disease is important for determining the underlying mechanisms of pathogenesis and disease outcome. There have been very few studies that approached the immune response to scrub typhus in an animal model. The lack of an adequate model was partly to blame, as trying to correlate immunological phenomena observed in a model that does not parallel human disease is difficult. The same can be said about *in vitro* studies, where the investigators can only focus on one or two cell types at a time. This is a two-dimensional approach to solve a three-dimensional question.

The immune response to a specific pathogen is a complex interaction that cannot be fully investigated *in vitro*. This sub-aim focused on identifying key inflammatory cytokines that would provide insight into the immune progression that occurs throughout the course of a scrub typhus infection. This study utilized female C57BL/6J mice from Jackson Laboratories, Bar Harbor, ME. This approach was a departure from the studies in sub-aim 1 that used B6 mice from Harlan Laboratories. This change was due to vendor notification that certain batches of their mice may have been exposed to bacterial pathogens, which may have an effect on our studies. The B6 mice from Jackson Laboratories had identical pathologic lesions as those from Harlan Laboratories.

Using the i.v. model previously developed in sub-aim 1, samples were collected early, mid-, and late during lethal infection to analyze the cytokine profile throughout the disease progression. A pro-inflammatory response as early as 2 dpi in all tissues except the kidney, and at 6 dpi all four tissues had cytokine expression levels that reflected a pro-inflammatory Th-1 response (**Table 4.4**). The mRNA levels from the respective tissues

revealed a distinct repression of type 2 (**Table 4.4-blue text**) responses while demonstrating activation of type 1 responses as early as 2 dpi. This trend continued until the animals were moribund. It could be hypothesized that this prominent type 1 response could be a contributing factor to the mortality in mice infected with *Orientia*. The pathology observed in this model and in human scrub typhus infections is predominantly associated with cellular infiltrates in response to the presence of *Orientia*, and the tissue damage is a direct result of the pathogen-host cell interactions and the cellular infiltrates' response to this interaction. When *Orientia* exits the host cell, it does so with minimal damage to the cell unlike other rickettsiae thus, the host's response is likely more responsible for the tissue damage observed in this disease than direct bacterial damage.

The concurrent up-regulation of IFN- $\gamma$  and IL-10 in the liver and lung is interesting and provides a paradox of the host trying to both up-regulate and down-regulate the immune response during infection. Kramme *et al.* (2009) reported elevated levels of IFN- $\gamma$  and IL-10 in the sera of scrub typhus patients, but serum data from my model only revealed elevated IFN- $\gamma$ . IL-10 was present but not at levels greater than the controls. IL-10 mRNA levels in the liver were also significantly up-regulated, but actual IL-10 levels, as measured by ELISA, did not change throughout the course of infection. The discrepancy between the mRNA levels and the protein levels may be due to a high uptake of IL-10 in the tissue or an unknown mechanism triggered during *Orientia* infection that reduces the translation of IL-10 mRNA to protein.

The data collected in this study demonstrate that a clear Th-1 activation response (**Table 4.4 black, red text**) begins as early as 2 dpi and lasts until 10 dpi, and strong down regulation in a tissue-specific manner (**Table 4.4 blue text**) when animals are moribund.

This pro-inflammatory environment coincides with severe weight loss and development of other signs of disease. This study will provide important information of the host's immune response to scrub typhus.

**Table 4.4. Cytokine expression profile summary**

	<b>qRT-PCR</b>				<b>Trends / Impacts</b> (immunopathogenesis)
	<b>Liver</b>	<b>Lung</b>	<b>Kidney</b>	<b>Spleen</b>	
<b>2 dpi</b>	IL-1 $\beta$ * ST2 * IL-33 **  IL-10 * IFN- $\gamma$ * CXCL9 *	IL-6 ** IL-1 $\beta$ *  IFN- $\gamma$ **		IFN- $\gamma$ *	Type I IFN__no major changes  IL-17__no major changes
<b>6 dpi</b>	IL-6 * ST2 ** IL-33 ** IL-10 **  TNF- $\alpha$ ** IFN- $\gamma$ ** CXCL9 ** CXCL10 * CXCL11 *	IL-6 ** <u>IL-33</u> ** <u>IL-13</u> ** IL-10 **  TNF- $\alpha$ ** IFN- $\gamma$ ** CXCL9 ** CXCL10 ** CXCL11 **	TGF- $\beta$ *  TNF- $\alpha$ ** IFN- $\gamma$ ** CXCL9 **	<u>ROR-<math>\gamma</math>t</u> ** <u>IL-4</u> ** <u>IL-13</u> ** <u>TGF-<math>\beta</math></u> **  TNF- $\alpha$ ** IFN- $\gamma$ ** CXCL9 ** <u>T-bet</u> **	IL-10 _____always increased  IL-4/IL-13_____always decreased  <b>Overwhelming Th1 cytokine response</b>
<b>10 dpi</b>	ST2 **  IL-10 **  TNF- $\alpha$ ** IFN- $\gamma$ ** CXCL9 ** CXCL10 *	IL-6 * ST2 * <u>IL-33</u> ** <u>IL-13</u> ** IL-10 **  TNF- $\alpha$ ** IFN- $\gamma$ ** CXCL9 ** CXCL10 ** CXCL11 **	IL-23 ** IL-33 ** TGF- $\beta$ **  TNF- $\alpha$ ** IFN- $\gamma$ ** CXCL9 **	<u>GATA3</u> ** <u>ROR-<math>\gamma</math>t</u> * <u>IL-4</u> ** <u>TGF-<math>\beta</math></u> **  TNF- $\alpha$ * IFN- $\gamma$ ** CXCL9 **	TGF- $\beta$ _____increased in kidney decreased in spleen  IL-33_____increased in kidney decreased in lung
<b>0 d</b>	<u>p &lt; 0.05</u> *	<u>p &lt; 0.01</u> **			

Black and red text denotes up-regulation, Blue text denotes down-regulation, and underlined text denotes mRNA of transcription factors. \*, change in gene expression was significant at p < 0.05; \*\*, change in gene expression was significant at p < 0.01.



## CHAPTER 5

### **Janus-like behavior of neutrophils during lethal *Orientia* infection.**

**Specific aim 2:** *Determine the effect of neutrophil depletion on disease progression using a hematogenously disseminated murine model of scrub typhus.*

**Hypothesis:** The neutrophilia observed in mice infected with *O. tsutsugamushi* is detrimental to disease outcome, and depletion of neutrophils at the appropriate time during infection will rescue lethally challenged mice.

**Rationale:** Neutrophils (PMN) are one of the most numerous circulating WBC in humans and up to 40% of circulating WBCs in the mouse (Amulic 2012, Harkness and Wagner 1989). PMNs are important innate immune cells that have multiple functions during the course of an infection. The role of PMNs during infections tends to be trivialized as these cells are nonspecific responders to a multitude of insults to their hosts. Recent studies suggest that neutrophils may have a more complex role in infectious diseases than previously thought (Nathan 2006, Jaeger 2012). During the initial stage of infections neutrophils are recruited by numerous cytokines and chemokines. Once they come into contact with one of these molecules, PMNs begin to home toward the source in a concentration dependent manner and, once at the source, begin to orchestrate the immune response via releasing chemokines and cytokines that recruit more PMNs, natural killer (NK) cells, and a variety of other cell types (Kolaczowska and Kubes 2013). How these cells respond to the PMN signals determines how the PMNs continue to perform, and it is at this crucial junction that the course of disease may be determined.

Neutrophils act on pathogens in a variety of means. When stimulated, they can release pre-packaged digestive enzymes that will punch holes into the pathogen or infected

cells or they can undergo NETosis that releases the PMN's DNA and histones into the extracellular creating a "net" that can stick to extracellular pathogens (Nathan 2006). This release of intracellular molecules also acts as a chemoattractant for APCs and other immune cells, assisting in the clearance of pathogens (Kolaczowska and Kubes 2013). PMNs have been studied in infections caused by several protozoan parasites, and their role is highly pathogen-dependent. In the case of *Trypanosoma cruzi*, the PMN's role in disease is host dependent (Abi Addallah 2012, Riberio-Gomez 2004, Luna-Gomes 2014).

The study of PMN involvement in obligatory intracellular bacterial infections is non-existent. Studying PMNs in scrub typhus *in vivo* is novel, as most immunological research has focused on macrophages and the adaptive immune response as described previously and the only studies involving PMNs were conducted *in vitro*. It is possible for PMNs to be infected with *O. tsutsugamushi* *in vitro*, but the physiological relevance to the disease has not been studied (Rikihisa and Ito 1982), and *Orientia*-infected neutrophils have not been detected *in vivo*. Preliminary studies using my i.v model demonstrated neutrophilia throughout the course of infection, and all case reports that included blood cell counts have described neutrophilia during acute scrub typhus. Additionally, my evaluation of the cytokine response during acute *Orientia* infection revealed chemokines and cytokines that are crucial for PMN recruitment to sites of infection (sE-selectin, sP-selectin, IL-12, Fas ligand, TNF- $\alpha$ , CXCL-15, CCL-12) and from the bone marrow (KC, G-CSF).

## **Characterization of the role of PMNs during *Orientia* infection**

### *PART I EXPERIMENTAL DESIGN:*

*Orientia tsutsugamushi* Karp strain, passaged and maintained as described above was diluted in PBS, and the bacteria were injected i.v. through the tail vein in a volume of 200  $\mu$ L. Control mice were inoculated with 200  $\mu$ L of similarly prepared material from

uninfected cells or tissue diluted in PBS. Animals were challenged with  $1.25 \times 10^6$  organisms. All infected and non-infected animals were monitored for signs of illness and body weight measured daily. Mice were necropsied at 0, 2, 6, and 10 dpi as described in **Chapter 4, sub-aim 2**. Four i.v. inoculated animals were euthanized, and blood, brain, heart, kidney, liver, lung, lymph nodes, and spleen were collected for histopathology and blood, brain, liver, lung, and spleen for bacterial load determination. IHC staining was performed for detecting *Orientia*, PMNs, and myeloperoxidase (MPO), as described in **Chapter 2**, to evaluate their presence in the tissues during the course of infection.

#### *PART 2 EXPERIMENTAL DESIGN:*

In order to address the effects of neutrophil depletion during lethal *Orientia* infection, I designed an experiment using 8-12 week old female C57/BL6 mice, Harlan Laboratories, lethally challenged with *Orientia* and neutrophil-depleted with an anti-Ly6G monoclonal antibody. Animals received 300  $\mu$ g of depleting antibody (1A8) or isotype antibody one day prior to infection (D-1), one (D+1), six (D+6), and one and six (D+1/6) days post infection. At 6 dpi, two animals that were depleted on day one, one uninfected, and one infected, isotype antibody-treated matched normal control animal were euthanized and tissues collected for histopathology and bacterial load determination to characterize the effects of early neutrophil depletion. At 12 dpi, two animals depleted on days 1 and 6, one animal depleted on day 6, one uninfected, and three infected isotype antibody-treated animals (all infected controls were moribund) were euthanized and tissues collected as on day 6. The remaining animals were monitored until 19 dpi.

## Results

*PART I: NEUTROPHIL LOCALIZATION-* As described previously, animals began to lose weight at 6 dpi and continued to lose weight until the end of the experiment. At days 0 and 2 pi, no pathologic lesions were detected, and animals appeared normal. PMNs were present at day 0 in all three tissues, with the spleen having the most abundant IHC staining (**Figure 5.1 A, D0**). At 6 dpi, animals had begun to show signs of illness, namely hunched posture and mildly ruffled fur. Spleens were enlarged as described previously, no oriental antigen was detected, but the red pulp had abundant PMN staining and focal MPO staining (**Figure 5.1 A, D6 and B, D6**). Oriental antigen was observed in sinusoids of the liver (**Figure 5.2 A**) and endothelium of the lung (**Figure 5.3 A**).

PMN staining in the liver was present in multicellular lesions throughout the section (**Figure 5.2-B left and top/bottom panels**). MPO staining was observed in these lesions as well. PMNs were also present in the interstitial infiltrates observed in the lung as was MPO (**Figure 5.3-B left top/bottom panel right panels, respectively**).

At 10 dpi, PMNs were detected throughout the red pulp of the spleen (**Figure 5.1 A, D10**). MPO was also confined to the red pulp with intense foci of positive staining (**Figure 5.1 B, D10**). In the liver, PMN staining was not confined to the lesions, but was also distributed throughout the parenchyma of the organ (**Figure 5.2 B, D10**). Although the PMNs were distributed throughout the liver, the strongest MPO signal was in the multicellular lesions (**Figure 5.2 C, D10**).

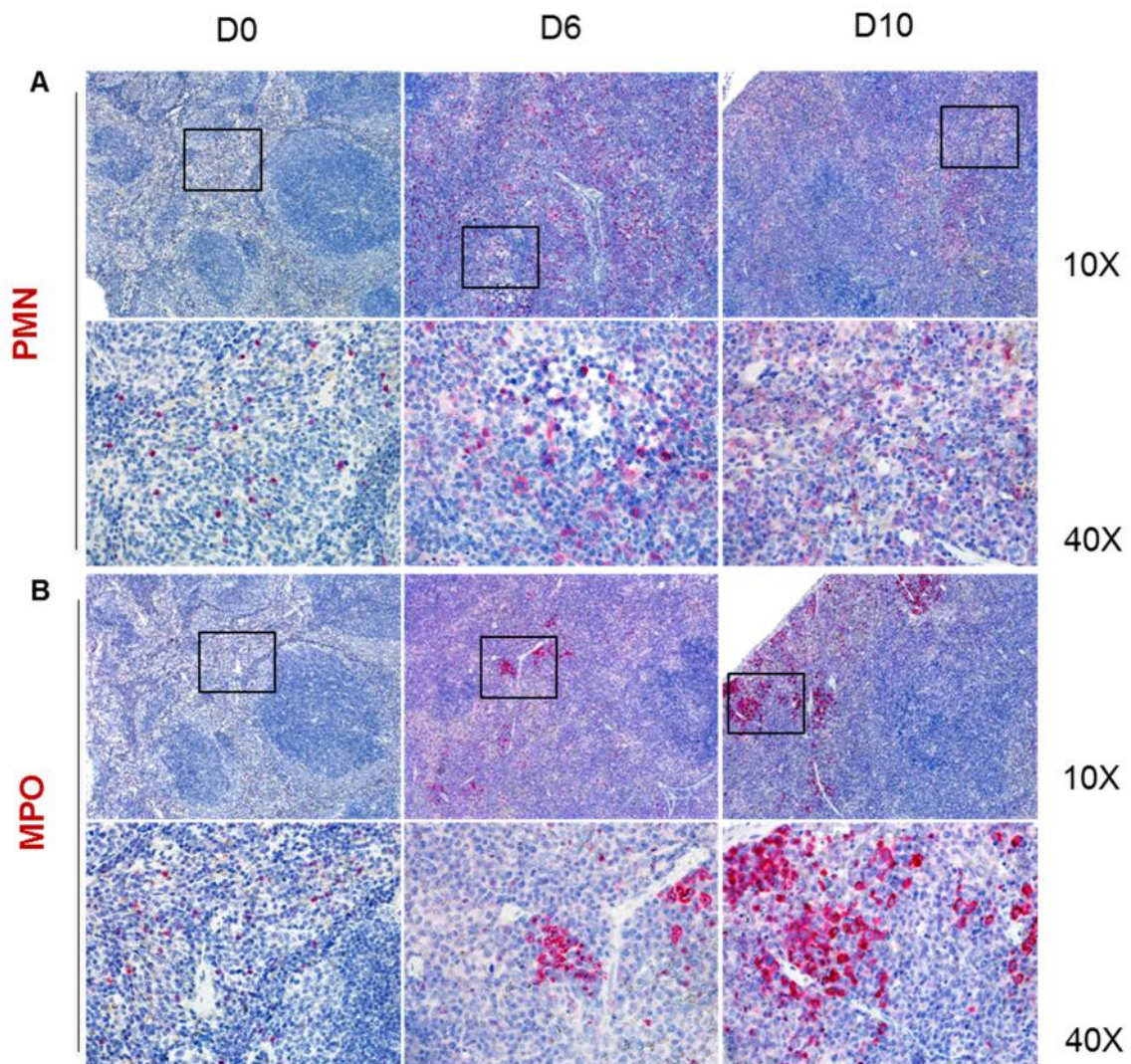


**Figure 5.1: IHC staining of PMNs in the spleen of mice lethally challenged with *Orientia*.**

PMN staining was generally localized to the red pulp on both days 6 and 10 (A). To measure the PMN activation status, MPO expression was measured (B). MPO staining was more prominent at 10 dpi.

PMNs were dispersed throughout the lung at this time, in the interstitium as well as in the perivascular infiltrates (**Figure 5.3 B, D10**). The MPO staining was diffuse and matched the dispersion of the PMNs throughout the lung. MPO was not concentrated in a specific area, such as was shown in the liver (**Figure 5.3 C, D10**). The PMN staining revealed an influx of PMNs into infected tissues at 6 and 10 dpi, which coincides with the



neutrophilia observed in **Chapter 4**. This provides further evidence that PMNs may play a significant role in scrub typhus pathology.

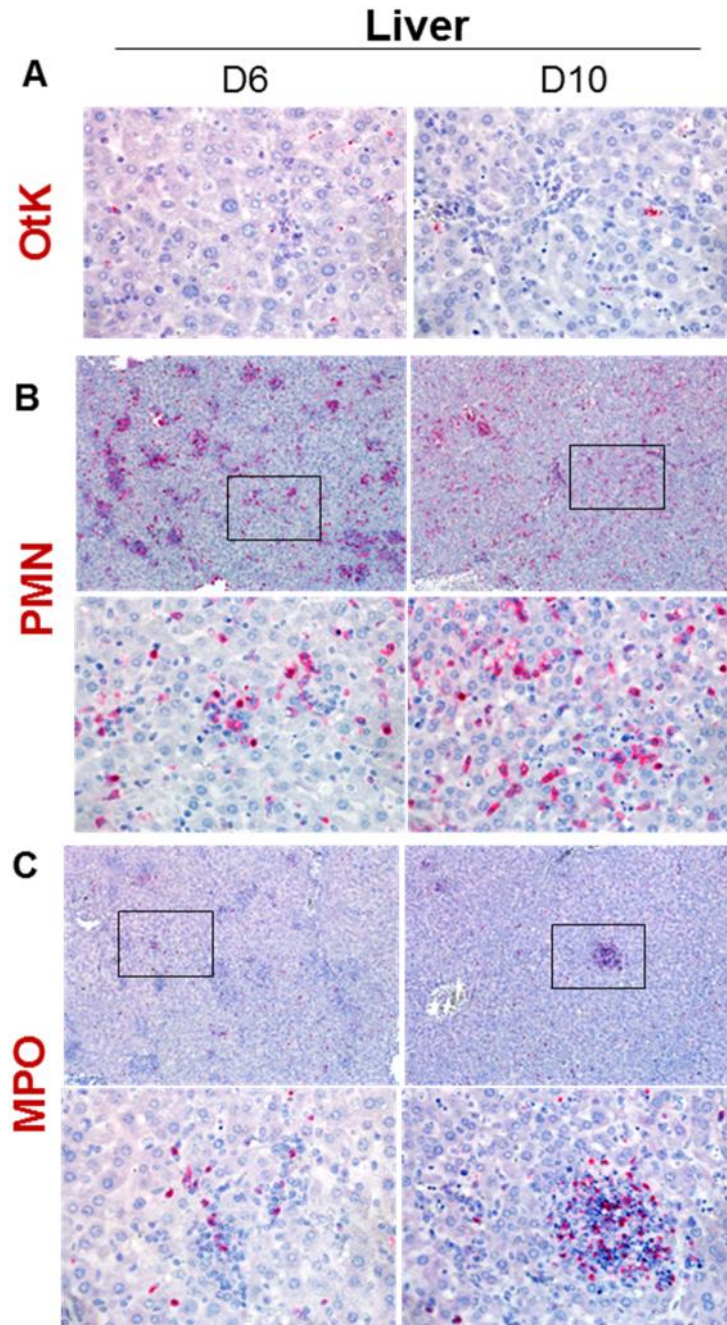


**Figure 5.2: IHC staining of liver from mice lethally challenged with *Orientia*.**

Oriental antigen was detected in the hepatic sinusoids of the liver at 6 dpi and 10 dpi (**A- 40x**). PMN staining had a focal distribution at 6 dpi (**B- left top-20x/bottom-40x panels**), but had a more diffuse localization by 10 dpi (**B-right top20x/bottom-40x panels**). To measure the PMN activation status, MPO expression was evaluated (**C**).

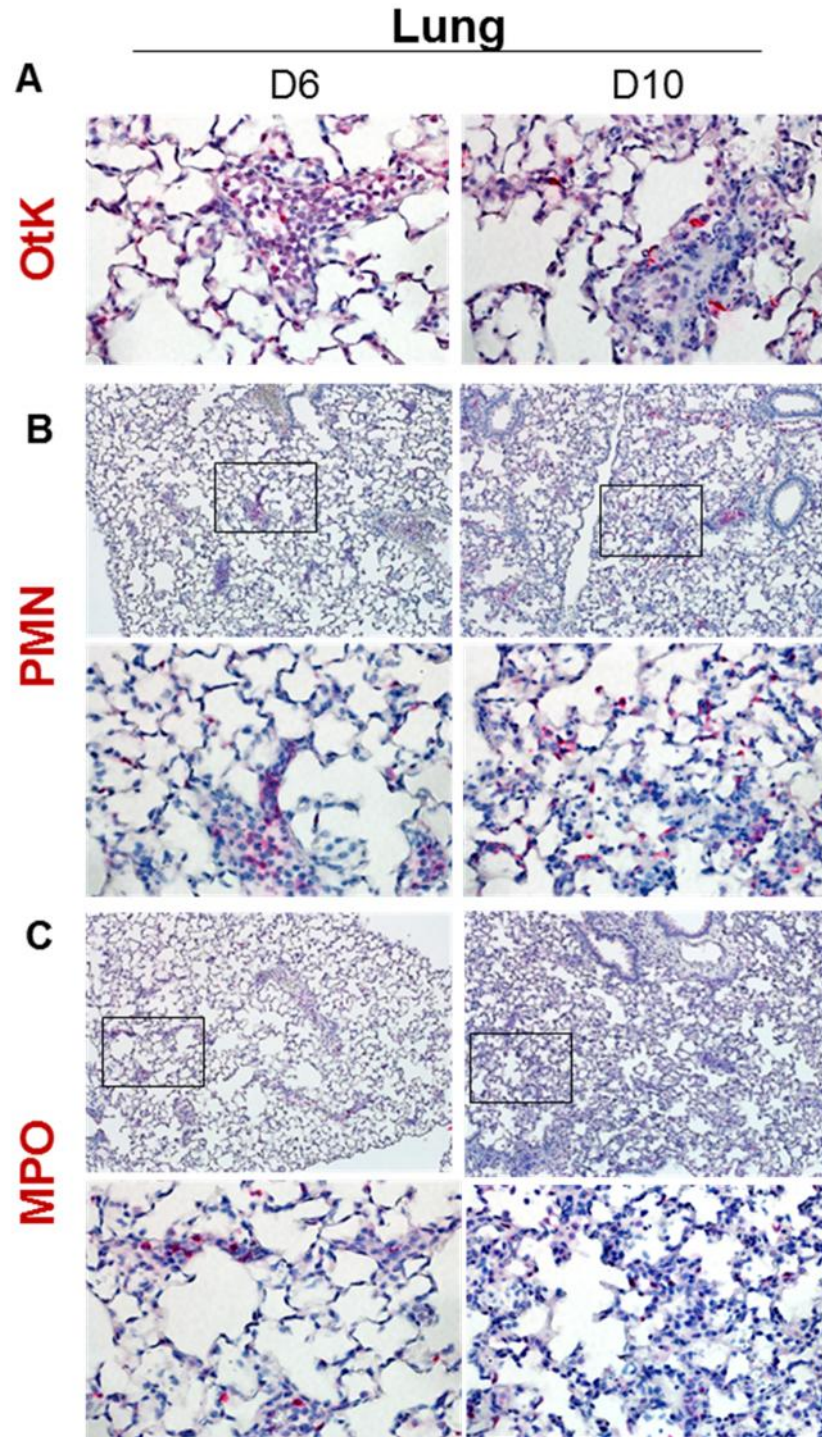


**Figure 5.3: IHC staining of lung from mice lethally challenged with *Orientia*.**

Oriental antigen was detected in the endothelial cells of the lung at 6 dpi and 10 dpi (**A- 40x**). PMN staining had a focal appearance at 6 dpi (**B- left top/bottom panels**), but had a more diffuse distribution by 10 dpi (**B-right top/bottom panels**). To measure the PMN activation status, MPO expression was evaluated (**C**).



*PART 2: NEUTROPHIL DEPLETION AND DISEASE PROGRESSION-* The antibody used to deplete PMNs in this experiment, binds only to Ly6-G, which is only expressed on PMNs. Administration of this antibody resulted in nearly 100% removal of PMNs from the circulation as determined by flow cytometry. The depletion strategy was designed to remove PMNs early during infection (D-1, D+1), thus studying the role of PMNs during the initial stages of infection, to remove PMNs at onset of signs of illness (D+6) to study the role of PMNs during the late stage of infection, and continual depletion (D+1/6), to assess the effect that neutrophil depletion would have on disease progression. Regardless of neutrophil depletion status, uninfected animals did not experience weight changes.

Isotype-treated, infected animals had disease progression as described in **Chapter 4**, with weight loss and signs of illness beginning on day 6 (**Figure 5.4**). Initially the D-1 depleted animals began to lose weight at 2 dpi, but this was attributed to a broken water supply, causing the animals to become dehydrated. Once the water source was replaced the animals recovered (**Figure 5.4**) and surpassed their starting weights by nearly 20%.

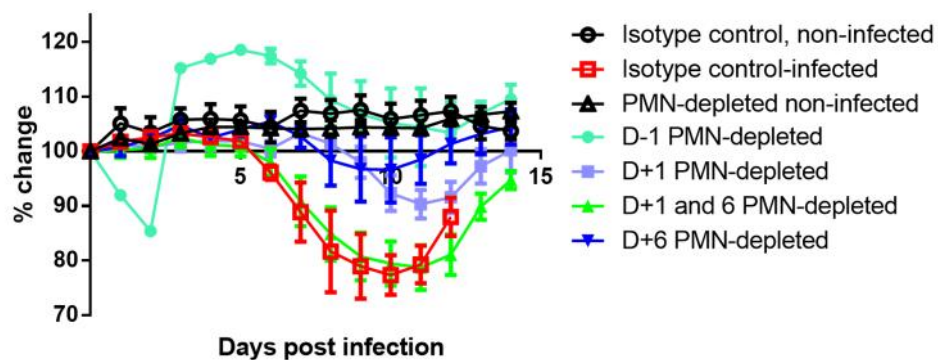


**Figure 5.4: Percent body weight change of mice following lethal challenge with *Orientia* and PMN-depletion.**

Body weights were measured daily. Each animal was compared to its own starting weight to express the percent change. Average percent change in weight is shown for each group. All animals lost weight during the course of infection.



Although they gained additional body weight, D-1 depleted animals began losing weight at the same time as the isotype controls. During this time they had similar signs as the controls, and one animal expired on day 10 pi (**Figure 5.5**). Histopathology of these animals was similar to that described in D+1 depleted animals. Signs of illness in D-1 depleted animals began to lessen by 12 dpi and were completely resolved by 19 dpi, although they had detectable *Orientia* in the kidney, lung, and spleen (**Figure 5.6**). Animals depleted on D+1 had a delayed onset of weight loss, ~2 days, compared to the isotype control animals. At this time, animals began to show signs of illness, i.e., hunched posture, ruffled fur and lethargy. Although these animals became ill, all animals survived (**Figure 5.5**, line parallels non-infected and D+6 PMN-depleted groups), and their body weights returned to baseline by day 15 (**Figure 5.4**).

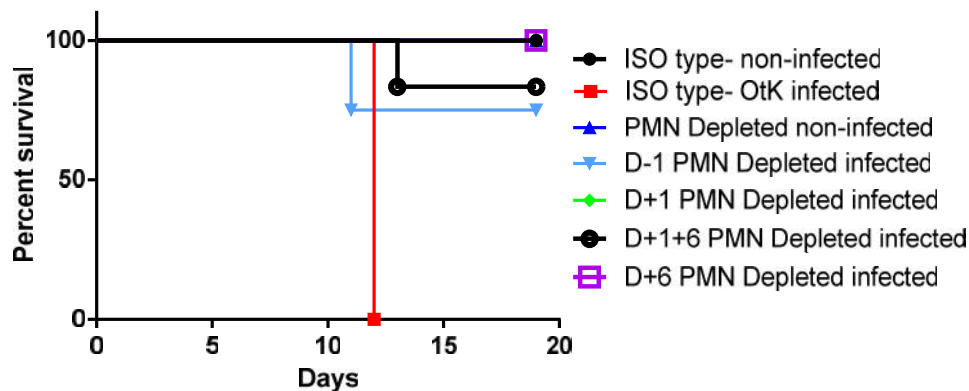


**Figure 5.5: Percent survival following lethal challenge with *Orientia* and PMN depletion.**

Isotype-control treated infected animals died on 12 dpi as expected. PMN depletion increased survival for all groups, but not did prevent disease development.

On day 6 pi, two animals from the D+1 depleted group and one isotype control animal were euthanized and tissues collected for histology. Typical histopathology of the lung for i.v. challenged mice at 6 dpi is illustrated in **Figure 5.7 B**. Depletion of neutrophils

on 1 dpi resulted in a dramatic increase of cellular infiltrate into the *Orientia*-infected lung (Figure 5.7 C, D). Cellular infiltration of this magnitude did not occur until 9 and 12 dpi typically in undepleted mice. Similar to the lung pathology, an increased cellular infiltrate was observed in the liver at this time point (Figure 5.8 C, D). Also observed, were infarcted areas in the liver that had not been observed previously in the i.v. model (Figure 5.8 D). At 19 dpi, the remaining animals still had copies of the 47 kD gene in the lung and spleen (Figure 5.6).

Animals depleted of PMNs on D+1/6 began to lose weight at the same time as isotype controls as well as exhibited hunched posture and ruffled fur. Throughout the course of the infection this group most closely resembled the behavior of the infected controls (Figure 5.4). Although they lost almost exactly the same percent of body weight as lethally infected controls, only one animal from this group expired on 13 dpi (Figure 5.5). By day 19, this group had recovered body weight but exhibited signs of severe illness and had detectable bacterial loads in all organs on day 19 (Figure 5.6).

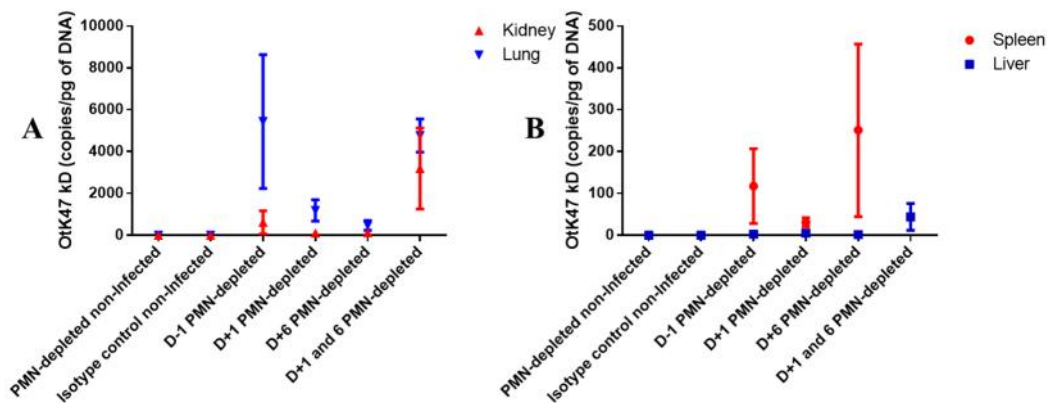


**Figure 5.6: *Orientia* 47 kD gene copies/pg of DNA at 19 dpi following neutrophil depletion.**

Bacterial loads were measured for the surviving animals from each group using the methods described in Chapter 3. All PMN-depleted animals had detectable *Orientia* in the lung and kidney; D+6 depleted animals had similar loads in the lung and kidney.

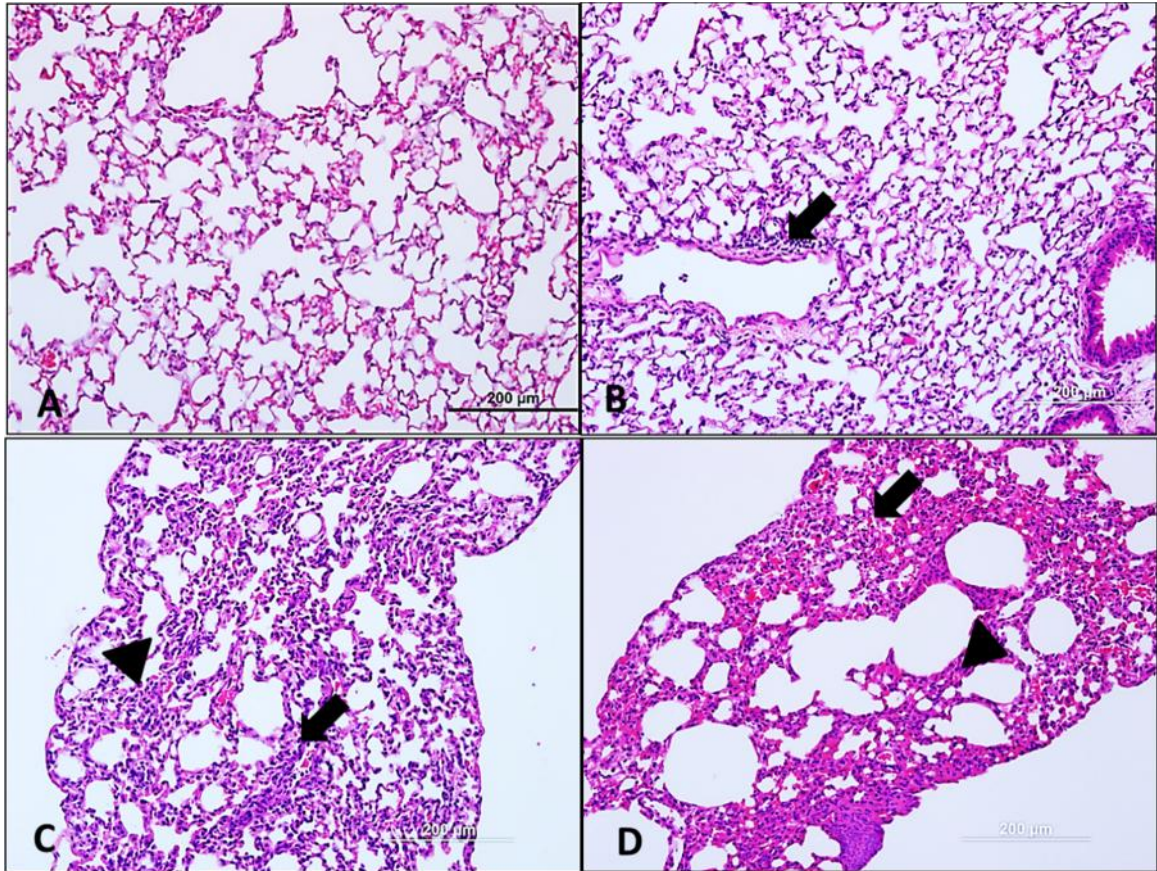


**Figure 5.7: Histopathology of the lung at 6 dpi of mice inoculated with *Orientia tsutsugamushi* following neutrophil depletion on day 1.**

Tissue morphology of the non-infected, neutrophil depleted animal appeared normal (A). The infected, isotype treated infected control mouse had mild vasculitis (arrow) (B). Depletion of neutrophils dramatically affected the tissue histopathology of infected animals at 6 dpi (C, D). The severity of cellular infiltrates varied from moderate vasculitis, and focal interstitial pneumonia, (C-arrow and triangle, respectively) to severe perivascular and peribronchial infiltration, interstitial pneumonia, and alveolar edema (D).



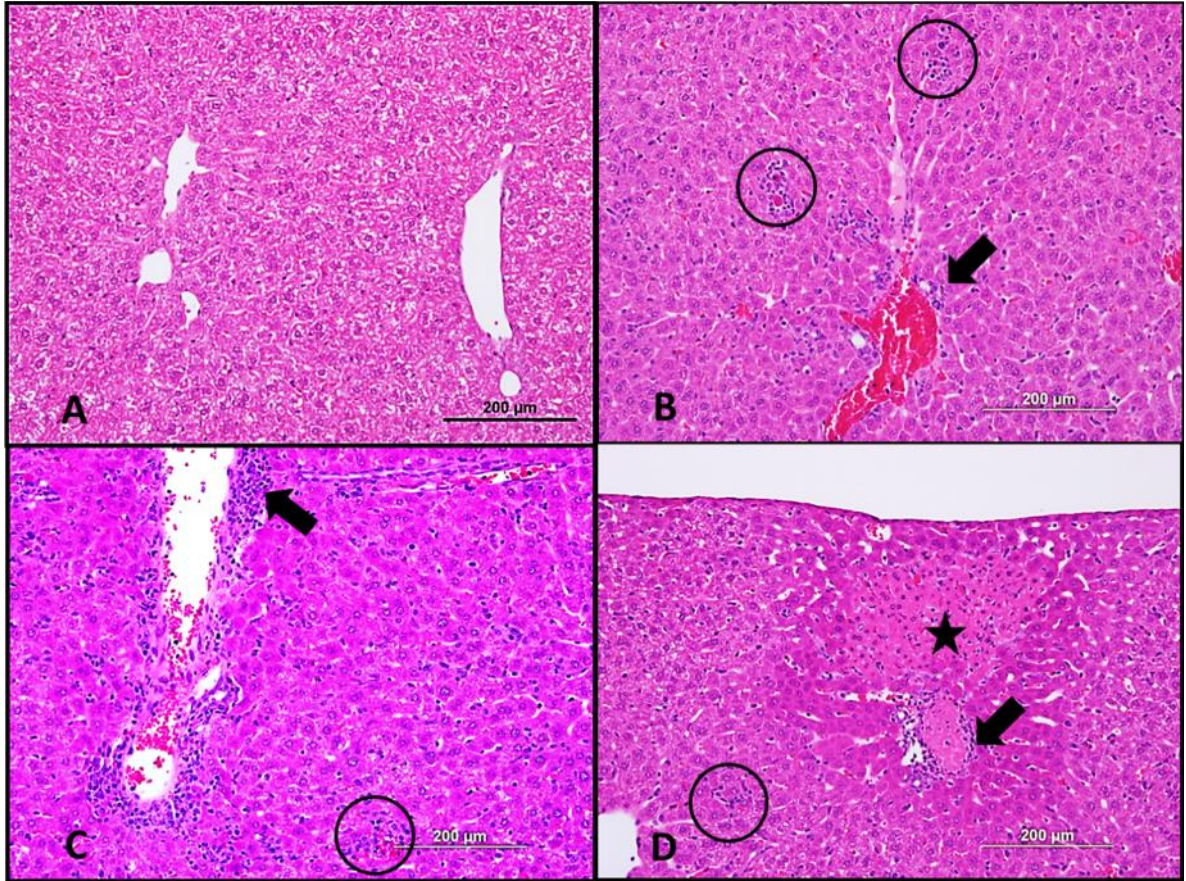


**Figure 5.8: Hepatic histopathology at 6 dpi of mice inoculated with *Orientia tsutsugamushi* following neutrophil depletion on day 1.**

Tissue morphology of the non-infected, neutrophil-depleted animal appeared normal (A). The infected, isotype-treated infected control mouse had mild vasculitis (arrow) and compact multifocal, mononuclear infiltrates (circles) on 6 dpi as previously reported (B). Depletion of neutrophils, by antibody treatment on day 1 affected the histopathology of infected animals at 6 dpi (C, D). Severe cellular infiltrates and associated pathology were multifocal. Mononuclear infiltrates were present, but less compact (C, D-circles). Both neutrophil-depleted animals (C and D) exhibited moderate-to-severe vasculitis (arrows) and had infarcted areas (D-star) indicating severe damage to the vasculature. Previously, infarcts were rarely seen following intravenous challenge.

Animals depleted of PMNs on day 6 had mild hunched posture at the time they received the neutrophil-depleting antibody and had begun to lose weight. After depletion, this group did not continue to lose weight like the other groups. In contrast to the other groups, D+6 depleted animals' signs of illness ameliorated and were completely resolved by 10 dpi while all other groups were severely lethargic or moribund. On day 12 pi, two D+6 animals and all isotype-treated, infected animals were euthanized, necropsied, and tissues collected for histology. The isotype-treated, infected animals were moribund, as expected. Extensive inflammation was observed at this time throughout the lung (**Figure 5.9 B**). Immunofluorescent staining of *Orientia* and PMNs at 6 dpi and 12 dpi demonstrated infiltrating PMNs and oriental antigen in the endothelium (**Figure 5.10 B**). Corresponding with their observed well being, the D+6 depleted animals had considerably less inflammation in the lung. The lungs of these animals manifested mostly normal appearance (**Figure 5.9 C**) with occasional areas of vasculitis (**Figure 5.9 C, D arrows**) and focal interstitial pneumonia (**Figure 5.9 D triangle**). No *Orientia* staining by IF was detected in the lungs of this animal nor positively stained PMNs (**Figure 5.10 D**). In the liver a similar trend was also observed on day 12 pi (**Figure 5.11 B-D**). Compared to the isotype-treated, infected animals, the D+6 depleted animals' liver histology was almost normal, with small, dispersed lesions (**Figure 5.11 D circles**). Similar to the lungs, non-depleted infected animals had detectable *Orientia* and PMNs at 6 and 12 dpi (**Figure 5.12 B, C**), the D+6 neutrophil-depleted animal was negative for both by IF (**Figure 5.12 D**). Animals depleted on day 6 also had the lowest bacterial loads in the kidney, liver, and lung



on day 19 pi (**Figure 5.6**). All tissues of PMN-depleted animals did not have positive PMN staining and virtually no positive staining for *Orientia*.

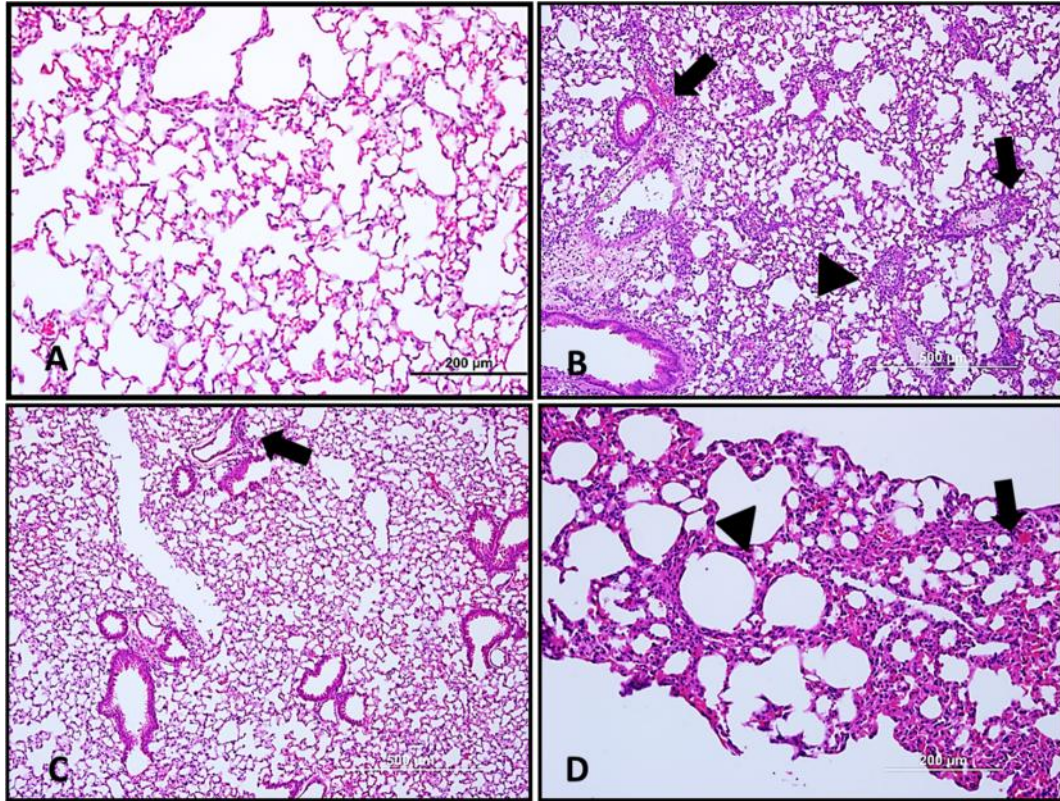


**Figure 5.9: Histopathology of the lung at 12 dpi of mice inoculated with *Orientia tsutsugamushi* following neutrophil depletion on day 6.**

Tissue morphology of the non-infected, neutrophil-depleted animal appeared normal (A). The infected, isotype-treated infected control mouse had severe vasculitis in all regions (**arrows**) and interstitial pneumonia (**triangle**) (B). Cellular infiltrates were diffuse. Depletion of neutrophils, by antibody treatment on 6 dpi dramatically reduced the cellular infiltrate of infected animals at 12 dpi (C, D). The severity of cellular infiltrates varied from absent-to-mild vasculitis (C, D-**arrows**), and focal interstitial pneumonia (D- **triangle**).

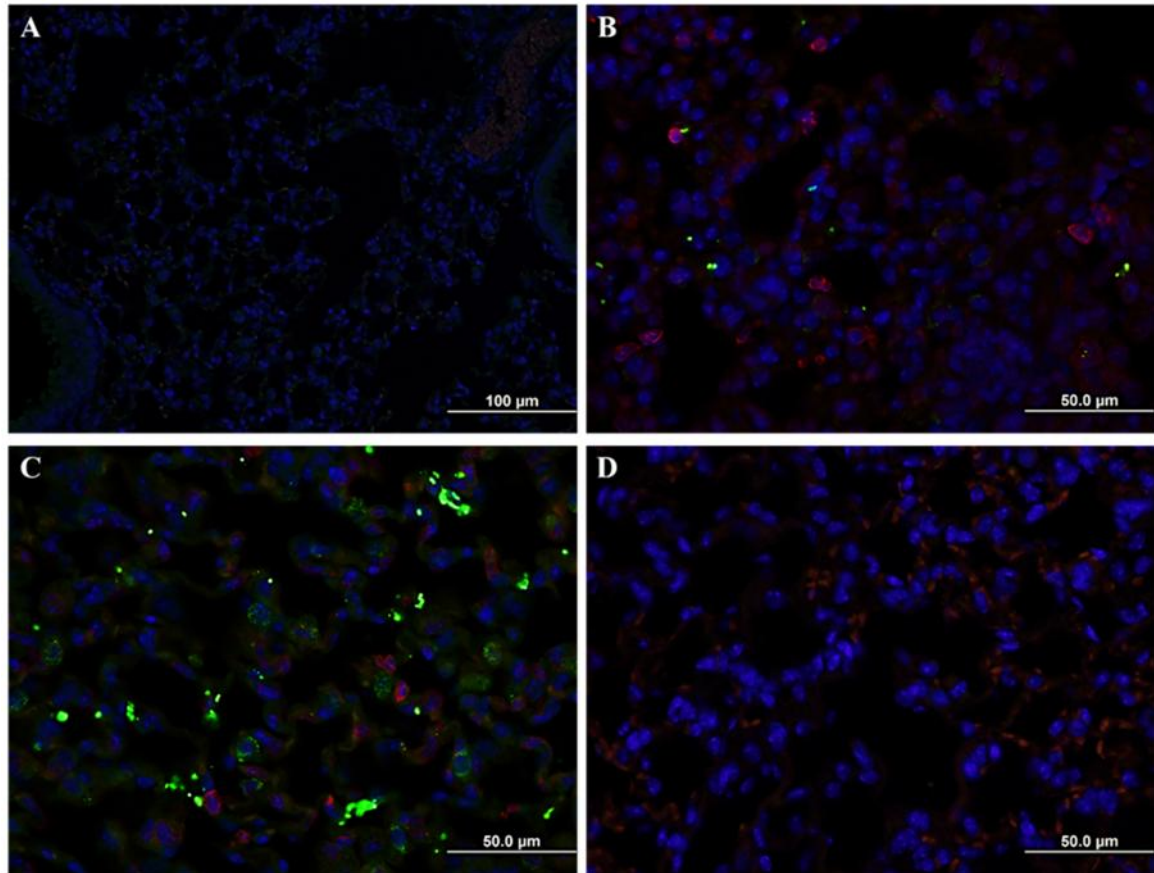


**Figure 5.10: Dual immunofluorescence staining for PMNs (red) and *Orientia* (green) in the lung of mice inoculated with *Orientia tsutsugamushi* following neutrophil depletion on day 6.**

Non-infected animals had little neutrophil staining in the lung and no *Orientia* (A). At 6 dpi, oriental antigen (green) was detected in the lung as were PMNs (red-punctate staining) in the interstitium (B). At 12 dpi, the lung of non-depleted animals was highly infected (green) with PMNs throughout the lung (C). Mice that were PMN-depleted at 6 dpi did not have staining for either *Orientia* or PMNs (D). Under these conditions, RBCs autofluoresce orange-red without the punctate staining that is observed in the PMNs.



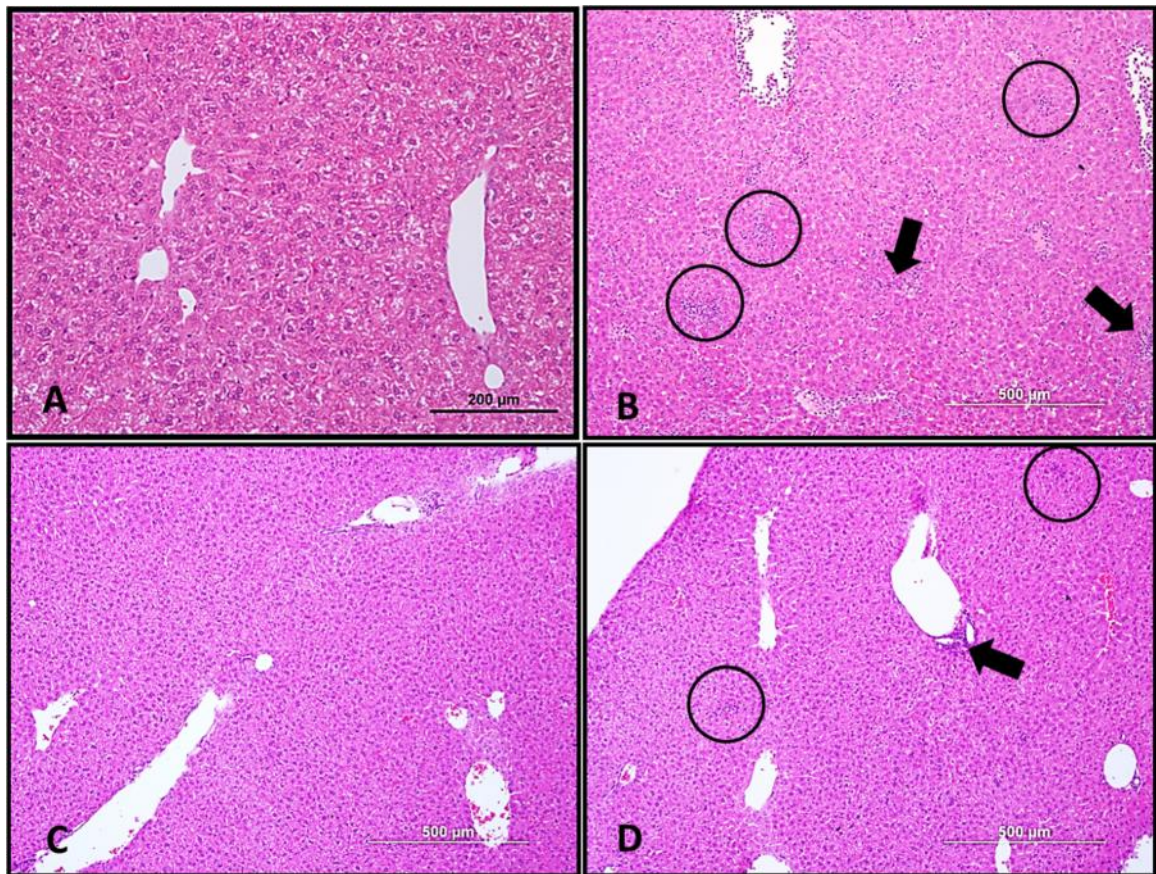


**Figure 5.11: Hepatic histopathology at 12 dpi of mice inoculated with *Orientia tsutsugamushi* following neutrophil depletion on day 6.**

Tissue morphology of the non-infected, neutrophil-depleted animal appeared normal (A). The infected, isotype-treated infected control mouse had severe vasculitis (**arrows**) and numerous compact, multifocal, mononuclear infiltrates (**circles**) at 12 dpi as previously reported (B). Depletion of neutrophils, by antibody treatment on day 6, like in the lung, reduced the cellular infiltration in infected animals at 12 dpi (C, D). Mononuclear infiltrates were present as in infected PMN-depleted animals, but were less numerous and decreased in size (C, D-circles). In both neutrophil-depleted animals (C and D), there was minimal vasculitis (**arrows**) and infarcts were absent.



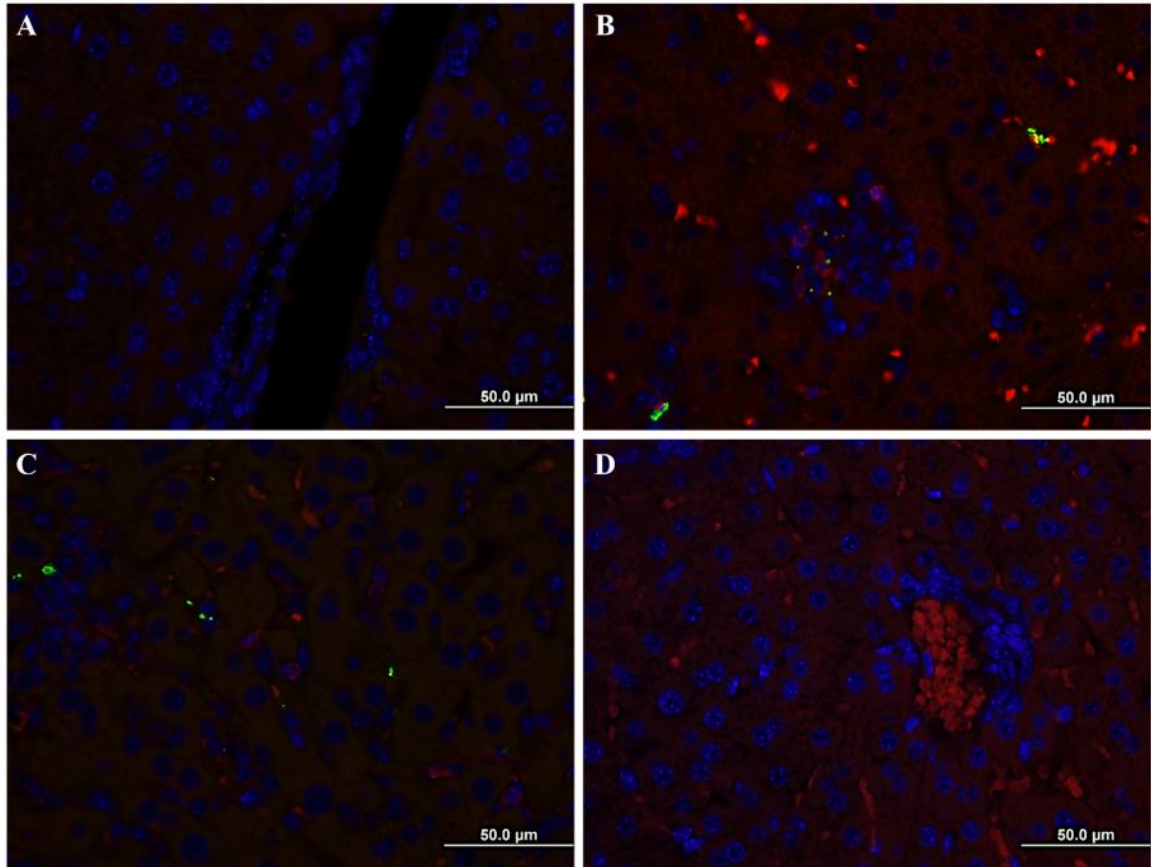


**Figure 5.12: Dual immunofluorescence staining for PMN (red) and *Orientia* (green) in the liver of mice inoculated with *Orientia tsutsugamushi* following neutrophil depletion on day 12.**

Non-infected animals had little neutrophil staining in the liver and no *Orientia* (A). At 6 dpi, oriential antigen (green) was detected in the liver as were PMNs (red-punctate staining) in the interstitium (B). At 12 dpi, the liver of non-depleted animals had detectable *Orientia* (green) and PMNs throughout the liver (C). Mice that were PMN-depleted at 6 dpi did not have staining for either *Orientia* or PMNs (D). Under these conditions, RBCs autofluoresce orange-red without the punctate staining that is observed in the PMNs.

## Discussion

PMNs are one of the most abundant WBCs and could possibly be one of the most important innate immune cells involved in infectious disease defense. Their multitude of functions and ever growing roles in the immune response necessitates that we further our understanding of their role in acute infections. It was the goal of this aim to elucidate the role of PMNs during scrub typhus infection using an i.v. mouse model that results in scrub typhus-like pathology described in human disease.

Data observed in **Chapter 4** suggested that PMNs may play a crucial role in determining the outcome of scrub typhus and its subsequent pathology. *Part 1* demonstrated the localization of PMNs in lesions in the liver and lungs of animals infected with *Orientia*. PMN and MPO staining was consistently associated with cellular infiltrates in both tissues. These data, in conjunction with our previously collected data, provided strong support for PMN involvement during scrub typhus infection.

*Part 2* demonstrated that the effects of PMN depletion were dependent on the time in the disease course when depletion occurred. Early depletion resulted in more severe pathology with earlier onset and disease progression similar to non-depleted animals but with increased survival. These animals were not able to clear infection, but it is likely that the intense cellular response of PMN-depleted animals reduced the number of bacteria present thus, allowing the animals to recover from the infection. The most striking observation was seen in the D+6 depleted animals.

Animals depleted on 6 dpi recovered weight and had less severe signs of illness. Signs of illness had resolved by 12 dpi. Histopathology demonstrated decreased cellular infiltrates when compared to infected, non-depleted animals. PMN depletion on day 6 pi

considerably reduced the bacterial burden on day 19 when compared to the other PMN-depleted groups. Why this group had lower bacterial loads needs to be further investigated, but it is possible that the decreased number of *Orientia* in the tissues of these animals may be due to the reduced recruitment of monocytes (possible shuttle cells for oriental dissemination) and therefore, decreasing their ability to disseminate, and allowing the host to reduce the bacterial burden but not clear the infection. Another possibility is that the activation of PMNs creates an environment that is permissive to oriental infection and PMN-depletion interferes with this. These animals also had the highest bacterial load in the spleen at 19 dpi. This could be the result of the PMN-depletion altering the available cell types that may assist in dissemination, thus creating an alternate niche in which *Orientia* can persist.

IF staining of non-depleted animals was observed for both of *Orientia* and PMNs at 6 and 12 dpi in heart (data not shown), liver, and lung. The IF PMN staining was similar in distribution to the IHC, but the IF was not as intense. This is most likely due to the inherent differences in the procedures as IF stain intensity is dependent on the number of cell protein molecules being expressed, and IHC is a precipitating reaction that amplifies the signal at the site of the primary antibody attachment, thus giving the impression that the PMNs were more numerous. The IF staining of PMNs demonstrated PMN localization in the interstitium of the lung and in lesions in the liver at 6 dpi (**Figure 5.10-B** and **Figure 5.12-B, respectively**). At 12 dpi, the PMN staining was observed throughout the tissue similar to that of IHC (**Figure 5.2-B 10** and **Figure 5.3- B 10**). The IF demonstrated that the *Orientia* and PMNs were associated with lesions at 6 dpi, but they were not co-localized. Although it has been shown that *Orientia* can infect PMNs *in vitro* (Rikihisa 1979), these

data suggest that PMNs are not infected during *Orientia* infection *in vivo* and are unlikely to be directly involved in oriental replication and dissemination. Further studies using multiple PMN markers or fluorescently tagged PMNs should be conducted to verify these studies possibly using tissues that were not formalin fixed in order to improve the epitope confirmation of the cellular proteins. Also, the creation of a fluorescent-tagged *Orientia* would be a great advantage in studying individual cellular interactions with *Orientia in vivo*.

Additional attempts were made to further clarify these results, but confounding factors, i.e., inconsistent bacterial stocks, resulted in mixed results that could not be fully applied to the elucidation of the role of neutrophils in scrub typhus. An important trend was observed; increased bacterial burden and D-1 depletion of PMNs results in earlier mortality. These data provide further support to the importance of PMNs as immune suppressors during early infection. During this experiment, 60% of animals depleted of PMNs on day 6 survived the same challenge, but without the promising recovery observed in the initial experiment.

PMNs are thought to strongly promote a pro-inflammatory response, calling in as many reinforcements as possible to deal with whatever is causing insult to the host. The animals that had their PMNs depleted early during infection exhibited an increased cellular infiltration into the liver and lung compared to non-depleted animals. This result would suggest that PMNs have an immunomodulatory role early in scrub typhus infection. This modulation may be important for limiting tissue damage that otherwise could occur in response to scrub typhus infection, but does the PMN's modulatory function benefit the *Orientia* by reducing the cellular response to sites of infection allowing the bacteria to

replicate unmolested while decreasing host cell damage? To answer this, a time course study should be performed during the first 6 days of infection to compare bacterial loads in depleted and non-depleted animals to determine whether the presence of PMNs actually benefits bacterial replication and conversely the conclusion that depletion of PMNs early in infection, while increasing the cellular response, benefits the host's survival.

On the other side of the coin, depletion of PMNs on day 6 resulted in a reduction in illness and eventual weight recovery. Histopathologically, the day 6 depleted animals appeared almost normal, especially compared to the non-depleted controls. This result suggests that the PMNs that are recruited after day 6 have a detrimental role in disease progression, thus possibly promoting a pro-inflammatory environment that results in the cellular infiltration and eventual death observed in non-depleted animals.

These data suggest a dual role of neutrophils in bacterial clearance and tissue pathology during scrub typhus infection. These roles may be determined by the initial recruitment factors and the environment in which the PMNs enter in response to the chemoattractants, i.e., KC and G-CSF (Kolaczowska and Kubes 2013). PMNs recruited early in infection may be induced to release a more suppressive payload, e.g., IL-10 or IL-33, allowing for a more gradual influx of cells to sites of infection limiting tissue damage to the host. This hypothetically delayed response may inadvertently allow the *Orientia* to further disseminate without being killed by the host's immune response, thus making the infection more difficult to control. Conversely, those PMNs recruited later in the course of infection, may arrive in a more pro-inflammatory environment, triggering them to release more chemoattractants, further recruiting more inflammatory cells to the sites of infection creating an environment that is detrimental to the host. It has been demonstrated that

monocytes in the eschar are infected and, therefore, may play a role in oriental dissemination from the eschar (Paris 2013); it is possible that these cells that are recruited may continue to shuttle the *Orientia* throughout the disease course.

## CHAPTER 6

### Conclusions and Future Studies

#### Summary

The aim of this dissertation project was to develop a scrub typhus model that parallels human disease and could be used to further our understanding of the progression of this neglected re-emerging disease. After reviewing more than 30 years of scrub typhus research, I decided that the biggest impediment to furthering our understanding was the lack of an adequate animal model.

The first sub-aim of **Aim 1 (Chapter 4)** compared the historically utilized intraperitoneal inoculation model to the uncharacterized intravenous model developed during this project. Intraperitoneally inoculated animals developed lethal peritonitis and accumulation of proteinaceous exudates in the peritoneum. Histopathology demonstrated prominent mesothelial hyperplasia and recruitment of inflammatory cells on the surface of the peritoneal organs, especially the liver and spleen. These mesothelial cells were heavily infected with *Orientia* as demonstrated by IHC. Endothelial infection was present at the time of death, which was the result of the severe peritonitis. During this comparison, I found that the i.v. inoculated animals developed disseminated endothelial infection and histopathology that paralleled severe human scrub typhus. Multicellular lesions were observed in the liver that were similar in structure to human lesions as described by Allen and Spitz (1945). IHC revealed *Orientia* infection of the endothelial cells of the microvasculature in the liver as well as the endothelial cells located in the larger vessels of the portal triads. The terminal pathology of the lung strongly paralleled that of human scrub typhus (Allen and Spitz 1945). Alveolar endothelial cells were heavily infected, and

the resulting perivascular infiltrates resulted in interstitial pneumonia and vasculitis throughout the lung. Cerebral nodules of perivascular infiltrating cells were evident in the brain as was meningoencephalitis and cerebral hemorrhages. The microvasculature of the brain was infected. The kidney of mice infected by i.v. challenge also exhibited extensive cellular infiltrates around the vasculature as was also described in humans by Allen and Spitz (1945). Bacterial dissemination occurred in both i.p. and i.v. inoculated animals, but only i.v. inoculated mice developed scrub typhus-like pathology, indicating that the pathology was dependent on the route the bacteria were given and how/where the host first contacts the bacteria. The overall histopathology of this model strongly paralleled that of human scrub typhus and will be a powerful tool for elucidating the disease mechanisms of scrub typhus.

Sub-aim 2 characterized the cytokine and chemokine responses during lethal scrub typhus infection using the model developed in sub-aim 1 (**Chapter 4**). As early as day 2 pi, a pro-inflammatory environment was being established in the lung and liver, and by day 6, the mRNA expression levels of IFN- $\gamma$ , TNF- $\alpha$ , and CXCL9-11 were all significantly elevated, strongly promoting a Th-1 response, while there was distinct repression of Th-2 and T-regulatory responses with significant down-regulation of GATA-3 and ROR $\gamma$ t. This environment continued until the animals were moribund. Serum cytokine levels matched the pro-inflammatory response observed at the mRNA level. The increased expression of pro-inflammatory cytokines and the up-regulation of the Th-1 promoting mRNA levels, coincided with the initial observation of signs of illness and decrease in body weight on day 6. After 6 days of infection, the animals began to show signs which occurred at the time in the course at which the humans with scrub typhus might present to the clinic. The



inflammatory responses observed in the acute phase of infection are similar to what has been reported in human scrub typhus cases at the time of admission (Kramme 2009, Paris 2008). These data and the histopathology of this model indicate that it is the best murine model for scrub typhus available.

In **Chapter 5**, this model was utilized to begin to understand the immunological events that occur during scrub typhus. During the course of characterizing the i.v. model, CBCs were done to evaluate the changes in circulating inflammatory cells. I observed that at 3 dpi, mice infected with *Orientia* began to have increased numbers of PMNs in the circulation when compared to uninfected and i.p. infected animals. By day 6 pi, these animals had neutrophilia, which was present at all time points until the animals succumbed to infection. Elevated levels of PMN-recruiting chemokines/cytokines (sE-selectin, sP-selectin, IL-12, Fas ligand, TNF- $\alpha$ , CXCL-15, CCL-12, KC (not shown), and G-CSF) were observed in the serum throughout the infection with a peak at day 6. All of these are potent recruiters of PMNs, especially KC and G-CSF. Infected or damaged endothelial cells are capable of releasing most, if not all, of these, providing homing signals for newly recruited PMNs. A review of the literature that actually reported CBC suggested that neutrophilia was common in acute infections as well as observed in tissue lesions of lethal cases (Allen and Spitz 1945, Bourgeois 1982). These reports plus my observations during the development of the i.v. model led to the development of the hypothesis that PMNs play a role in the disease outcome in scrub typhus.

To confirm that PMNs were actually in the lesions and activated, PMN and MPO were stained, respectively. At day 6 pi, PMNs were strongly associated with the lesions observed in the liver and in the perivascularitis in the lung. MPO staining was also present. At day 10 pi, PMNs were observed in the lesions in the liver as well as throughout the parenchyma. MPO staining was mainly observed in the lesions. In the lung, PMNs and MPO staining were observed in the interstitium as well as in the perivascular infiltrates.

This staining provided solid evidence that PMNs were indeed present in the tissues and could be contributing to disease pathology.

To assess the role of PMNs in scrub typhus, a depleting antibody specific for Ly6-G was utilized. Administration of this antibody resulted in nearly 100% removal of PMNs from the circulation as determined by flow cytometry. The animals that had their PMNs depleted the day before infection and on days 1 and 6 after infection exhibited similar signs and weight loss as the non-depleted animals, but with increased survival. Animals depleted on the day after infection had a two day delay in onset, when compared to non-depleted animals, before signs and weight loss began. At the time of depletion, animals depleted on day 6 of infection were exhibiting signs of illness and slight weight loss. After depletion, they lost weight for two more days, but not as severely as the non-depleted, D-1, or D+1/6 groups. By day 10 pi, this group no longer had signs and had begun to recover weight while all other groups continued to lose weight. D+6 and D+1 groups had 100% survival while the D-1 and D+1/6 groups had 75% and 89% survival, respectively. All non-depleted animals expired.

Depletion of PMNs early in *Orientia* infection resulted in increased cellular infiltrates in the lung and liver at day 6 pi when compared to the non-depleted animals. Infarcts were also observed at this time in D+1 depleted animals. This was the first time that this type of lesion was observed in this model at this early time point. Although they had an increase in cellular infiltrates earlier in the disease course, it did not have a negative impact on survival. Animals that were PMN-depleted on the day prior to infection exhibited similar signs as non-depleted animals with one animal expiring on day 10. In a subsequent experiment animals depleted one day prior to infection had 100% mortality at 10 dpi. The differences observed in these experiments can be partially attributed to the poor stability of my oriental stocks. These experiments were conducted using two different stocks. I feel that the second experiment (0% survival) is more in line with the hypothesis of PMNs being immunomodulators that reduce the tissue damage that could

occur early infection and without PMNs, this tissue damage results in an increased mortality for *Orientia* infected animals. This suggests that PMNs may be crucial for maintaining a balance between infection control and tissue damage.

Animals that were depleted throughout the course of infection had similar signs as non-depleted animals. These animals began to recover weight on day 13, but they continued to have signs until day 19 when the experiment ended. Bacterial load analysis at this time revealed a higher bacterial burden in the lung and kidney of these animals than the other groups at this time. These data suggest that the continuous depletion of PMNs is detrimental to the ability of the host to reduce the bacterial burden as well as its ability to recover from the infection.

Animals that had their PMNs depleted on day 6 pi were relatively healthy by day 12 when two animals of the group were euthanized for histology. As with the outward appearance, the histopathology was nearly normal when compared to non-depleted animals. The liver of the animals depleted of PMNs on day 6 had very few lesions and practically no vasculitis while the non-depleted animals had numerous lesions and extensive vasculitis as described previously. The lungs of these mice were similarly devoid of pathology compared to the non-depleted animals and lacked oriental staining by IF. On day 19 pi, this group had the lowest bacterial burden in the kidney, liver, and lung when compared to the other groups and had surpassed their initial body weight. These data suggest the PMNs recruited on day 6 and later are detrimental to disease outcome.

The results of this aim provide evidence that PMNs may play two distinct roles during the course of scrub typhus: 1) PMNs have an immunomodulatory role early in scrub typhus infection, thus limiting tissue damage while possibly providing a favorable environment, or least less hostile, for the *Orientia* to survive; 2) PMNs that are present on/after day 6 of infection are detrimental to disease outcome, possibly by promoting an overwhelming immune response that results in severe tissue damage without effectively clearing the bacteria. It should be noted that during completion of this aim, an article was

published indicating that the depleting antibody that we used for these studies does not actively deplete PMNs, but instead inhibits their chemotactic capabilities (Wang 2012). More specific staining for alternative PMN markers (work done by Eric Carlsen, in the Soong laboratory) demonstrated the PMNs were still in circulation, but their ability to respond to stimuli or activate has not been assessed. Inhibiting PMN chemotaxis effectively removes them from the site of infection, but if they are still capable of activating and releasing their anti-bacterial payloads indiscriminately creating conditions that we can not account for. Further analysis of the PMNs' functionality must be conducted in order to verify that their general presence in the circulation, but not at the site of infection, does not have deleterious effects.

In conclusion, the completion of this dissertation project has provided a hematogenously disseminated mouse model of human scrub typhus that has pathology, cytokine, and chemokine expression that parallels human disease. This project also has provided solid evidence of PMN involvement in scrub typhus pathogenesis and demonstrated that neutralization of PMNs at disease onset at day 6 pi results in decrease in the fatal disease outcome. Together, these data suggest that the host's immune response, and not direct tissue damage by *Orientia*, determines the disease course in scrub typhus.

Prior to this research project, almost all *in vivo* studies had been conducted using an intraperitoneal inoculation of mice. This model is effective at inducing mortality of infected animals, but stimulates the host immune response in the peritoneum is not observed in human infections. This model results in the infection of the peritoneal surface of the organs in the peritoneum and peritoneal macrophages further stimulating the host's immune response in an artificial manner. Intravenous inoculation of *Orientia* into mice results in endothelial infection similar to that observed in human scrub typhus, although this route bypasses the skin, the natural portal of entry, it results in a target cell tropism the same as a mite transmitted infection. This model will allow for elucidation of the immune mechanisms that may lead to scrub typhus pathology as well as an understanding of the

correlates of protection that occur immediately after infection. Development of this model opens new avenues in scrub typhus research. Although this dissertation project has come to its completion, there are still numerous unresolved questions in the field of scrub typhus research.

### **Future studies**

Now that an accurate model of scrub typhus has been developed and characterized, we can begin determining the immune mechanisms that occur during infection and what factors influence disease outcome. In this study, it was demonstrated that PMNs play a role in scrub typhus, but their role was not elucidated fully. With this in mind, it should be determined how PMNs affect disease outcome by repeating the study in my second aim focusing on D-1 and D+6 depletion, and employing an oriental stock with a very defined concentration so that direct comparisons can be made to the previous experiments. I think it would be interesting to determine whether PMNs actively phagocytose (Abi Abdallah 2011) *Orientia* or if their behavior during infection is mediated by other cellular signals, such as infected endothelial cells or macrophages.

It is possible that PMNs are not directly responsible for the disease course, but rather act through their ability to communicate with other cells that generates a negative influence in severe scrub typhus. Communication between PMNs and NK cells may play a pivotal role in early innate immunity to scrub typhus. There is a growing number of articles that provide evidence for PMN and NK cell cross-talk and that in the absence of PMNs leads to NK cells failure to mature and function properly (Nathan 2006, Costantini and Cassatella 2011, Jaeger 2012). It could be that the depletion of PMNs early in infection

results in poor NK cell activation or differential NK cell activation resulting in aberrant activity that results in the increase of cellular infiltrates observed in this study. This study would require elucidation of the NK cell activation status during scrub typhus infection with and without PMNs in early and late infection. The alternative could be true as well; early immunomodulatory effects of PMNs may inhibit NK cell maturation and function allowing the bacterial infection to persist. The depletion of PMNs on day 6 could possibly remove activated NK cells from the pro-inflammatory response, allowing the host to reduce the collateral tissue damage that could be occurring, which would result in a non-lethal outcome for this disease. Ultimately, an increased understanding of PMN-NK cell cross-talk during *Orientia* infection should be pursued.

Assessment of the role of monocytes, and their subsequent recruitment to sites of infection in dissemination of *Orientia* during infection would increase our understanding of how *Orientia* spread throughout the host. This can be done by using a similar strategy to my PMN-depletion studies. If monocytes actively transport *Orientia* during infection, then their removal should have similar effects to PMN-depletion.

Another aspect I think should be pursued is the role of innate lymphoid cells (ILC) in disease progression and outcome. ILCs are not well understood, but are highly capable of impacting the direction that a disease course will take (**Figure 6.1**). The results from this study suggest that ILCs, particularly group 1 ILCs, may be important in determining the disease outcome in scrub typhus. These cells are relatively abundant and can be found in almost all tissues, and cross-talk between groups of ILCs and other cells may prove important in scrub typhus immunity (Spits 2013).

By studying the host immune response during scrub typhus, we may be able to identify possible biomarkers they predict severity of disease, i.e., the ratio of Angiotensin 1/Angiotensin 2 can be used to predict the severity and outcome of cerebral malaria (Kim H 2011), and a specific cytokine profile can do the same thing. Studying the cytokine/chemokine response during scrub typhus will provide avenues of research that will help us understand what immunological pathways are being triggered, and with this knowledge we could possibly manipulate the host response to effectively clear the infection.

An important, but understudied, phenomenon of scrub typhus, is the short-lived immunity to homologous and heterologous challenge with different *Orientia* strains. Many strains of *Orientia* circulate in the same geographic regions, but infection with one strain only provides 3-6 months of protection against heterologous challenge. Homologous immunity lasts for a couple of years, but wanes over time, allowing individuals to be re-infected. Why this occurs is not understood and is a huge hurdle that needs to be overcome in order to develop an efficacious vaccine for scrub typhus.

*Orientia* has endothelial tropism, but little is known of the events that occur in *Orientia* infected endothelial cells. All studies with an endothelial focus in scrub typhus research have been performed *in vitro* and under static conditions (Cho KA 2010, Cho NH 2001, 2002). These studies demonstrated that upon *Orientia* infection, pro-inflammatory pathways are activated, but they did not evaluate how the endothelial cells and bacteria interact. Endothelial cells under static conditions behave differently than those under sheer stress induced by blood flow (Ziegler 1994, Stanness 1996, Yuan 2011); thus, these studies need to be repeated in a system that mimics the *in vivo* environment (Strelow 2002) to

ensure that the endothelial signaling that was observed was not a product of the experimental design. Continuing with the endothelial theme, I think it would be important to study the interaction of infected endothelial cells with innate immune cells to determine how this communication affects vascular permeability and its role in scrub typhus pathology.

Ultimately, characterization of a mite-transmission model for scrub typhus would be the most important advance in scrub typhus research. This model would eliminate the need for other models as all of the factors involved in scrub typhus infections would be present in one model instead of researchers having to extrapolate from models that bypass the initial site of infection. With a mite-transmission model, we could study the immunological events occurring at the site of infection as well as how the *Orientia* disseminates, but until that model is developed and characterized, the intravenous inoculation of *Orientia tsutsugamushi* provides the most potent research tool in understanding the complex immune reactions that occur during scrub typhus infection.

Any one of these studies could provide for a solid research career in scrub typhus and emerging infectious disease. It is my hope to continue on these research avenues because an understanding of the underlying immunological events that occur during scrub typhus infections will produce promising avenues for vaccine development.



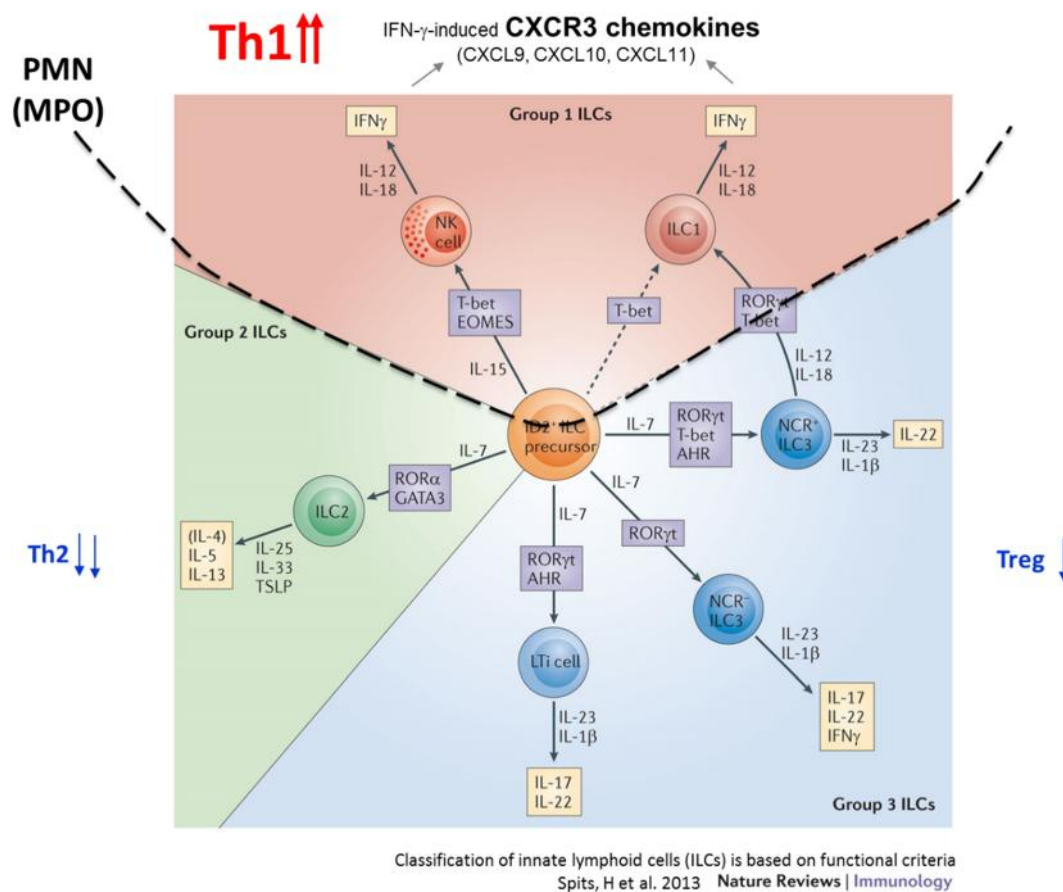


**Figure 6.1: The role of ILCs in promotion of a Th-1 response in scrub typhus.<sup>4</sup>**

Image modified from Spits *et al.* 2013. Appropriate stimulation of ILCs during *Orientia* infection may promote a Th-1 response resulting in the disease pathology of scrub typhus.

<sup>4</sup> Modified from Spits *et al.* 2013 with permission from Nature Publishing Group (NPG).

## REFERENCES

- Abi Abdallah DS, Egan CE, Butcher BA, Denkers EY (2011). Mouse neutrophils are professional antigen-presenting cells programmed to instruct T<sub>h</sub>1 and T<sub>h</sub>17 T-cell differentiation. *Int Immunol* 23(5): 317-326.
- Abi Abdallah DS, Denkers EY (2012). Neutrophils cast extracellular traps in response to protozoan parasites. *Front Immunol* 3: 382.
- Allen AC and Spitz S (1945). A comparative study of the pathology of scrub typhus (tsutsugamushi disease) and other rickettsial diseases. *Am J Pathol* 21(4): 603-681.
- Audy JR (1947). Scrub typhus as a study in ecology. *Nature* 159: 295-96.
- Ben RJ, Feng NH, Ku CS (1999). Meningoencephalitis, myocarditis and disseminated intravascular coagulation in a patient with scrub typhus. *J Microbiol Immunol Infect* 32(1): 57-62.
- Bergsbaken T and Cookson BT (2009). Innate immune response during *Yersinia* infection: critical modulation of cell death mechanisms through phagocyte activation. *J Leukc Biol* 86(5): 1153-1158.
- Berman SJ and Kundin WD (1973). Scrub typhus in South Vietnam. A study of 87 cases. *Ann Intern Med* 79(1): 26-30.
- Bourgeois AL, Olson JG, Fang RCY, Huang J, Wang CL, *et al.* (1982). Humoral and cellular responses in scrub typhus patients reflecting primary infection and reinfection with *Rickettsia tsutsugamushi*. *Am J Trop Med Hyg* 31(3 Pt 1): 532-540.
- Carl M, Ching WM, Dasch GA (1988). Recognition of typhus group rickettsia-infected targets by human lymphokine-activated killer cells. *Infect Immun* 56(9): 2526-2529.
- Catanzaro PJ, Shirai A, Hilderbrandt PK, Osterman JV (1976). Host defenses in experimental scrub typhus: histopathological correlates. *Infect Immun* 13(3): 861-875.
- Catanzaro PJ, Shirai A, Agniel LD, Osterman JV (1977). Host defenses in experimental scrub typhus: role of spleen and peritoneal exudate lymphocytes in cellular immunity. *Infect Immun* 18(1): 118-123.

- Chattopadhyay S and Richards AL (2007). Scrub typhus vaccines: past history and recent developments. *Hum Vaccin* 3(3): 73-80.
- Chattopadhyay S, Jiang J, Chan TK, Manetz TS, Chao CC, *et al.* (2005). Scrub typhus vaccine candidate Kp r56 induces humoral and cellular immune responses in cynomolgus monkeys. *Infect Immun* 73(8): 5039-5047.
- Cho BA, Cho NH, Seong SY, Choi MS, Kim IS (2010). Intracellular invasion by *Orientia tsutsugamushi* is mediated by integrin signaling and actin cytoskeleton re-arrangements. *Infect Immun* 78(5): 1915-1923.
- Cho KA, Jun YH, Suh JW, Kang JS, Choi HJ, Woo SY (2010). *Orientia tsutsugamushi* induced endothelial cell activation via the NOD1-IL-32 pathway. *Microbial Pathog* 49(3): 95-104.
- Cho NH, Seong SY, Huh MS, Han TH, Koh YS, *et al.* (2000). Expression of chemokine genes in murine macrophages infected with *Orientia tsutsugamushi*. *Infect Immun* 68(2): 594-602.
- Cho NH, Seong SY, Choi MS, Kim IS (2001). Expression of chemokine genes in human dermal microvascular endothelial cell lines infected with *Orientia tsutsugamushi*. *Infect Immun* 69(3): 1265-1272.
- Cho NH, Seong SY, Huh MS, Kim NH, Choi MS, Kim IS (2002). Induction of the gene encoding macrophage chemoattractant protein 1 by *Orientia tsutsugamushi* in human endothelial cells involves activation of transcription factor activator protein 1. *Infect Immun* 70(9): 4841-4850.
- Chrispal AH, Boorugu H, Gopinath KG, Prakash JAJ, Chandy S, *et al.* (2010). Scrub typhus: an unrecognized threat in South India - clinical profile and predictors of mortality. *Trop Doct* 40(3): 129-133.
- Chu H, Lee JH, Han SH, Kim SY, Cho NH, *et al.* (2006). Exploitation of the endocytic pathway by *Orientia tsutsugamushi* in nonprofessional phagocytes. *Infect Immun* 74(7): 4246-4253.
- Chung DR, Lee YS, Lee SS (2008). Kinetics of inflammatory cytokines in patients with scrub typhus receiving doxycycline treatment. *J Infect* 56(1): 44-50.
- Costantini C and Cassatella MA (2011). The defensive alliance between neutrophils and NK cells as a novel arm of innate immunity. *J Leukoc Biol* 89(2): 221-233.
- de Fost M, Chierakul W, Pimda K, Dondorp AM, White NJ, Poll TVD (2005). Activation of cytotoxic lymphocytes in patients with scrub typhus. *Am J Trop Med Hyg* 72(4): 465-467.

- Ewing EP, Takeuchi A, Shirai A, Osterman JV (1978). Experimental infection of mouse peritoneal mesothelium with scrub typhus rickettsiae: an ultrastructural study. *Infect Immun* 19(3): 1068-1075.
- Feng HM, Lo LJ, Shih-en P (1964). Tissue culture of *Rickettsia tsutsugamushi*. ii. Rabbit testis monolayer tissue culture for cultivation of *Rickettsia tsutsugamushi*. *Sci Sin* 13: 1275-1279.
- Feng HM and Walker DH (1993a). Interferon-gamma and tumor necrosis factor-alpha exert their antirickettsial effect via induction of synthesis of nitric oxide. *Am J Pathol*. 143(4): 1016-23.
- Feng HM, Wen J, Walker DH (1993b). *Rickettsia australis* infection: a murine model of a highly invasive vasculopathic rickettsiosis. *Am J Pathol* 142(5): 1471-1482.
- Feng HM, Popov VL, Walker DH (1994). Depletion of gamma interferon and tumor necrosis factor alpha in mice with *Rickettsia conorii*-infected endothelium: impairment of rickettsicidal nitric oxide production resulting in fatal, overwhelming rickettsial disease. *Infect Immun* 62(5): 1952-1960.
- Feng HM and Walker DH (2000). Mechanisms of intracellular killing of *Rickettsia conorii* in infected human endothelial cells, hepatocytes, and macrophages. *Infect Immun* 68(12): 6729-6736.
- Frances SP, Watcharapichat P, Phulsuksombati D (2001). Vertical transmission of *Orientia tsutsugamushi* in two lines of naturally infected *Leptotrombidium deliense* (Acari: Trombiculidae). *J Med Entomol* 38(1): 17-21.
- Ge Y and Rikihisa Y (2011). Subversion of host cell signaling by *Orientia tsutsugamushi*. *Microbes Infect* 13(7): 638-648.
- Geng P and Jerrells TR (1994). The role of tumor necrosis factor in host defense against scrub typhus rickettsiae. I. Inhibition of growth of *Rickettsia tsutsugamushi*, Karp strain, in cultured murine embryonic cells and macrophages by recombinant tumor necrosis factor-alpha. *Microbiol Immunol* 38(9): 703-711.
- Granger DN and Senchenkova E (2010). Inflammation and the microcirculation. Integrated Systems Physiology—From Cell to Function #8. D. N. Granger and J. Granger editors. Morgan & Claypool Publishers. ISBN: 9781615041664.
- Groves MG and Kelly DJ (1989). Characterization of factors determining *Rickettsia tsutsugamushi* pathogenicity for mice. *Infect Immun* 57(5): 1476-1482.
- Groves MG and Osterman JV (1978). Host defenses in experimental scrub typhus: Genetics of natural resistance to infection. *Infect Immun* 19(2): 583-588.

- Hanson B (1991a). Comparative susceptibility to mouse interferons of *Rickettsia tsutsugamushi* strains with different virulence in mice and of *Rickettsia rickettsii*. *Infect Immun* 59(11): 4134-4141.
- Hanson B (1991b). Susceptibility of *Rickettsia tsutsugamushi* Gilliam to gamma interferon in cultured mouse cells. *Infect Immun* 59(11): 4125-4133.
- Harkness JE and Wagner JE (1989). The Biology and Medicine of Rabbits and Rodents. 3<sup>rd</sup> ed. Lea & Febiger; Philadelphia, PA.
- Hsu YH and Chen HI (2008). Pulmonary pathology in patients associated with scrub typhus. *Pathology* 40(3): 268-271.
- Ikedo M, Takahashi H, Yoshida S (1994). HLA-DR<sup>+</sup> CD3<sup>+</sup> and CD8<sup>+</sup> cells are increased but CD4<sup>+</sup> CD45RA<sup>+</sup> cells are reduced in the peripheral blood in human scrub typhus. *Clin Immunol Immunopathol* 72(3): 402-04.
- Irons NE (1946). Clinical and laboratory variation of virulence in scrub typhus. *Am J Trop Med Hyg* 26: 165-174.
- Iwasaki H, Mizoguchi J, Takada N, Tai K, Ikegaya S, Ueda T (2010). Correlation between the concentrations of tumor necrosis factor-alpha and the severity of disease in patients infected with *Orientia tsutsugamushi*. *Int J Infect Dis* 14(4): e328-333.
- Iwasaki H, Takada N, Nakamura T, Ueda T (1997). Increased levels of macrophage colony-stimulating factor, gamma interferon, and tumor necrosis factor alpha in sera of patients with *Orientia tsutsugamushi* infection. *J Clin Microbiol* 35(12): 3320-3322.
- Jaeger BN, Donadieu J, Cognet, C, Bernat C, Ordonez-Rueda D, *et al.* (2012). Neutrophil depletion impairs natural killer cell maturation, function, and homeostasis. *J Exp Med* 209(3): 565-580.
- Jeong YJ, Kim S, Wook TD, Lee JW, Kim KI, Lee SH (2007). Scrub typhus: clinical, pathologic, and imaging findings. *Radiographics* 27(1): 161-172.
- Jerrells TR (1985). Immunosuppression associated with the development of chronic infections with *Rickettsia tsutsugamushi*: adherent suppressor cell activity and macrophage activation. *Infect Immun* 50(1): 175-182.
- Jerrells TR and Eisemann CS (1983). Role of T-lymphocytes in production of antibody to antigens of *Rickettsia tsutsugamushi* and other *Rickettsia* species. *Infect Immun* 41(2): 666-674.

- Jerrells TR and Osterman JV (1981). Host defenses in experimental scrub typhus: inflammatory response of congenic C3H mice differing at the Ric gene. *Infect Immun* 31(3): 1014-1022.
- Jerrells TR and Osterman JV (1982). Role of macrophages in innate and acquired host resistance to experimental scrub typhus infection of inbred mice. *Infect Immun* 37(3): 1066-1073.
- Jerrells TR and Osterman JV (1983a). Development of specific and cross-reactive lymphocyte proliferative responses during chronic immunizing infections with *Rickettsia tsutsugamushi*. *Infect Immun* 40(1): 147-156.
- Jerrells TR and Osterman JV (1983b). Parameters of cellular immunity in acute and chronic *Rickettsia tsutsugamushi* infections of inbred mice. *Adv Exp Med Biol* 162: 355-360.
- Jerrells TR and Geng P (1994). The role of tumor necrosis factor in host defense against scrub typhus rickettsiae. II. Differential induction of tumor necrosis factor-alpha production by *Rickettsia tsutsugamushi* and *Rickettsia conorii*. *Microbiol Immunol* 38(9): 713-719.
- Jiang J, Chan TC, Temenak JJ, Dasch GA, Ching WM, Richards AL (2004). Development of a quantitative real-time polymerase chain reaction assay specific for *Orientia tsutsugamushi*. *Am J Trop Med Hyg* 70(4): 351-356.
- Kasuya S, Nagano I, Ikeda T, Goto C, Shimokawa K, Takahashi Y (1996). Apoptosis of lymphocytes in mice induced by infection with *Rickettsia tsutsugamushi*. *Infect Immun* 64(9): 3937-3941.
- Kee SH, Cho KA, Kim MK, Lim BU, Chang WH, Kang JS (1999). Disassembly of focal adhesions during apoptosis of endothelial cell line ECV304 infected with *Orientia tsutsugamushi*. *Microb Pathog* 27(5): 265-271.
- Kelly DJ, Fuerst PA, *et al.* (2009). Scrub typhus: the geographic distribution of phenotypic and genotypic variants of *Orientia tsutsugamushi*. *Clin Infect Dis* 48 Suppl 3: S203-230.
- Kelly DJ, Richards AL, Temenak J, Strickman D, Dasch GA (2002). The past and present threat of rickettsial diseases to military medicine and international public health. *Clin Infect Dis* 34(Suppl 4): S145-169.
- Kim DM, Kim SW, Choi SH, Yun NR (2010). Clinical and laboratory findings associated with severe scrub typhus. *BMC Infect Dis* 10: 108.

- Kim H, Higgins S, Liles WC, Kain KC (2011). Endothelial activation and dysregulation in malaria: a potential target for novel therapeutics. *Curr Opin Hematol* 18: 177-185.
- Kim MJ, Kim MK, Kang JS (2006). *Orientia tsutsugamushi* inhibits tumor necrosis factor alpha production by inducing interleukin 10 secretion in murine macrophages. *Microb Pathog* 40(1): 1-7.
- Kim MK, Seong SY, Seoh JY, Han TH, Song HJ, *et al.* (2002). *Orientia tsutsugamushi* inhibits apoptosis of macrophages by retarding intracellular calcium release. *Infect Immun* 70(8): 4692-4696.
- Kim MK, Kee SH, Cho KA, Chung MH, Lim BU, *et al.* (1999). Apoptosis of endothelial cell line ECV304 persistently infected with *Orientia tsutsugamushi*. *Microbiol Immunol* 43(8): 751-757.
- Koh YS, Yun JH, Seong SY, Choi MS, Kim IS (2004). Chemokine and cytokine production during *Orientia tsutsugamushi* infection in mice. *Microb Pathog* 36(1): 51-57.
- Kolaczowska E and Kubes P (2013). Neutrophil recruitment and function in health and inflammation. *Nat Rev Immunol* 13(3): 159-175.
- Kouwenaar W and Esseveld H (1948). The nature of immunity against scrub typhus in guinea-pigs. *Qt. J Trop Med Hyg* 1(1): 34-40.
- Kramme S, An le V, Khoa ND, Trin Le V, Tannich E, *et al.* (2009). *Orientia tsutsugamushi* bacteremia and cytokine levels in Vietnamese scrub typhus patients. *J Clin Microbiol* 47(3): 586-589.
- Kundin WD, Liu C, Harmon P, Rodina P (1964). Pathogenesis of scrub typhus infection (*Rickettsia tsutsugamushi*) as studied by immunofluorescence. *J Immunol*. Nov 93: 772-81.
- Kundin WD and Jones GS (1972). Isolation of *Rickettsia tsutsugamushi* from rodents, insectivores, carnivores, and ectoparasites from Danang, South Vietnam. *Southeast Asian J Trop Med Public Health* 3(3): 310-313.
- Lee JH, Cho NH, Kim SY, Bang SY, Chu H, *et al.* (2008). Fibronectin facilitates the invasion of *Orientia tsutsugamushi* into host cells through interaction with a 56-kDa type-specific antigen. *J Infect Dis* 198(2): 250-257.
- Levine HD (1946). Pathologic study of thirty-one cases of scrub typhus fever with especial reference to the cardiovascular system. *Am Heart Jd Mar* 31: 314-328.

- Lim TS, Twartz JC, Groves MG (1986). Suppression of lymphocyte responsiveness during acute *Rickettsia tsutsugamushi* infection in mice. Jpn J Med Sci Biol 39(3): 129-138.
- Luna-Gomes T, Filardy AA, Rocha JDB, Decote-Ricardo D, LaRocque-de-Freitas IF, *et al.* (2014). Neutrophils increase or reduce parasite burden in *Trypanosoma cruzi*-infected macrophages, depending on host strain: Role of neutrophil elastase. PLoS One 9(3): e90582.
- Moron CG, Popov VL, Feng HM, Wear D, Walker DH (2001). Identification of the target cells of *Orientia tsutsugamushi* in human cases of scrub typhus. Mod Pathol 14(8): 752-759.
- Murata M, Sudo K, Suzuki K, Aoyama Y, Nogami S, *et al.* (1985). Proliferating sites of *Rickettsia tsutsugamushi* in mice by different routes of inoculation evidenced with immunofluorescence. Jpn J Exp Med 55(5): 193-199.
- Nacy CA (1983). Activation of macrophages for killing of rickettsiae: analysis of macrophage effector function after rickettsial inoculation of inbred mouse strains. Adv Exp Med Bio 162: 335-53.
- Nacy CA and Osterman JV (1979). Host defenses in experimental scrub typhus: role of normal and activated macrophages. Infect Immun 26(2): 744-750.
- Nacy CA and Groves MG (1981). Macrophages in resistance to rickettsial infections: early host defense mechanisms in experimental scrub typhus. Infect Immun 31(3): 1239-1250.
- Nacy CA and Meltzer MS (1979). Macrophages in resistance to rickettsial infection: macrophage activation in vitro for killing of *Rickettsia tsutsugamushi*. J Immunol 123(6): 2544-2549.
- Nagayo M, Miyagawa Y, Mitamura T, Imamura A (1917). On the nymph and prosopon of the tsutsugamushi, *Leptotrombidium akamushi*, n. sp. (*Trombidium akamushi brumpti*), carrier of the tsutsugamushi disease. J Ex Med 25(2): 255-77.
- Nagayo M, Tamiya T, Mitamura T, Sato K (1939). On the virus of tsutsugamushi disease and its demonstration by a new method. J Ex Med 8: 309-17.
- Nathan C (2006). Neutrophils and immunity: challenges and opportunities. Nat Rev Immunol 6(3): 173-182.
- Ni YS, Chan TC, Chao CC, Richards AL, Dasch GA, Ching WM (2005). Protection against scrub typhus by a plasmid vaccine encoding the 56-KD outer membrane protein antigen gene. Am J Trop Med Hyg 73(5): 936-941.



- Niu D, Chen W, Zhang X, Chen M, Cui H, Wei W, Wen B, Chen X (2003). Immunogenicity of a 40 kDa fragment of the 47 kDa recombinant protein and DNA vaccine from Karp strain of *Orientia tsutsugamushi*. *Ann N Y Acad Sci* 990: 527-534.
- Oaks SC Jr, Ng FK, Elwell MR, Groves MG, Lewis GE Jr (1985). Pathology of toxic death in mice following intravenous injection of *Rickettsia tsutsugamushi* strain Gilliam: examination by light and scanning electron microscopy. *Jpn J Med Sci Biol* 38(2): 67-72.
- Ohashi N, Fukuhara M, Shimada M, Tamura A (1995). Phylogenetic position of *Rickettsia tsutsugamushi* and the relationship among its antigenic variants by analyses of 16S rRNA gene sequences. *FEMS Microbio Lett.* 125(2-3): 299-304.
- Palmer BA, Hetrick FM, Jerrells TR (1984). Production of gamma interferon in mice immune to *Rickettsia tsutsugamushi*. *Infect Immun* 43(1): 59-65.
- Palmer BA, Hetrick FM, Jerrells TR (1984). Gamma interferon production in response to homologous and heterologous strain antigens in mice chronically infected with *Rickettsia tsutsugamushi*. *Infect Immun* 46(1): 237-244.
- Paris DH, Jenjaroen K, Blacksell SD, Phetsouvanh R, Wuthiekanun V, *et al.* (2008). Differential patterns of endothelial and leucocyte activation in 'typhus-like' illnesses in Laos and Thailand. *Clin Exp Immun* 153(1): 63-67.
- Paris DH, Phetsouvanh R, Tanganuchitcharnchai A, Jones M, Jenjaroen K, *et al.* (2012). *Orientia tsutsugamushi* in human scrub typhus eschars shows tropism for dendritic cells and monocytes rather than endothelium. *PLoS Negl Trop Dis* 6(1): e1466.
- Paris DH, Shelite TR, Day NP, Walker DH (2013). Unresolved problems related to scrub typhus: a seriously neglected life-threatening disease. *Am J Trop Med Hyg* 89(2): 301-307.
- Park JS, Jee YK, Lee KY, Kim KY, Myong NH, *et al.* (2000). Acute respiratory distress syndrome associated with scrub typhus: diffuse alveolar damage without pulmonary vasculitis. *J Korean Med Sci* 15(3): 343-345.
- Payne AF, Binduga-Gajewska I, Kauffman EB, Kramer LD (2006). Quantitation of flaviviruses by fluorescent focus assay. *J Virol Methods* 134(1-2): 183-189.
- Phommasone K, Paris DH, Anantatat T, Castonguay-Vanier J, Keomany S, *et al.* Concurrent infection with murine typhus and scrub typhus in southern Laos—the mixed and the unmixed. *PLoS Negl Trop Dis* 7(8): e2163.

- Ribeiro-Gomes FL, Otero AC, Gomes NA, Moniz-De-Souza MCA, Cysne-Finkelstein L, *et al.* (2004) Macrophage interactions with neutrophils regulate *Leishmania major* infection. *J Immunol* 172: 4454–4462.
- Rights FL and Smadel JE (1948). Studies on scrub typhus (Tsutsugamushi disease) III. Heterogenicity of strains of *R. tsutsugamushi* as demonstrated by cross-vaccination studies. *J Exp Med* 87(4): 339-351.
- Rikihisa Y and Ito S (1979). Intracellular localization of *Rickettsia tsutsugamushi* in polymorphonuclear leukocytes. *J Exp Med* 150(3): 703-708.
- Rikihisa Y and Ito S (1982). Entry of *Rickettsia tsutsugamushi* into polymorphonuclear leukocytes. *Infect Immun* 38(1): 343-350.
- Rollwagen FM, Dasch GA, Jerrells TR (1986). Mechanisms of immunity to rickettsial infection: characterization of a cytotoxic effector cell. *J Immunol* 136(4): 1418-1421.
- Saunders JP, Brown GW, Shirai A, Huxsoll DL (1980). The longevity of antibody to *Rickettsia tsutsugamushi* in patients with confirmed scrub typhus. *Trans R Soc Trop Med Hyg* 74(2): 253-257.
- Sayen JJ, Pond H, Forrester JS, Wood FC (1946). Scrub typhus in Assam and Burma: A clinical study of 616 cases. *Medicine* 25(2): 155-214.
- Shieh GJ, Chen HL, Chen HY, Horng CB (1995). Detection of *Rickettsia tsutsugamushi* specific DNA from the lymphocyte of patients by polymerase chain reaction. *Proc Natl Sci Counc Repub China B* 19(1): 43-46.
- Shirai A, Catanzaro PJ, Phillips SM, Osterman JV (1976). Host defenses in experimental scrub typhus: role of cellular immunity in heterologous protection. *Infect Immun* 14(1): 39-46.
- Shirai A, Huxsoll DL, Montrey RD, Werner RM, Arimbalam S (1979a). Experimental *Rickettsia tsutsugamushi* infections in dogs. *Jpn J Med Sci Biol* 32(3): 175-178.
- Shirai A, Montrey RD, Werner RM, Arimbalam S, Huxoll DL (1979b). Clinical responses of silvered leaf monkeys to infection with selected strains of *Rickettsia tsutsugamushi*. *J Infect Dis* 140(5): 811-814.
- Shirai A, Saunders JP, Dohany AL, Huxsoll DL, Groves MG (1982). Transmission of scrub typhus to human volunteers by laboratory-reared chiggers. *Jpn J Med Sci Biol* 35(1): 9-16.

- Sirisanthana V, Puthanakit T, Sirisanthana T (2003). Epidemiologic, clinical and laboratory features of scrub typhus in thirty Thai children. *Pediatr Infect Dis J* 22(4): 341-345.
- Spits H, Artis D, Colonna M, Dieffenbach A, Di Santo JP, *et al.* (2013). Innate lymphoid cells—a proposal for uniform nomenclature. *Nat Rev Immunol* 13(2): 145-149.
- Stanness KA, Guatteo E, Janigro D (1996). Dynamic model of the blood-brain barrier in vitro. *Neurotoxicology* Summer 17(2): 481-96.
- Strelow L, Janigro D, Nelson JA (2002). Persistent SIV infection of a blood-brain barrier model. *J Neurovirol* 8(4): 270-280.
- Tamura A (1988). Invasion and intracellular growth of *Rickettsia tsutsugamushi*. *Micrbiol Sci* 5(8): 228-232.
- Tamura A, Ohashi N, Urakami H, Miyamura S (1995). Classification of *Rickettsia tsutsugamushi* in a new genus, *Orientia* gen. nov., as *Orientia tsutsugamushi* comb. nov. *Int J Syst Bacteriol* 45(3): 589-591.
- Traub R, Wisseman CL Jr, Jones MR, O’Keefe JJ (1975). The acquisition of *Rickettsia tsutsugamushi* by chiggers (trombiculid mites) during the feeding process. *Ann N Y Acad Sci* 266: 91--114.
- Walker DH, Popov VL, Wen J, Feng HM (1994). *Rickettsia conorii* infection of C3H/HeN mice. A model of endothelial-target rickettsiosis. *Lab Invest* 70(3): 358-68.
- Walker DH, Popov VL, Crocquet-Valdes PA, Welsh CJ, Feng HM (1997). Cytokine-induced, nitric oxide-dependent, intracellular antirickettsial activity of mouse endothelial cells. *Lab Invest* 76(1): 129-38.
- Walker DH, Popov VL, Feng HM (2000). Establishment of a novel endothelial target mouse model of a typhus group rickettsiosis: Evidence for critical roles for gamma interferon and CD8 T lymphocytes. *Lab Invest* 80(9): 1361-1372.
- Wang JX, Bair AM, King SL, Shnayder R, Huang YF, *et al.* (2012). Ly6G ligation blocks recruitment of neutrophils via a  $\alpha$ 2-integrin-dependent mechanism. *Blood* 120: 1489-1498.
- Woods ME and Olano JP (2008). Host defenses to *Rickettsia rickettsii* infection contribute to increased microvascular permeability in human cerebral endothelial cells. *J Clin Immunol* 28(2): 174-185.
- Xu G, Chattopadhyay S, Jiang J, Chan TC, Chao CC, *et al.* (2005). Short- and long-term immune responses of CD-1 outbred mice to the scrub typhus DNA vaccine candidate: p47Kp. *Ann N Y Acad Sci* 1063: 266-269.

- Yuan SY and Rigor RR (2011). Regulation of endothelial barrier function. Integrated Systems Physiology: From Molecule to Function to Disease. D. N. Granger and J. Granger editors. Morgan & Claypool Publishing. ISBN: 9781615041213.
- Yun JH, Koh YS, Lee KH, Hyun JW, Choi YJ, *et al.* (2005). Chemokine and cytokine production in susceptible C3H/HeN mice and resistant BALB/c mice during *Orientia tsutsugamushi* infection. *Microbiol Immunol* 49(6): 551-557.
- Yun JH, Koo JE, Koh YS (2009). Mitogen-activated protein kinases are involved in tumor necrosis factor alpha production in macrophages infected with *Orientia tsutsugamushi*. *Microbiol Immunol* 53(6): 349-355.
- Zarafonetis CJD (1945). The susceptibility of the rodents, *Gerbillus pyramidum* and *Gerbillus gerbillus*, to experimental Tsutsugamushi infection (Scrub typhus). *Proc Soc Exp Biol Med*. 59: 113-116.-116.
- Ziegler T and Nerem RM (1994). Effect of flow on the process of endothelial cell division. *Arterioscler Thromb* 14(4): 636-643.

## VITA

Thomas Robert Shelite was born on October 23, 1980 in Hutchinson, Kansas to Bobbie L. and Barbara A. Shelite. Thomas graduated from Pratt High School in Pratt, Kansas in 1999, and attended Pratt Community College on the Above and Beyond Scholarship. He received his Associates of Science degree in May 2001 and then transferred to Wichita State University (WSU), Wichita, Kansas where he was awarded a Bachelor of Science degree in biological sciences in December 2003. Thomas continued at Wichita State, earning a Master of Science degree in biological sciences, with an emphasis on ecology and epidemiology of West Nile virus, May 2006. While attending WSU, Thomas taught microbiology laboratories to undergraduate biology majors and nursing students. He also taught laboratories for anatomy and physiology and ecology courses while doing his research. In August 2006, Thomas enrolled at the University of Texas-Medical Branch in the Ph.D. program.

While at UTMB, Thomas was awarded a T32 Biodefense Training grant that provided support for two years. After entering UTMB, Thomas became a member of American Association for the Advancement of Science (AAAS), American Society for Microbiology (ASM), American Society for Rickettsiology (ASR), American Society of Tropical Medicine and Hygiene (ASTMH), and International Society of Infectious Diseases (ISID). As a Blomberg Scholar, Thomas has mentored three Ball High School students in the UTMB Bench Mentor program where he received the Robert C. Braiser Award for Outstanding Performance as a Bench Tutorial; Scientific Research and Design Mentor. Thomas has collaborated on several research projects while working on his Ph.D.

that has resulted in eight papers which he was a co-author. In addition to his work at UTMB, Thomas is the primary caregiver for his 15-year old nephew.

Permanent address: 8100 Seawall Blvd Apt 319  
Galveston, TX 77551  
Email address: tshelite@hotmail.com

#### Education

Associates of Science, May 2001, Pratt Community College, Pratt, KS  
B.S., Dec 2003, Wichita State University, Wichita, KS  
M.S., May 2006, Wichita State University, Wichita, KS; MS

#### Publications

Saito TB, Thirumalapura N, **SHELITE TR**, Brower D, Walker DH. *Ehrlichia muris*-like infection of mice as model of a newly emerging monocytotropic ehrlichiosis. Manuscript to be submitted to Journal of Infectious Diseases April 2014.

**SHELITE TR**, Saito TB, Mendell NL, Gong B, Xu G, Soong L, Valbuena G, Bouyer DH, Walker DH. A hematogenously disseminated *Orientia tsutsugamushi* infected mouse model of scrub typhus. Manuscript submitted to PLoS Neglected Tropical Diseases March 2014.

Soong L\*, Wang H\*, **SHELITE TR**\*, Mendel NL, Valbuena GA, Bouyer DH, Walker DH. Elevated type 1 cytokines and repressed type 2 immune modulators at early *Orientia tsutsugamushi* infection in mice contribute to disease pathogenesis. Manuscript to be submitted to Infection and Immunity April 2014 (\*equal contribution).

Gong B, **SHELITE TR**, Mei FC, Ha T, Xu G, Chang Q, Hu Y, Wakamiya M, Ksiazek TK, Boor P, Bouyer DH, Popov VL, Chen J, Walker DH, Cheng X. Exchange protein directly activated by cAMP plays a critical role in bacterial invasion during fatal rickettsioses, Proc Natl Acad Sci Nov 2013; 110(48): 19615-620.

Paris DH, **SHELITE TR**, Day N, Walker DH. Unresolved problems related to scrub typhus: A seriously neglected life-threatening disease. Am J Trop Med Hyg 2013 Aug; 89(2): 301-307.

Gong B, Lee YS, Lee I, **SHELITE T**, Kunkeaw N, Xu G, Lee K, Jeon SH, Johnson B, Chang Q, Ha Ha T, Mendell N, Bouyer D, Boor P, Ksiazek T, Walker DH. Compartmentalized, functional role of angiogenin during spotted fever group rickettsia-induced endothelial barrier dysfunction: Evidence of possible mediation by tRNA-derived small noncoding RNAs. BMC Infectious Diseases June 23; 13: 285.

Gong B, Ma L, Liu Y, Gong Q, **SHELITE T**, Bouyer D, Boor PJ, Lee YS, Oberhauser A spotted fever group rickettsiae induce microvascular hyperpermeability via phosphorylation of VE-cadherins: Evidence from atomic force microscopy and biochemical studies in human cerebral microvascular endothelial cells. PLoS Negl Trop Dis. 2012 Jun; 6 (6): e1699.

Xin L, **SHELITE TR**, Gong B, Soong L, Fang R, Walker DH. Systemic treatment with CpG-B after sublethal rickettsial infection induces mouse death through indoleamine 2,3-dioxygenase (IDO). PLoS ONE 2012 Mar; 7(3): e34062.

Oliveira KA, Pinter A, Medina-Sanchez A, Boppana VD, Wikel SK, Saito TB, **SHELITE T**, Blanton L, Popov V, Teel PD, Walker DH, Galvao MA, Mafra C, Bouyer DH. *Amblyomma imitator* ticks as vectors of *Rickettsia rickettsii*, Mexico. Emerg Infect Dis. 2010 Aug;16(8):1282-4.

Fang R, Ismail N, **SHELITE T**, Walker DH. CD4+CD25+Foxp3- T regulatory cells produce both IFN- and IL-10 during acute severe murine spotted fever rickettsiosis. Infect Immun. 2009 Sep 77(9):3838-49.

**SHELITE TR**, Rogers CM, Litzner BR, Johnson RR, Schneegurt MA. 2008. West Nile virus antibodies in permanent resident and overwintering migrant birds in south-central Kansas. Vector-borne and Zoonotic Diseases. (8)3: 321-29.

## Abstracts

**Shelite TR**, Mendell NL, Xu G, Carlsen E, Gong B, Valbuena GA, Bouyer DH, Soong L, Walker DH. Neutrophils exhibit Janus-like behavior during *Orientia tsutsugamushi* infection in a murine model of scrub typhus. American Society of Tropical Medicine and Hygiene, November 2013.

Xu G\*, **Shelite TR**, Mendell NL, Goetz-Rivillas Y, Gong B, Valbuena GA, Soong L, Olano JP, Walker DH, Bouyer DH. Studies of *Orientia tsutsugamushi* persistence in newly developed animal models. American Society of Tropical Medicine and Hygiene, November 2013.

**Shelite TR**, Mendell NL, Xu G, Carlsen E, Gong B, Valbuena GA, Bouyer DH, Soong L, Walker DH. The Janus-like behavior of neutrophils during scrub typhus infection. American Society for Rickettsiology June 2013

Gong B, **Shelite TR**, Chang Q, Ha TH, Xu G, Mendell N, Cheng X, Bouyer D, Boor PJ, Walker DH. Compartmentalized, functional role of angiogenin in rickettsia-induced endothelial barrier dysfunction. American Society for Rickettsiology June 2013

Mendell NL\*, Goetz-Rivillas Y, Brouwer D, **Shelite TR**, Xu G, Gong B, Valbuena GA, Soong L, Olano JP, Walker DH, Bouyer DH. Assessment of the efficacy of antibiotics in an intradermal mouse model of scrub typhus. American Society for Rickettsiology June 2013

Xu G\*, **Shelite T**, Mendell NL, Brouwer D, Walker DH, Bouyer DH. Studies of *Orientia tsutsugamushi* persistence in newly developed animal models. American Society for Rickettsiology June 2013

**Shelite TR**, Mendell NL, Xu G, Gong B, Soong L, Walker DH. Friend, foe, or both? The Janus-like behavior of neutrophils during scrub typhus infection. Experimental Pathology Day. May 2013

Mendell NL\*, Goetz-Rivillas Y, Brouwer D, **Shelite TR**, Xu G, Gong B, Valbuena GA, Soong L, Olano JP, Walker DH, Bouyer DH. Characterizing the histopathology of intradermal infection model of human scrub typhus disease. Experimental Pathology Day. May 2013

Xu G\*, **Shelite T**, Mendell NL, Brouwer D, Walker DH, Bouyer DH. Persistence of *Orientia tsutsugamushi* in a newly developed intradermally inoculated mouse model. Experimental Pathology Day. May 2013

**Shelite TR**, Mendell NL, Xu G, Gong B, Soong L, Walker DH. Friend, foe, or both? The Janus-like behavior of neutrophils during scrub typhus infection. IHII/McLaughlin Symposium, March 2013.

Xu G, **Shelite TR**, Mendell NL, Brouwer D, Goetz-Rivillas Y, Gong G, Soong L, Olano JP, Valbuena GA, Walker DH, Bouyer DH. Studies of *Orientia tsutsugamushi* persistence in newly developed animal models. IHII/McLaughlin Symposium, March 2013.

**Shelite TR\***, Saito TB, Xu G, Gong B, Walker DH. Characterization of a murine model for human scrub typhus Abstract # 1058. American Society Tropical Medicine and Hygiene, November 2012. Oral and Poster presentation.

Gong B, Ma L, Gong Q, **Shelite T**, Mendell NL\*, Chang Q, Olano J, Walker DH, Oberhauser A. Tracking adhesion forces between VE-cadherin and human cerebral microvascular endothelial cell during infection of *Rickettsia montanensis* using atomic force microscopy. American Society for Rickettsiology, July 2012.



Gong B, Ma L, Liu Y, Gong Q, **Shelite T\***, Bouyer DH, Boor PJ, Lee YS, Oberhauser A. *Rickettsiae* induce microvascular hyperpermeability via phosphorylation of VE-cadherins: Evidence from atomic force microscopy and biochemical studies. American Society for Rickettsiology, July 2012.

Mendell NL\*, Goetz-Rivillas Y, Brouwer D, **Shelite TR**, Xu G, Gong B, Valbuena GA, Soong L, Olano JP, Walker DH, Bouyer DH. Characterizing the histopathology of intradermal infection model of human scrub typhus disease. American Society for Rickettsiology, July 2012.

Saito TB\*, Thirumalapura N, **Shelite TR**, Walker DH. Development of a mouse model of human ehrlichiosis caused by emerging new pathogenic *Ehrlichia* species. American Society for Rickettsiology, July 2012.

**Shelite TR**, Saito TB, Xu G, Gong B, Walker DH. Characterization of hematogenously disseminated *Orientia tsutsugamushi*: A human scrub typhus disease model in mice. American Society for Rickettsiology, July 2012.

Xu G\*, **Shelite T**, Mendell NL, Brouwer D, Walker DH, Bouyer DH. Persistence of *Orientia tsutsugamushi* in a newly developed intradermally inoculated mouse model. American Society for Rickettsiology, July 2012.

**Shelite TR**, Saito TB, Xu G, Gong B, Walker DH. Characterization of a murine model for human scrub typhus. Pathology Research Day-Poster, May 2012.

**Shelite TR**, Saito TB, Xu G, Gong B, Walker DH. Characterization of a murine model for human scrub typhus. IHII/McLaughlin Symposium-Poster, April 2012.

**Shelite TR**, Saito TB, Gong B, Walker DH. Development of a model of hematogenously disseminated scrub typhus disease in mice. 6th International Meeting on Rickettsiae and Rickettsial Diseases, Heraklion, Crete, Greece, June 2011. (Presented by David H. Walker)

**Shelite TR**, Saito TB, Gong B, Walker DH. Development of a model of hematogenously disseminated scrub typhus disease in mice. Pathology Poster Day, April 2011.

Xin L, **Shelite TR**, Gong B, Fang R, Walker DH. The role of indoleamine 2,3-dioxygenase in rickettsial infection. Pathology Poster Day, April 2011.

Xin L, **Shelite TR**, Walker DH. The role of indoleamine 2,3-dioxygenase in rickettsial infection. American Association of Immunologists-Poster, May 2011.

**Shelite TR**, Saito TB, Gong B, Walker DH. Development of a model of hematogenously disseminated scrub typhus disease in mice. IHII/McLaughlin Symposium-Poster, March 2011.

**Shelite TR**, Walker DH. Ehrlichial and rickettsial diseases: Vector-borne, intracellular pathogens of animals and humans. GSBS Program Fair-Poster, October 2010.

**Shelite TR**, Saito TB, Gong B, Walker DH. Development of a scrub typhus disease model via intravenous inoculation of mice. ASR-Poster, August 2010.

**Shelite TR**, Walker DH. Development of a relevant disease model for scrub typhus, *Orientia tsutsugamushi*. IHII/McLaughlin/UK Controlling Infectious Disease in the 21<sup>st</sup> Century Symposium- February 2010.

**Shelite TR**, Rong F, Pinter A, Ismail, N, Walker DH. The effects of tick saliva on the dendritic cell-*Rickettsia* interaction, *in vitro*. Sealy Center for Vaccine Development Symposium-Poster November 2009.

**Shelite TR**, Rong F, Pinter A, Ismail, N, Walker DH. The effects of tick saliva on the dendritic cell-*Rickettsia* interaction, *in vitro*. ASR-Poster August 2009.

**Shelite TR**, Rong F, Pinter A, Ismail, N, Walker DH. The effects of tick saliva on the dendritic cell-*Rickettsia* interaction, *in vitro*. McLaughlin Symposium-Poster. February 2009.

**Shelite TR**, Rong F, Pinter A, Ismail, N, Walker DH. The effects of tick saliva on the dendritic cell-*Rickettsia* interaction, *in vitro*. Fourteenth Annual Pathology Day-Poster. May 2008.

**Shelite TR**, Rong F, Pinter A, Ismail, N, Walker DH. The effects of tick saliva on the dendritic cell-*Rickettsia* interaction, *in vitro*. McLaughlin Symposium-Poster. May 2008.

**Shelite TR**, Rong F, Pinter A, Ismail, N, Walker DH. The effects of tick saliva on the dendritic cell-*Rickettsia* interaction, *in vitro*. 49<sup>th</sup> National Science Research Forum-Poster. April 2008.

**Shelite TR**, Rogers CM, Litzner BR, Johnson RR, Schneegurt MA. West Nile virus and natural bird populations: Two hypotheses. Graduate Research and Scholarly Projects Symposium-Poster. April 2006.

This dissertation was typed by Thomas Robert Shelite